TRANSFER AND DEVELOPMENT LENGTH OF FULLY BONDED 15.2 MM (0.6 IN) DIAMETER PRESTRESSING STRAND IN STANDARD AASHTO TYPE I CONCRETE BEAMS

BY

HEATHER LYNNE JOBSON, BSARCHE

THESIS

Presented to the Faculty of the Graduate School of

The University of Texas at Austin

in Partial Fulfillment

of the Requirements

for the Degree of

MASTER OF SCIENCE IN ENGINEERING

THE UNIVERSITY OF TEXAS AT AUSTIN

AUGUST 1997

TRANSFER AND DEVELOPMENT LENGTH OF FULLY BONDED 15.2 MM (0.6 IN) DIAMETER PRESTRESSING STRAND IN STANDARD AASHTO TYPE I CONCRETE BEAMS

Approved by
Supervising Committee:

Ned H. Burns

Michael E. Kreger

DEDICATION

For the glory of

my Lord and Savior and Best Friend

Jesus Christ

"For God so loved the world that He gave His one and only Son,

that whoever believes in Him

shall not perish but have eternal life.

For God did not send his Son into the world to condemn the world,

but to save the world through Him."

John 3:16-17

ACKNOWLEDGEMENTS

First and foremost, I want to thank my Father in Heaven for "willing in me to work and to act according to His good purpose (Philippians 2:13)," from the beginning of time until now. After all, it is only by His grace and for His glory that I live and work.

My deepest gratitude also belongs to all of those who supported me during my graduate education and in the execution of this research project. Specifically, I want to thank the Federal Highway Administration and the Texas Department of Transportation, whose financial support made this research project and my graduate education possible. The supervisors on this project were Dr. Ned H. Burns and Dr. Michael E. Kreger, whose encouragement to and confidence in me are greatly valued. I also appreciate both their enthusiasm and commitment to the field of engineering.

Additionally, words cannot express the depth of my appreciation for the hard work and dedication of Robert Barnes, Jon Kilgore, John Grove, Usnik ?, and Cem Topkaya to this project. I appreciate their patience and the laughter they provided as we worked side by side, sometimes under very difficult circumstances. I want to specifically thank Robbie for overseeing the project and for his guidance and insight. Special gratitude also belongs to Usnik for going above and beyond the call of duty as an undergraduate helper.

I also want to thank the people at Texas Concrete in Victoria, TX, for their cooperation and contribution to this project. Likewise, the technical support of the lab technicians was essential and extremely valuable to this project. I want to thank all of them for their patience and ingenuity, which helped to overcome some very difficult

hurdles. Also, the friendship and encouragement, as well as the hard work, of Laurie Golding, Sharon , Kelly, and April Jenkins was truly a blessing to me. This project could not have been completed without the help of many other students, too, who graciously volunteered their precious time to help cast the concrete beams and decks for this project.

On a more personal level, I want to thank the many members of the "dinner group" over the last two years, who provided encouragement, friendship, and support, through our common bond of engineering. Each member brought to the group a unique perspective on life and touched my life in a special way. I will never forget the many Sunday nights we spent together eating, drinking, and talking about "anything, except school."

Acknowledgements would not be complete without expressing my deep love and gratitude to my family for their unconditional love and prayers. I want to especially thank my mother for the important role she played in my life these last two years through our endless conversations on the phone. As we laughed, cried, and prayed together, we were able to share our life experiences, in spite of the many miles between us.

Special thanks also goes to Rebecca Martin for her encouragement and support over the last semester. As a fellow Christian, female in graduate school in engineering, we strove together to serve and glorify the Lord in our research and in the completion of our thesis. Additionally, I want to express deep gratitude to Tiffany Willingham, Karen Schelter, Regina Connor, Kristin Cooper, Jana Holley, Kimberly Megason, and Molly Cowan for their friendship, unconditional love, encouragement, and prayers. Last, but not least, I want to thank those at First Evangelical Free Church, for truly being a family to me and giving me a glimpse of what heaven will be like, worshipping God together.

May 20, 1997

ABSTRACT

TRANSFER AND DEVELOPMENT LENGTH OF FULLY BONDED 15.2 MM (0.6 IN) DIAMETER PRESTRESSING STRAND IN STANDARD AASHTO TYPE I CONCRETE BEAMS

Heather Lynne Jobson, M.S.E.

The University of Texas at Austin, 1997

Supervisor: Ned H. Burns

It is necessary to use 15.2 mm (0.6 in) diameter prestressing strand in order to fully utilize the properties of high-strength concrete currently used in standard pretensioned prestressed concrete beams. Therefore, tests were performed to further investigate the previously questioned anchorage characteristics of 15.2 mm (0.6 in) diameter prestressing strand at 51 mm (2 in) grid spacing. Conclusions based on test results, regarding such issues as transfer length, development length, and strand pull-out, are presented and compared with related literature. The specimens are AASHTO Type I highway bridge girders containing bright, fully bonded 15.2 mm (0.6 in) diameter prestressing strand. Each specimen has a composite concrete deck. Also, the beams in the test program have varying concrete strengths, as well as the variable of horizontal shear reinforcement.

TABLE OF CONTENTS

List of Tables

List of Figures

List of Illustrations

CHAPTER ONE

INTRODUCTION

1.1 PROJECT BACKGROUND

Prestressed concrete is a widely used material today, especially for highway overpasses and bridges. Prestressed concrete is a combination of high-strength steel and high-strength concrete, utilizing the best properties of both materials as they actively interact through bond stresses. However, as modern technology develops, more efficient structures are desired which utilize longer spans, contain wider spaces between girders, and support larger loads. Since more is demanded of the materials in order to meet these needs, it is important to have a thorough understanding of the interaction between the steel prestressing strand and the concrete.

Due to the increasing demands on prestressed concrete, as well as changes in strand technology and results from some recent research studies [1,2,3,4], concerns arose regarding the applicability of the equations, developed in the 1950's, that are still used today for transfer and development length [5]. Also, concerns existed regarding the practice of using 15.2 mm (0.6 in) diameter strand, instead of 12.7 mm (0.5 in) diameter strand, to increase the efficiency and capacity of flexural members. The issue of concern was the capability of the 15.2 mm (0.6 in) diameter strand to develop sufficient bond because the bond forces act on a surface area only 20% larger in size, and yet, sustain a 40% larger pretensioning force [6].

Therefore, for the purpose of further investigation, the Federal Highway Administration (FHWA) issued a memorandum on October 26, 1988 [7], imposing several restrictions on seven-wire strands in pretensioning applications. The memorandum prohibited the use of 15.2 mm (0.6 in) diameter strand, increased the minimum spacing requirement (center-to-center of strand) to four times the nominal strand diameter, restricted the development length, for all strand sizes less than or equal to 14.3 mm (9/16 in), to 1.6 times AASHTO equation 9-32, and restricted the

development length of debonded strands, for which tension is allowed at service load in the precompressed tensile zone, to 2.0 times the AASHTO requirement.

However, in order to fully utilize the properties of the high-strength concrete available today, it *is* necessary to use the 15.2 mm (0.6 in) prestressing strand at 50 mm (2 in) grid spacing. This is because the 15.2 mm (0.6 in) strand, due to its 40% larger area, can carry 40% more force than the 12.7 mm (0.5 in) strand, at the same level of steel stress. Since the extensive research performed after the FHWA memorandum in 1988 yielded results favorable to the bond performance of the 15.2 mm (0.6 in) diameter at 50 mm (2 in) grid spacing in pretensioned specimens, a portion of the restrictions imposed by the FHWA memorandum [7] was lifted. More specifically, the FHWA memorandum issued on May 8, 1996 [8], allows unrestricted use of 15.2 mm (0.6 in) diameter strand at 50.8 mm (2 in) grid spacing and 12.7 mm (0.5 in) diameter strand at 44.5 mm (1.75 in) grid spacing. All other restrictions remain until further review of proposed development length equations and current research is completed and commented upon by the AASHTO Bridge Subcommittee on Bridges and Structures.

It is important to reiterate that major portions of the 1988 FHWA memorandum remain in effect; therefore, more information is still urgently needed to develop more accurate equations for transfer and development length. This research project will provide some of that much needed data by examining the behavior of 15.2 mm (0.6 in) diameter prestressing strand with two different strand surface conditions, in specimens containing three different ranges of concrete strength, different percents of debonded strands, and the possible presence of horizontal shear reinforcement.

1.2 OBJECTIVES OF RESEARCH PROGRAM

The research program which provides the basis for this thesis is entitled *Development Length of 15-mm (0.6-inch) Diameter Prestressing Strand at 50-mm (2-inch) Grid Spacing in Standard I-shaped Pretensioned Concrete Beams* and is funded by Texas Department of Transportation (TxDOT) and the Federal Highway Administration (FHWA). The test program consists of 36 beams (72 tests) with the following variables:

strand surface condition, percent debonded strands, concrete strength, and horizontal shear reinforcement. The length of each beam was designed to effectively perform two tests per beam.

One objective of the research program is to measure the transfer and development length of 15.2 mm (0.6 in) prestressing strand at 50.8 mm (2 in) grid spacing in tests of standard AASHTO Type I highway bridge girders with composite concrete decks. The concrete deck is used to obtain a desired strain of 0.035, 3.5%, in the strand under applied load at ultimate and to more accurately represent field conditions. The results from the tests will then be used to further evaluate and refine the existing equations for transfer and development length. Another important objective is to provide much needed experimental data on the performance of debonded strands in pretensioned beams. In general, the results from the tests performed for this research project will add to the overall understanding of the bond performance of 15.2 mm (0.6 in) diameter strand in concrete for both fully bonded and partially debonded pretensioned applications.

1.3 OBJECTIVES OF THIS STUDY

The purpose of this study is to present and discuss the first portion of results in the total research program described in Section 1.2. The findings and conclusions discussed in this study include transfer length, development length, and strand pull-out for the specimens containing bright, fully bonded 15.2 mm (0.6 in) diameter prestressing strand. The results from the testing of these specimens is important because strand with a "mill condition" surface represents a "worst case" scenario for the strand condition variable. A more complete understanding of the interaction between concrete and the bright strand will be obtained by considering the behavior of the bright strand in test specimens with different concrete strengths and a possible presence of longitudinal shear reinforcement.

Another objective of this study is to evaluate the effectiveness of using the previously mentioned horizontal shear reinforcement (H-bars) to arrest crack growth in

the transfer zone, and subsequently reduce the possibility of and/or magnitude of the slipping of the prestressing strand.

1.4 ORGANIZATION OF THIS STUDY

Eight total chapters are included in this report. The first chapter gives an introduction to this project, including the objectives of the research program and the related portion of the program to this study, namely the specimens with bright, fully bonded prestressing strand. The second chapter contains a discussion of previous literature related to this work, as well as discussion and definitions of essential terminology, such as bond and transfer and development length. The third chapter describes details related to the specimens: their design, designation, properties, and fabrication. The fourth, fifth, and sixth chapters describe transfer length, development length, and strand pull-out testing, respectively. Finally, Chapter Seven presents a discussion of all the test results, and Chapter Eight gives a summary of this study and conclusions made from the test results.

CHAPTER TWO

THEORETICAL BACKGROUND

2.1 INTRODUCTION

In order to better understand the test results presented in this study it is important to first define essential terminology and review relevant literature. Therefore, this chapter first defines the nature of bond and its importance to pretensioned concrete. Then, following the discussion of bond, sections on transfer length, development length, and strand pull-out are presented which each include definitions and a brief discussion of literature pertaining to the section topic.

2.2 THE NATURE OF BOND IN PRETENSIONED CONCRETE

2.2.1 Bond Behavior

As discussed by Russell [6], although the existence and importance of bond between prestressing strands and concrete is certain, it is difficult to quantify bond mathematically in a formula based on physical properties. This difficulty exists for several reasons, including the variability and unpredictability of the frictional component, material discontinuities due to local cracking resulting from tangential stresses between the strand and the surrounding concrete [9], and complicated interaction between Hoyer's effect and mechanical interlocking as untwisting of the strand is restrained.

Some effort as been made to develop equations for bond based on experimental results [1,5,9,10,11,12,13,14], but more important is a qualitative understanding of bond stresses. Bond between a steel prestressing strand and the surrounding concrete can be adequately described by three separate mechanisms: Hoyer’s effect, adhesion, and mechanical interlock. A qualitative understanding of these mechanisms not only provides a means of understanding bond, but also aids the prediction of anchorage failure of pretensioned seven-wire strand.

2.2.1.1 Hoyer's Effect

Hoyer's effect was developed in 1939 by E. Hoyer [15], who investigated the mechanism which anchored the pretensioned force in the concrete. At the time this research was conducted, the pretensioning steel consisted of small diameter smooth wire containing no deformations, and therefore, eliminating the influence of mechanical interlocking.

As the strand is pretensioned, reduction in the strand diameter proportional to Poisson's ratio occurs simultaneously with the elongation of the strand. Then, after the concrete is cast and set around the strand, the prestressing force in the strands is released, causing the wire to lose its initial prestress. Upon the loss of the initial prestress, the wire attempts to regain its original shape. As the strand begins to expand laterally, however, the concrete restrains the strand, inducing a normal force on the concrete. A frictional force is activated by this normal force, preventing relative movement of the steel strand to the concrete, and therefore, holding the strand in tension, as detailed in Figure 2.1.

Hoyer's effect exists mostly in the transfer zone and is independent of the other two mechanisms.

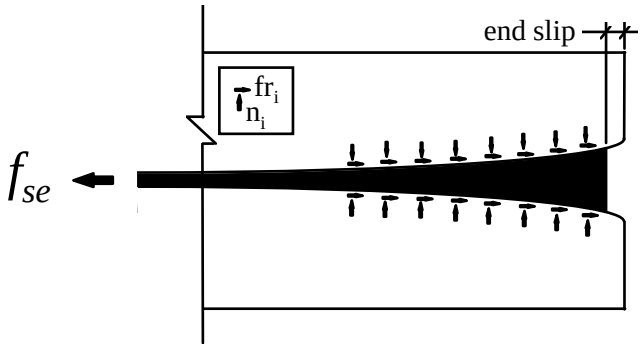

Figure 2.1- Diagram of Hoyer's Effect [6]

2.2.1.2 Adhesion

Adhesion is the chemical mechanism which fastens the concrete to the steel pretensioning strand before slip occurs. In other words, adhesion aids strand anchorage only until a critical stress is reached. At the critical stress, a rigid-brittle failure of the bond stress versus slip occurs, ending any contribution to bond by adhesion. Therefore, the contribution of adhesion to bond must be compensated by the other two mechanisms.

Slip of the strand relative to the concrete occurs both at the release of the strands through the transfer zone and in a development bond failure. Therefore, adhesion realistically contributes little to the prevention of a bond failure, at transfer or in the achievement of full flexural capacity.

2.2.1.3 Mechanical Interlock

Mechanical interlocking occurs when the strand tries to pull through the concrete without twisting. Since the concrete conforms to the helical pattern of the seven-wire prestressing strand, the helical ridges prevent this motion of the strand. Mechanical interlocking is also dependent upon Hoyer's effect and/or adhesion to restrain the strand and prevent twist. It is important to note, however, that for mechanical interlocking to aid strand anchorage, the strand must be prevented from twisting.

If the prevention of twisting is ensured, mechanical interlocking is probably the largest contributor to flexural bond, especially in cracked regions. At the appearance of a crack, slipping of the strand occurs. Mechanical interlocking is then activated as the concrete encasing the strand on either side of the crack prevents slipping of the strand.

2.2.2 Importance of Bond

The existence of an active bond between the prestressing strand and the concrete is the primary reason that prestressed concrete exists as an option in construction today. If the steel tendons and concrete were not connected together in an integral fashion, prestressed concrete would merely act like standard reinforced concrete.

Research shows that bond is important during both parts of the history of a non-end-anchored pretensioned member: at transfer and in flexure. Bond is activated at release through the transfer of the prestress from the strand to the concrete, and flexural bond is activated as external loading causes cracking and possibly failure [16]. The concept of transfer and flexural bond stresses was first introduced by Janney [9] and was later confirmed by tests performed by Hanson and Karr [11].

2.2.2.1 Transfer Bond Stresses

Transfer bond stresses are responsible for the increase in steel stress from zero at the beginning of bond between the concrete and steel to the effective prestress (f_{se}) at the end of the transfer zone. As shown in Figure 2.2, theoretically, the steel stress varies linearly over the transfer zone and remains constant in the central portion of the beam. Therefore, since total bond stress is the derivative, or proportional to the rate of change, of the steel stress, the bond stresses must be uniform over the transfer zone.

It is the combination of Hoyer's effect and mechanical interlocking that creates this uniform bond stress through the transfer zone [6]. Hoyer's effect contributes more toward strand anchorage at the beams ends because resistance to twisting has not developed for mechanical interlocking to be entirely effective. However, as the strand expands laterally along the transfer length, Hoyer's effect provides the needed twist restraint for mechanical interlocking to contribute to bond. Then, since the steel loses a smaller portion of its initial stress near the center of the beam, the contribution to bond stresses by Hoyer's effect is nearly eliminated and mechanical interlocking becomes the primary bonding mechanism. As stated in Section 2.2.1.2, adhesion does not contribute to transfer bond stresses due to slipping of the strands.

2.2.2.2 Flexural Bond Stresses

Flexural bond stresses are responsible for the increase in steel stress from the effective prestress (f_{se}) to the ultimate stress (f_{ps}) under applied loads, as shown in Figure

2.2. These “flexural” bond stresses, however, must resist the additional strand tension due to both flexural and shear loads.

Before cracking, the additional bond stresses are very minor. However, once cracking occurs, the concrete contributes nothing to resist the additional tensile stresses, causing a dramatic increase in the steel stress at crack locations. Since the rate of change of the steel stress is very high near crack locations, high bond stresses are present. Once a limiting stress is reached, though, small slipping of the strands occurs, which relieves some of the bond stresses.

Once the crack opens, mechanical interlocking develops to prevent the strand from pulling through the concrete. For this reason, mechanical interlocking is the primary bond mechanism which contributes to flexural bond stresses [6]. Adhesion does not exist in the presence of slip, and Hoyer’s effect is negated by the elongation of the strand as the beam deforms under load.

2.2.2.3 Relationship between Transfer and Flexural Bond Stresses

Janney [9] made two important observations related to transfer and flexural bond stresses. The first observation was that as loading increased and the appearance of cracks spread toward the end regions of the beams, the maximum values of flexural bond stresses also spread outward from a crack and moved toward the beam ends. The second observation was that little interaction exists between transfer and flexural bond stresses. Even in the occurrence of a bond failure, evidenced by end-slip of the strands, the maximum flexural bond stresses barely overlapped the region of transfer bond due to prestress.

The combination of the transfer and flexural bond regions yields the development length of the prestressing strand, as shown in Figure 2.2 and defined in Section 2.3.1.3.

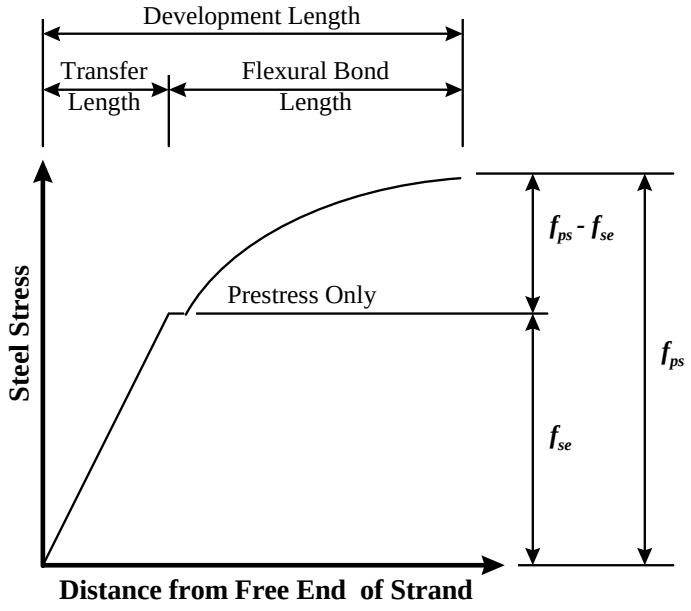

Figure 2.2- Variation of Steel Stress with Distance from Free End of the Strand [17]

2.3 DISCUSSION OF TRANSFER AND DEVELOPMENT LENGTH

This section discusses the importance of, as well as definitions, variables, literature, and equations related to transfer and development length.

2.3.1 Definitions

2.3.1.1 Transfer Length

Transfer length is the distance required to transfer the fully effective prestressing force from the strand to the concrete. In other words, the transfer length is the length from the beginning of bond, where the stress in the strands is zero, to the point where the prestressing force is fully effective. The beginning of bond, or location of zero stress, occurs at the end of the beam for fully bonded strands and at the location of debonding for debonded strands.

2.3.1.2 Flexural Bond Length

As indicated by Figure 2.2, the *flexural bond length* is the additional bond length, beyond the transfer length, necessary to develop the strand bond stresses from the fully effective prestress (f_{se}) to the ultimate strand stress (f_{ps}). The flexural bond length results entirely from the application of external loads.

2.3.1.3 Development Length

Development length is the distance required to fully anchor the prestressing strand as it resists externally applied loads to the concrete member. A fully anchored strand refers to a strand adequately secured by bond stresses, ensuring a flexural failure and preventing slipping of the strands under increasing load. As shown in Figure 2.2, the development length is the combination of the transfer and flexural bond lengths.

2.3.1.4 Embedment Length

Embedment length is the bonded length of the strand from the beginning of bond to the critical section. The critical section occurs where the steel stresses are maximum, which is usually the point of maximum moment. However, it is important to note that the critical section does not *always* occur at the location of the maximum moment.

As described in the development length definition, it is important for the strand to be fully anchored by bond stresses. Therefore, it is necessary for the embedment length to be longer than the required development length ($L_e \geq L_d$).

2.3.2 Importance of the Transfer and Development Lengths

2.3.2.1 Importance of the Transfer Length

In this study the transfer length is important because it is related to the contribution of the concrete to shear strength and associated shear cracking, as discussed in Section 2.3.5.1.

The transfer length is also important, though, because in the transfer zone the prestressing force in the strand is not yet fully effective. Therefore, the stress in the strands is somewhere between zero, at the beginning of the length over which bond occurs between the strand and the concrete, and f_{se}, at the end of the transfer zone. This means that along the transfer length, the prestressed member has less resistance to cracking.

Also, the transfer length is important for the prediction of development failures. If a crack occurs in the transfer zone, the member is likely to experience a bond failure. Therefore, the prevention of both flexural and shear cracking within the transfer length is important for the development of the strength of the beam.

On the other hand, the importance of the transfer length should not be exaggerated. In normal practice, the design or performance of pretensioned members will most likely not be affected by a significant variation in the transfer length. Therefore, it is not always necessary to know the exact value for the transfer length to ensure structural integrity.

2.3.2.2 Importance of the Development Length

As described in Section 2.3.1.3, the development length is important because it defines the boundary between a flexural and a bond failure. It is the length required to fully anchor the strand as external loads are resisted by the member; therefore, assuring the full flexural capacity of the member is reached.

Unfortunately, determining the development length in reality is not as straight forward as the definition might indicate. The development length must be determined experimentally by testing specimens at various embedment lengths and noting the failure types that results from each embedment length.

The development length is not only important as a requirement for flexural resistance, but also for the prevention of anchorage failures resulting from the propagation of web shear cracking. The prestressing steel must have a development

length capable of supporting the additional tensile stresses which exist after the concrete cracks, and therefore, loses its tensile capacity

2.3.3 Variables Affecting Transfer and Development Length

Although the current equations used to calculate the transfer and development length in the design of prestressed specimens only include the use of the effective prestressing steel stress (f_{se}) and the strand diameter (d_b), several other variables can affect transfer length and development length [13]. Some of these variables are listed below with references given to research related to each variable:

1. Type of steel (wire, strand) [18]
2. Size of steel (diameter) [1,3,6,12,19,20,21,22,23]
3. Steel stress level [20]
4. Steel surface condition (i.e. clean or rusted) [1,6,9,11,18,20,23,24,25,26,27]
5. Concrete compressive strength [12,28,29]
6. Type of loading (static, repeated, impact) [6]
7. Type of release (gradual, sudden) [12,21,24,28,]
8. Confining reinforcement around steel (helix, stirrups) [21]
9. Time-dependent effects [12]
10. Consolidation and consistency of concrete around steel
11. Concrete cover around steel [6,21]
12. Debonding strands [6,21,22,30]

In brief, some general observations can be made regarding the previously listed variables effect on the transfer length and development length. Transfer length tends to increase as the strand diameter increases, as the steel effective prestressing stress increases, with a smoother strand surface, as the concrete compressive strength decreases, with sudden release of the prestress in the strands, as time increases, and in fully bonded

specimens. Development length increases especially with an increase in strand diameter and with a smoother strand surface.

It is important, however, to note that not *all* the research conducted to date follows the trends. A more detailed discussion of the research regarding the variables related to this thesis is included in Section 2.4.

2.3.4 Related Research on Transfer and Development Length

This section discusses some of the major studies conducted on transfer and development length, which relate to the variables and materials used in this study. The relationship of the research reported in this section and the data in this thesis will be discussed in Chapter Seven.

2.3.4.1 Cousins, Johnston, and Zia- North Carolina State University (1986) [1,3]

The primary purpose of the research performed by Cousins, Johnston, and Zia was to study the effect of epoxy-coating on the transfer and development length of the prestressing strand. The variables included in the research were strand size, including 9.5, 12.7, and 15.2 mm (0.375, 0.5, and 0.6 in.) diameter strands, and epoxy grit density. Also, the specimens with coated strands were compared to specimens with uncoated strands. All of the specimens were rectangular with one concentric strand and contained concrete with a compressive strength at transfer (f'_{ci}) and 28-days (f'_c) of approximately 27.5 and 34.5 MPa (4000 and 5000 psi), respectively. One group of specimens was used exclusively for transfer length study and the remaining group of specimens was used for development length study.

The epoxy inundated with grit improved bonding characteristics of the strand to the concrete, which resulted in a reduction in the transfer and development lengths. Also, it was observed that the transfer and development length increased as the strand diameter increased. An average transfer length of 864, 1270, 1372 mm (34, 50, and 54 in) and an average development length of 1.4, 3.0, 3.4 m (57, 119, 132 in) was reported for the 9.5, 12.7, and 15.2 mm (0.375, 0.5, and 0.6 inch) strand, respectively. However, more

important than these findings was the occurrence of unconservative transfer and development lengths for the uncoated strands. This lack of conservatism in the ACI [17] and AASHTO [31] code equations strongly influenced the decision to issue the FHWA Memorandum [7], per Section 1.1, until further research could be performed. As given in Table 2.1, Cousins, Johnston, and Zia also developed suggested revisions to the transfer and development equations which account for surface condition.

2.3.4.2 Castrodale, Burns, and Kreger - The University of Texas at Austin (1988) [18]

Castrodale, Burns, and Kreger performed some transfer tests as a small part of a research project on pretensioned high-strength concrete girders in composite highway bridges. The project variables included concrete strength and type of release. All the specimens were rectangular, concentrically prestressed with a Grade 270, stress-relieved, 12.7 mm (0.5 in) single prestressing strand, and contained concrete with either a 28-day compressive strength (f'_c) of 34.5 MPa (5000 psi) or 68.9 MPa (10,000 psi).

It was observed that the type of release did not have a significant effect on the transfer length. More significant, though, is the observation that the transfer length seemed to decrease in the specimens with higher concrete strengths. For example, the average transfer lengths for the 102x102 mm (4x4 in) specimens with concrete compressive strengths of 35.2 and 64.8 MPa (5.1 and 9.4 ksi) were 559 and 381 mm (22 and 15 in), respectively. Also, unlike the findings of Cousins, Johnston, and Zia [1,3], the transfer lengths reported were less than those calculated from the ACI [17] and AASTO [31] equations given in Section 2.3.6.

2.3.4.3 Burdette, Deatherage, and Chew (1991) [20,27]

Burdette, Deatherage, and Chew performed research to determine the effects primarily of strand size on the transfer and development length of pretensioned members. The strand sizes used were 12.7, 14.3, and 15.2 mm (0.5, 9/16, and 0.6 in). The program utilized specimens with two different cross-sections: rectangular and I-shaped. All the specimens contained Grade 270, low-relaxation strands and a concrete compressive

strength at transfer (f'_{ci}) and at 28 days of 27.6 MPa (4000 psi) and 35.4-55.0 MPa (5130-7980 psi), respectively.

The effects of the strand diameter on the transfer and development were observed to partially agree with previously determined trends; namely, as the strand diameter increases, so does the transfer and development length. The average transfer lengths of 813, 889, and 610 mm (32, 35, and 24), and the approximate development lengths of 2.0, 2.7, and 2.2 m (80, 105, and 85) were measured for the 12.7, 14.3 and 15.2 mm (0.5, 9/16, and 0.6 in), respectively. Therefore, the transfer and development length of the 15.2 mm (0.6 in) diameter strand did not coincide with the trend of previous research. Also, due to the effects of weather, the strand surface condition became a variable. Strands with a rougher surface condition yielded shorter transfer and development lengths.

In addition, as observed by Cousins, Johnston, and Zia [1,3], Burdette, Deatherage, and Chew found the ACI [17] and AASHTO [31] provisions to be unconservative. Therefore, a modification to the equations was proposed and is listed in Section 2.3.6.

2.3.4.4 Shahawy, Issa, and deV Batchelor - Florida Dept. of Transportion (1992) [22]

Shahawy, Issa, and deV Batchelor performed an experimental and analytical investigation of the transfer lengths of prestressing strand in full scale AASHTO Type II girders. The variables included in the project were the diameter of the prestressing strand [12.7 and 15.2 mm (0.5 and 0.6 in)], debonding, and web shear reinforcement ratio. The specimens contained Grade 270, low-relaxation prestressing strand, which were released suddenly by flame-cutting, and concrete with a compressive strength at transfer (f'_{ci}) of 38.9 MPa (5640 psi).

It was observed that debonding did not greatly affect the transfer length. Also, similar to other research, the specimens with the larger strands yielded longer transfer lengths. Unfortunately, Shahawy, Issa, and deV Batchelor additionally discovered the ACI and AASHTO specifications to be inadequate, and therefore, recommended

revisions to the transfer length equation. Another important finding was that the 50 mm (2 in) grid spacing used was adequate for 0.6 in diameter strands, which aided the decision to remove part of the moratorium imposed by FHWA [6,7], per Section 1.1.

2.3.4.5 Russell and Burns - The University of Texas at Austin (1993) [6]

Russell and Burns executed an extensive research program on the transfer and development length of pretensioned members, including several of the variables listed in Section 2.3.3. The transfer length variables included the number of strands (1,3,4,5,8 and 24), diameter of the strand [12.7 and 15.2 mm (0.5 and 0.6 in)], confining reinforcement (with or without), size and shape of the cross-section, and debonding (fully bonded or debonded strands). The variables of the development testing included the diameter of the strand [12.7 and 15.2 mm (0.5 and 0.6 in)] and the specimen cross-section (rectangular or I-shaped).

The transfer length did not appear to be affected by the variables of strand spacing and confinement. However, as seen in previous literature, the specimens with larger diameter strands yielded longer transfer and development lengths. Also, longer transfer lengths were observed in specimens with smaller cross-sections and fully bonded strands. It was also noted that some of the specimens had much longer transfer and development lengths than expected, which did not conform to the observed trends. It was subsequently concluded that the strand in these specimens had become contaminated with oil. Furthermore, the longer lengths caused by the oil confirmed findings in previous research, as discussed in Section 2.3.3, that smoother strand surface conditions result in longer transfer and development lengths.

Two other important developments came from the research performed by Russell and Burns [6]. First, some of the bond failures in AASHTO-type beams were preceded by web shear cracking, not flexural cracking, in the transfer zone. This observation is important because it demonstrates the fact that shear cracking may govern the bond requirements in a pretensioned beam. Second, as listed in Section 2.3.6, a new

development length equation is proposed which prevents cracking in the transfer zone by limiting the applied loads.

2.3.4.6 Mitchell, Cook, Tham, and Khan- McGill University (1993) [29]

Mitchell et. al. investigated both the influence of high strength concrete and strand diameter on the transfer and development length of pretensioned concrete members. The specimens contained concrete with compressive strengths at transfer (f'_{ci}) and at 28-days (f'_c) ranging from 21.0 to 50.0 MPa (3050 to 7250 psi) and 31.0 to 88.9 MPa (4500 to 12,900 psi), respectively. All the specimens were rectangular and contained a concentrically placed, Grade 270, low-relaxation, prestressing strand with a diameter of 9.5, 12.7, or 15.7 mm (0.375, 0.5, and 0.62 in).

The specimens with lower concrete strengths and larger diameter strands yielded longer transfer and development lengths. Due to the apparent influence of concrete strength on the transfer and development lengths, Mitchell et. al. proposed new equations, which contain concrete strength as a variable, for inclusion in the ACI [17] and AASHTO [31] codes. These equations are given in Section 2.3.6.

2.3.4.7 Tawfiq- Florida State University (1995) [32]

Tawfiq performed research on full-scale AASHTO Type II girders to investigate the cracking and shear capacity of high strength prestressed concrete girders, which involved the study of transfer length. The two variables included in the study were concrete strength and amount of shear reinforcement. The concrete compressive strengths at transfer (f'_{ci}) ranged from 36.8 to 56.5 MPa (5340-8200 psi). The specimens all contained 12.7 mm (0.5 in) diameter, Grade 270, low-relaxation prestressing strand.

Most of the measured transfer lengths decreased with increasing concrete strengths; however, it is important to note that not all of the results followed this pattern. In addition, the test results agreed with Russell's finding [6] that it is possible for shear to govern the bond requirements in a pretensioned beam. It was also observed that the

quantity of shear reinforcement did not seem to affect the strength of the beams and that most of the beams had a bond failure.

2.3.4.8 Gross, Burns- The University of Texas at Austin (1995) [33]

Gross investigated the use of 15.2 mm (0.6 in) diameter prestressing strands in rectangular concrete beams with the purpose of determining the transfer and development length. The concrete beams contained concrete with a compressive strength at transfer and at 28-days of 48.5 and 81.7 MPa (7040 and 11,850 psi), respectively, and rusted, Grade 270, low-relaxation prestressing strands.

The average transfer and development length were found to be 363 mm (14 in) and 2.0 m (78 in), respectively, and to be conservative with respect to the current ACI [17] and AASHTO [31] specifications.

2.3.5 Current Transfer and Development Length Expressions

The current provisions for transfer and development length will be discussed in the next two sections. It is important to mention that both expressions are based on English units, and therefore, yield lengths in inches.

2.3.5.1 Transfer Length Expression

A required specification for transfer length does not exist in either the current ACI 318-95 [17] or AASHTO code [31]. Both codes, however, suggest the use of 50 times the strand diameter for the transfer length when calculating V_{cw} in shear provisions of the codes (ACI 11.4.3 and AASHTO 9.20.4). V_{cw} is the nominal shear strength provided by concrete when diagonal cracking results from excessive principal tensile stress in the web.

The specification of $L_t \approx 50 * d_b$ is an approximation for the following equation provided in the commentary to the ACI Building Code (R12.9) for transfer length:

$$L_t = (f_{se}/3) * d_b \quad (1)$$

The approximation is based on f_{se} = 150 ksi.

2.3.5.2 Development Length Expression

As in the case of the transfer length expression, the development length provisions in the ACI 318 [17] and AASHTO [31] codes are nearly identical, both requiring an embedment length less than or equal to the specified development length. The ACI 318 Code contains the following requirements for development length:

> *12.9.1 Three- or seven-wire pretensioning strand shall be bonded beyond the critical section for a development length, in inches, not less than*
>
> $$\left(f_{ps} - \frac{2}{3} f_{se} \right) d_b \qquad (2)$$
>
> *where d_b is strand diameter in inches, and f_{ps} and f_{se} are expressed in kips/in^2*
>
> *12.9.2 Limiting the investigation to cross sections nearest each end of the member that are required to develop full design strength under specified factored loads shall be permitted.*

The ACI Commentary (R12.9) to these provisions gives an alternate form of equation (2):

$$l_d = \frac{f_{se}}{3} d_b + (f_{ps} - f_{se}) d_b \qquad (3)$$

where l_d and d_b are in inches, and f_{ps} and f_{se} are in ksi. The first term represents the transfer length of the strand and the second term represents the flexural bond length, as defined in Section 2.3.1.

Also, the ACI Commentary mentions that these code equations are based on tests performed on prestressed members containing normal weight concrete, a minimum strand cover of 50.8 mm (2 in),.and clean, 6.4, 9.5, 12.7 mm (0.25, 0.375, and 0.5 in) strands. The research was performed in the 1950's and 1960's by by Hanson and Kaar [11], Kaar et. al. [12], and Kaar and Magura [30]

2.3.6 Summary of Suggested Transfer and Development Length Expressions

As a result of the unconservative results from some of the research discussed in Section 2.3.4, and changes in materials use since development of the current transfer and

development length expressions, several attempts have been made to revise the transfer and development length guidelines.

The equations are antiquated because they were developed for inclusion in the 1963 ACI 318 Building Code, at which time Grade 250, stress-relieved, seven-wire strand was used [4]. Today, however, low-relaxation Grade 270 seven-wire strand is most commonly used for pretensioned applications. This Grade 270 strand theoretically results in slightly longer transfer lengths than the Grade 250 strand used as the basis for the transfer and development length equations.

Since most of the suggested revisions are empirical, the equations must be compared and examined carefully as new research is performed, creating an even larger data base of test results. Even with a continuously expanding data base, however, the difficulty remains in developing one equation that is accurate and applicable to all cases. This difficulty is due to the variety of variables affecting the transfer and development length. Therefore, each suggested equation in Table 2.1 should be used with discretion. Also, Table 2.1 is not a comprehensive list; analytically derived equations have also been developed, but are too complicated to list [34,35]. The calculated transfer and development lengths from the equations in Table 2.1 will be compared to the results of this study in Chapter Seven.

Table 2.1- Proposed Equations for Transfer and Development Length [33,36]

Author(s)	Year	Transfer Length Equation	Development Length Equation	Ref. #
ACI 318/ AASHTO	1963	$L_t = \frac{f_{se}}{3} d_b$ $L_t \approx 50 d_b$	$l_d = L_t + (f_{ps} - f_{se}) d_b$	17, 31
Martin & Scott[(1)]	1976	$L_t = 80 d_b$	$f_{ps} \le \frac{L_e}{80 d_b}\left(\frac{135}{d_b^{1/6}} + 31\right) \quad L_e \le 80 d_b$ $f_{ps} \le \frac{135}{d_b^{1/6}} + \frac{0.39 L_e}{d_b} \quad L_e > 80 d_b$	37
Zia & Mostafa	1977	$L_t = 1.5 \frac{f_{si}}{f_{ci}^{'}} d_b - 4.6$	$l_d = L_t + 1.25(f_{pu} - f_{se}) d_b$	13
Cousins, Johnston, & Zia[(2)]	1990	$L_t = \frac{\left(U_t^{'}\sqrt{f_{ci}^{'}}\right)}{2B} + \frac{f_{se} A_{ps}}{\pi d_b U_t^{'}\sqrt{f_{ci}^{'}}}$	$l_d = L_t + (f_{ps} - f_{se})\left(\frac{A_{ps}/(\pi d_b)}{U_d^{'}\sqrt{f_c^{'}}}\right)$	1, 2, 3
Russell & Burns[(3)]	1993	$L_t = \frac{f_{se}}{2} d_b$	$M_{cr} > L_t V_u$ *Fully Bonded* $\frac{L_b + L_t}{Span} \le \frac{1}{2}\left(1 - \sqrt{1 - \frac{M_{cr}}{M_u}}\right)$ *Debonded*	5
Mitchell et. al.	1993	$L_t = \frac{f_{si} d_b}{3}\sqrt{\frac{3}{f_{ci}^{'}}}$	$l_d = L_t + (f_{ps} - f_{se}) d_b \sqrt{\frac{4.5}{f_c^{'}}}$	29
Burdette, Deatherage, & Chew	1994	$L_t = \frac{f_{si}}{3} d_b$ [(4)]	$l_d = L_t + 1.50(f_{ps} - f_{se}) d_b$	20,27
Buckner (FHWA)[(5)]	1994	$L_t = \frac{1250 f_{si} d_b}{E_c}$ $\approx \frac{f_{si}}{3} d_b$	$l_d = L_t + \lambda(f_{ps} - f_{se}) d_b$ $\lambda = (0.6 + 40\varepsilon_{ps})\, or \left(0.72 + 0.102\frac{\beta_1}{\omega_p}\right)$ $(1.0 \le \lambda \le 2.0)$	36

Notes: All equations result in transfer and development lengths with standard inch units

Notes to Table 2.1 (continued):

1 inch = 25.4 mm

All units of stress in ksi

Some notation changed to provide consistency between equations

See Appendix A for notation definitions

(1)Development length equations limit f_{ps} as a funcion of L_e.

(2)B = 300 psi/in on average; U'_t and U'_d are coefficients based on strand surface conditions

(3)Development length criteria based on preventing cracking in the transfer zone

(4)Shahawy et. al. [22] recommends the same equation for transfer length

(5)Development length equation based on minimum strand strain at failure

2.5 STRAND PULL-OUT

2.5.1 Definition

A *direct tension pull-out test* is an experimental arrangement which tests the bond characteristics of seven-wire strand that is not tensioned before loading.

Mechanical interlocking contributes to the bond behavior exhibited in a pull-out test through friction. Unlike an actual pretensioned application, however, the Hoyer effect does not contribute to the development of bond stresses. In fact, the cross-sectional areas of the strands reduce during testing [32]. As discussed in Section, any bond due to adhesion is lost when slip occurs. Therefore, the bond performance is minimally affected by adhesion in strand pull-out testing.

2.5.2 Importance of Strand Pull-Out Testing

Direct tension pull-out testing is important to gain a qualitative understanding of the bond performance between a concrete mix and the steel prestressing strand. The test results provide an understanding of the quality of bond performance which can be expected in the actual prestressed application.

2.5.3 Related Literature

All of the pull-out testing to date has been primarily on 12.7 mm (0.5 in) diameter prestressing strand. Therefore, no previous literature exists containing results using 15.2 mm (0.6 in) diameter strand. However, in order to give an adequate background on pull-out testing, the comprehensive study performed by Donald Logan [38] on the bond performance of 12.7 mm (0.5 in) diameter strand will be discussed in this section. Other related literature can be obtained through the PCI Journal article written by Logan and published in the March/April 1997 issue.

The research program executed by Logan was developed primarily due to the inconclusive and inconsistent nature of previous test results. Therefore, Logan, funded by Stresscon Corporation, developed a testing program to provide an acceptance criteria for the bond quality of prestressing strand. The test program included pull-out tests, end slip at prestress release and at 21 days, and development length tests which were performed on samples of Grade 270, 12.7 mm (0.5 in) diameter prestressing strand. This strand was obtained from six locations across North America. Thirty-six pull-out tests were performed using the method developed by Saad Moustafa in 1974 at an embedment length of 457 mm (18 in).

The most important conclusion made by Logan was that the pull-out test was an accurate method to predict a qualitative bond performance of a 12.7 mm (0.5 in) prestressing stand. Specifically, it was concluded that strands with an average pull-out capacity exceeding 160 kN (36 kips) yielded conservative transfer and development length results with respect to the ACI [17] and AASHTO [31] provisions. However, "strands with an average pull-out capacity less than 53.3 kN (12 kips) were unable to meet the ACI transfer length criteria and failed prematurely in bond at the ACI development length, without noticeable warning deflection."

CHAPTER THREE

TEST SPECIMENS

3.1 INTRODUCTION

The portion of the research program being reported on consists of six 12.2 m (40 ft) long AASHTO Type I prestressed highway bridge girders with composite cast-in-place concrete decks. All of the beams contain 15.2 mm (0.6 in) diameter prestressing strand with a bright mill finish, spaced on a 50 mm (2 in) grid. The variables in the test program are concrete strength and longitudinal shear reinforcement, or H-bars. The beams were cast in pairs, with each pair having a given concrete strength and one end of one beam containing longitudinal shear reinforcement.

3.2 SPECIMEN DESIGNATION AND DESIGN

3.2.1 Specimen and Test Designation

Each beam is identified by a four digit code (XXXX). Table 3.1 lists the description of each digit in the code and Table 3.2 gives a description of the possible variables for each place order. In order to distinguish between each beam end and each test, however, further clarification is necessary. Each beam end is designated by adding an A or B to the beam identification (e.g. XXXXA) and the individual tests are further distinguished by adding a hyphen plus the test number (1, 2, 3, or 4). Test 4 is always the test of the end containing the H-bars.

Table 3.1-Beam I.D. Description

Place Order	Description
1	Concrete Strength
2	Number of Debonded Strands
3	Strand Surface Condition
4	Longitudinal Shear Reinforcement Indicator

Table 3.2- Place Order Variable Description

Place Order	Variable	Description
1	L	Normal Strength Concrete (5000-7000 psi)
	M	Medium Strength Concrete (9500-11500 psi)
	H	High Strength Concrete (13000-15000 psi)
2	0	Fully Bonded (0 Strands Debonded)
	4	50% Debonded (4 strands debonded, staggered)
	6	Y% Debonded (6 strands debonded, staggered)
3	B	Bright Strand Surface (Mill Finish)
	R	Rusty Strand Surface
4	0	Does not contain H-bars
	1	Contains H-bars

3.2.2 Specimen Design

Each specimen consists of an AASHTO Type I girder, a composite cast-in-place concrete deck, prestressing strand, and mild shear reinforcement with a cross-section similar to Figure 3.1.

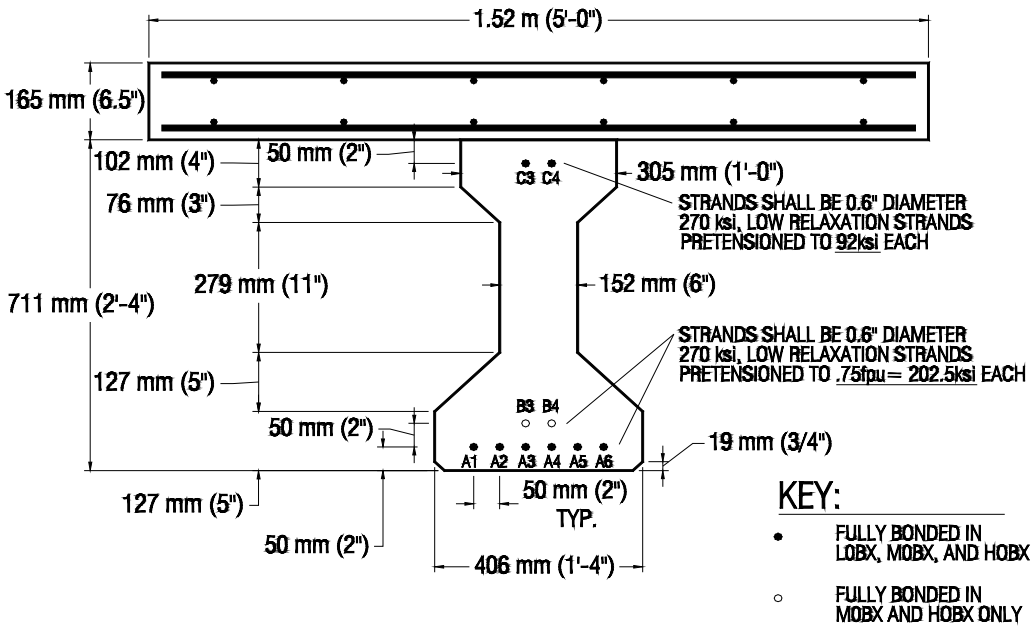

Figure 3.1- Sample Specimen Cross-Section fix drawing

This cross-section was developed through an iterative process, resulting in the optimum size concrete deck and the optimum number and location of prestressing strands. Furthermore, the design was based on the project proposal requirement that the bottom row(s) of prestressing strand reach an ultimate strain of 0.035, or 3.5%. Also, the design was required to contain a full bottom row of strands (6 strands). On top of the explicit requirements, it was desirable to produce a configuration of strands that could be debonded symmetrically in several configurations for later tests in the total test program, and to use cast-in-place concrete which would reach a reasonable strength in possibly less than 14 days, depending on the project schedule.

3.2.1.1 Flexural Design of Specimens

In order to begin the iterative flexural design process, estimates were made for the prestrain present in the strand [1.10 Gpa/197 Gpa ≈ 0.00561 mm/mm (160 ksi/28500 ksi ≈ 0.00561 in/in)] and for the slab concrete strength [37.9 MPa (5.5 ksi)]. The existence of prestrain reduced the required strain at ultimate to 0.0294. Therefore, using strain compatibility [nn], this new value of strain was used to calculate a minimum allowable neutral axis depth, c, for several deck thicknesses. Then, equilibrium equations were developed for several strand configurations, leaving both the neutral axis depth, c, and the width of the slab, b, as variables. It was assumed during these calculations in the design phase, that any slab steel would have very little effect on the ultimate moment or strand elongation. Also, it is important to note that according to typical TxDOT details, which were used to detail the mild reinforcement in the beams and are shown in Appendix I, extra longitudinal mild reinforcing #5 bars are placed in the top flanges of the beams. Therefore, this additional reinforcement was included in the equilibrium equations.

Before the strand configuration could be chosen for each pair of beams, however, it was necessary to determine the size concrete deck which would be used for all the test specimens. Consistency of the beam cross-sections was important for the testing program to ensure the comparability of the results. An approximate slab thickness of 165 mm (6.5 in) was chosen, and then, iterating with several deck widths, the number of strands and their arrangement was designed. After several iterations, it was apparent that the optimal solution was a slab width of 1.5 m (5 ft).

Next, the strand configurations and stresses for each pair of concrete beams was finalized. Since transfer stresses at the beam ends were critical and all strands were fully bonded to the end of the beam, it was necessary to put top strands some of the specimens. Also, the transfer stresses were extremely critical in the normal strength beams, so it was necessary to include a total of only six bottom strands, in contrast to the eight total bottom strands used in the other specimens. Only two extra strands were allowed into a second row of stands in the medium and high strength concrete specimens to minimize

the inconsistency between specimen cross-sections. Using more than two extra strands would not only require a changing the cross-section to a cast-in-place deck larger than 1.5 m (5 ft).

The total number of prestressing strands in the top and bottom flanges, as well as the determined value of prestress for each strand, is shown in Table 3.1.

Table 3.1- Prestressing Strand Design Stresses for Each Pair of Specimens

Pair of Specimens	**No. of Top Strands**	**Stress in Top Strands**	**No. of Bottom Strands**	**Stress in Bottom Strands**
L0BX	2	634 MPa (92 ksi)	6	.75*f_{pu} = 1.40 GPa (202.5 ksi)
M0BX	2	634 MPa (92 ksi)	8	.75*f_{pu} = 1.40 GPa (202.5 ksi)
H0BX	2	634 MPa (92 ksi)	8	.75*f_{pu} = 1.40 GPa (202.5 ksi)

As stated previously and shown in Figure 3.1, the cast-in-place concrete deck was designed to be 1.52 m (5 ft) wide and 165 mm (6.5 in) thick and the concrete strength was approximately 37.9 MPa (5.5 ksi). Although there were no strength requirements for the deck reinforcement, it was important to satisfy minimum reinforcement requirements and to represent a typical bridge deck reinforcement pattern. Therefore, the reinforcement pattern was designed to use #4 bars, maintain a 19 mm (3/4 in) clear cover, and locate the transverse bars closest to the concrete surface. The #4 bars were placed at 254 mm (10 in) and 305 mm (12 in) center-to-center in the transverse and longitudinal direction, respectively, with outside bars in both cases being placed at one-half the center-to-center distance (s/2) from the surface of the concrete.

3.2.1.2 Shear Design of Specimens

After the flexural design of the specimens was completed, the quantities of vertical and longitudinal shear reinforcement were determined. An approximate value for the shear strength of the beam was calculated. Then, using ACI requirements [17], the amount of vertical shear reinforcement was calculated and optimized according to the possible shear spans to be tested. This resulted in a placement of double #4 bars at 102 mm (4 in) for 2.2 m (7.33 ft) starting at 152 mm (6 in) from each end of the beam and single #4 bars at 102 mm (4 in) in the remainder of the beam, as shown in Figure 3.2. Also, additional vertical reinforcement was placed in the end regions of the beams according to TxDOT standard details shown in Appendix I. The additional vertical mild reinforcement helps to confine the concrete in the end regions of the beam and to arrest possible longitudinal end splitting cracks which might develop due to high stresses at transfer. See Appendix I for bar details.

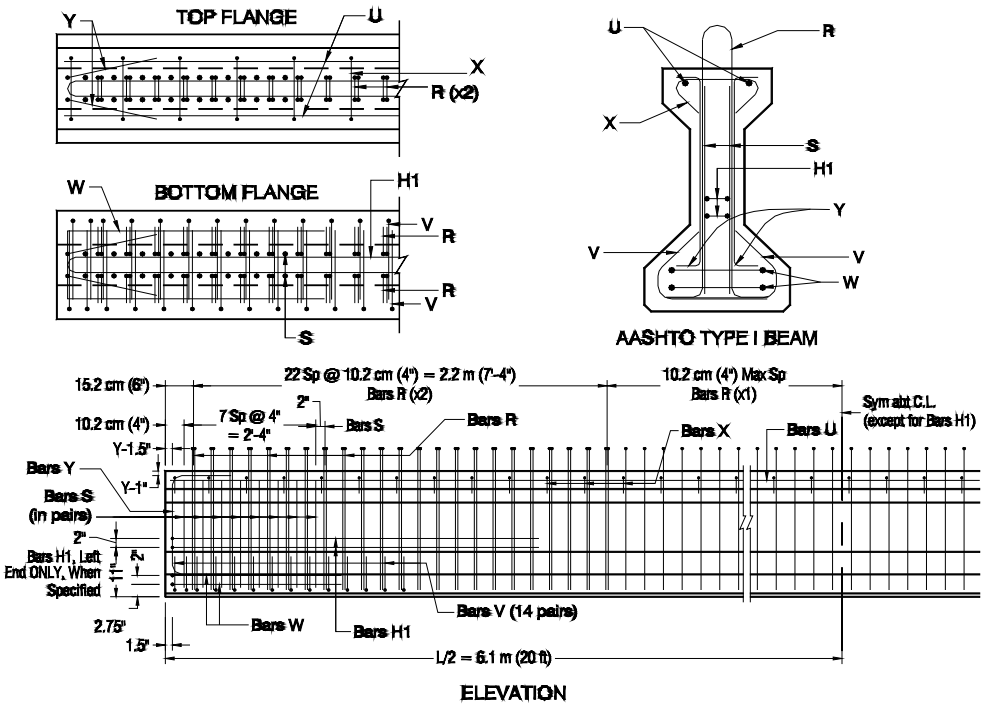

Figure 3.2- Mild Shear Reinforcement Details of Test Specimens

The longitudinal mild shear reinforcement (i.e. H-bars) was included at one end of one beam in each pair of beams. As shown in Figure 3.2, H-bars 19.8 m (6.5 ft) in length were placed in the web at approximately 279 mm (11 in) from the bottom of the beam. The length of these bars was based an approximated length for the transfer zone plus an additional conservative development length.

3.3 MATERIAL PROPERTIES

Material properties were determined by performing standard tests for each of the materials used. For the concrete in the beam and in the slab, modulus of elasticity [39] and cylinder strength tests [40] were performed according to ASTM standards, whereas tensile tests were performed on samples of the prestressing strand [41].

3.3.1 Concrete

3.3.1.1 Prestressed beams

The concrete mix designs for the three pairs of prestressed beams in the test program were developed at Texas Concrete in Victoria, Texas, and are described in detail in Tables 3.3, 3.4, and 3.5. The first pair of beams, designated as normal strength, was required to have a release strength (f'_{ci}) of approximately 27.6 MPa (4 ksi) and a 28-day strength (f'_c) of 34.5-48.3 MPa (5-7 ksi). The second pair of beams, designated as medium strength, was required to have a f'_{ci} = 48.3 MPa (7 ksi) and f'_c = 65.5-79.3 MPa (9.5-11.5 ksi). Finally, the third pair of beams, designated as high strength, was required to have a f'_{ci} = 65.5 MPa (9 ksi) and f'_c = 89.6-103.4 MPa (13-15 ksi). The f'_{ci} strength of the concrete was assumed to occur at 24 hours of age for the concrete.

Table 3.3- Mix Design for Normal Strength Concrete

Material	Quantity per 0.763m^3 (yd^3) of Concrete
Water	1.08 kN (242 lbs)
Cement (Type III)	2.35 kN (528 lbs)

Fly Ash	0.91 kN (205 lbs)
19.1mm (3/4 in) Coarse Aggregate	8.00 kN (1799 lbs)
Fine Aggregate	4.98 kN (1120 lbs)
Rheobuild 1000	?
Pozzolith 300R	?
Air-entrainment	5%

Table 3.4- Mix Design for Medium Strength Concrete

Material	Quantity per 0.763m^3 (yd^3) of Concrete
Water	0.90 kN (202 lbs)
Cement (Type III)	2.51 kN (564 lbs)
Fly Ash	0.72 kN (162 lbs)
19.1mm (3/4 in) Coarse Aggregate	8.89 kN (1999 lbs)
Fine Aggregate	5.13 kN (1153 lbs)
Rheobuild 1000	4.5 kg (160 oz)
Pozzolith 300R	0.48 kg (17 oz)
Air-entrainment	6.8%

Table 3.5- Mix Design for High Strength Concrete

Material	Quantity per 0.763m^3 (yd^3) of Concrete
Water	1.09 kN (246 lbs)
Type II Cement	2.98 kN (671 lbs)
Fly Ash	1.42 kN (319 lbs)
19.1mm (3/4 in) Coarse Aggregate	8.37 kN (1882 lbs)
Fine Aggregate	4.68 kN (1052 lbs)
Rheobuild 1000	5.6 kg (198 oz)
Pozzolith 300R	0.76 kg (27 oz)
Air-entrainment	4.9%

Cylinder breaks and modulus of elasticity tests were performed on predetermined dates with a special emphasis placed on days 1 (at transfer), 3, 7, 14, and 28, as well as

the days of development length testing. These tests on the beam concrete cylinders were performed using 102x203 mm (4x8 in) cylinders. The concrete strength versus time was then plotted in order to monitor the gain in strength of the concrete, so that the beams were tested within the desired range of strengths as indicated by the project proposal. The plots of the concrete strength curves are shown in Appendix C.

The average of the modulus of elasticity (E_c), or Young's modulus, tests performed on the cylinders cured in the field with each pair of beams (beam cured) and the cylinders cured at the same temperature as the beams (sure cured) are listed in Tables 3.6 and 3.7, respectively. The modulus of elasticity at release (E_{ci}) is also given in both tables.

The cylinder compressive strength and modulus of elasticity results from the beam cured cylinders are used for the comparison of transfer and development length results. However, the sure cure results are used in any calculations which require the exact properties of the specimen. For example, the sure cure results were used in the determination of the moment-curvature relationship. The sure cure results are also given for future reference, allowing for an accurate comparison of transfer and development length results on a future project, which also implements the sure cure system.

Table 3.6- Modulus of Elasticity Test Results for Beam Cured Cylinders

Pair of Beams	**Ave. E_{ci} (MPa)**	**Ave. E_{ci} (psi)**	**Ave. E_c (MPa)**	**Ave. E_c (psi)**
Normal Strength Concrete	32.2	4670	35.0	5080
Medium Strength Concrete	43.9	6370	46.3	6710
High Strength Concrete	51.7	7500	48.8	7080

Table 3.7- Modulus of Elasticity Test Results for Sure Cured Cylinders

Pair of Beams	**Ave. E_{ci}**	**Ave. E_{ci}**	**Ave. E_c**	**Ave. E_c**

	(MPa)	(psi)	(MPa)	(psi)
Normal Strength Concrete	32.2	4670	33.9	4910
Medium Strength Concrete	45.2	6550	45.4	6590
High Strength Concrete	52.7	7650	50.3	7300

3.3.1.2 Cast-in-place slabs

The concrete for the cast-in-place slabs was purchased from Capitol Aggregates in Austin, Texas, and had the mix design detailed in Table 3.8. This mix design was previously used on TxDOT Project 589 [42] to achieve a 28-day design strength of approximately 41.4 MPa (6 ksi).

Table 3.8- Mix Design for Cast-in-Place Slabs

Material	Quantity per 0.763m^3 (yd^3) of Concrete
Water	1.1 kN (250 lbs)
Cement (Type II)	2.3 kN (517 lbs)
19.1mm (3/4 in) Coarse Aggregate	8.3 kN (1869 lbs)
Fine Aggregate	6.0 kN (1355 lbs)
Admixture (Retarder)	586.8g (20.7 oz)

Cylinder breaks and modulus of elasticity (E_c) tests were also performed on the slab concrete on days 3, 7, 14, 28, and of development length testing. As appropriate, cylinder tests were performed on day 1 to determine whether or not the deck had adequate strength to enable the removal of the deck forms. The cast-in-place slab concrete strength curves are in Appendix C and the results from the modulus of elasticity tests are shown in Table 3.9.

Table 3.9- Modulus of Elasticity Test Results for Cast-in-Place Slabs

Slab I.D.	Average E_c (MPa)	Average E_c (psi)
L0B0	32.3	4684
L0B1	32.9	4767
M0B0	36.1	5232
M0B1	33.8	4897
H0B0	36.4	5279
H0B1	35.1	5093
Average of All Slabs	**34.4**	**4992**

3.3.2 Steel

The prestensioning steel reinforcement used in the test specimens was manufactured by Shinko Wire America, Inc., and was shipped to Texas Concrete Company in large coils of 15.2 mm (0.6 in) diameter, Grade 270, low-relaxation, seven-wire strand. This 15.2 mm (0.6 in) diameter strand has a nominal area of 140 mm^2 (0.217 in^2) and a modulus of elasticity of approximately 196 GPa (28,500 ksi). In order to determine properties specific to the particular coil of pretensioning strand used in the test specimens, tensile tests were performed on samples from the coils [41]. The results from these tests are summarized in Table 3.10, and the stress-strain plots for each test can be found in Appendix C.

It should be noted that the first strand test for the H0BX beams was omitted from Table 3.10 due to erroneous data. Also, the first strand test for the L0BX and M0BX beams was not fractured; therefore, no data appears in the corresponding columns. In order to utilize the stress-strain relationship for the prestressing strand in calculations, the modified Ramberg-Osgood equation [43] to derive an equation to fit the data. These derived curves are plotted along with the data in Appendix C.

Table 3.10- Tensile Test Results for 15.2 mm (0.6 in) Diameter Prestressing Strand

Beam I.D.	Strand Test No.	Load @ 1% kN *(kips)*	Stress @ 1% kN *(ksi)*	Ultimate Load kN *(kips)*	Ultimate Stress Gpa *(ksi)*	Ultimate Strain mm/mm or *in/in*
L0BX, M0BX	1	241 *(54.3)*	1.72 *(250)*	----	----	----
L0BX, M0BX	2	242 *(54.5)*	1.73 *(251)*	265 *(59.5)*	1.89 *(274)*	0.0946
H0BX	2	241 *(54.3)*	1.72 *(250)*	265 *(59.6)*	1.90 *(275)*	0.0968

The strand had a bright, or "mill finish," surface condition. The brightness of the strand was protected by storing the coils in a sheltered environment in between casting dates. The protection of the strand was important to ensure the uniformity of the brightness of the strand in all the test specimens and to clearly differentiate the strands in these specimens from specimens which will have a "rusty," or "weathered," surface condition. Specimens with the "rusted" strand will be tested later in the research program. The protection of the brightness of the strand surface was also important in order to ensure that the "worst case" scenario for bond is properly investigated.

All the mild reinforcing steel used in the beam and in the slab was Grade 60 steel.

3.4 BEAM FABRICATION

The beams were fabricated at Texas Concrete in Victoria, Texas, on July 1, 1996, July 5, 1996, and October 2, 1996. First, the strands were aligned along the prestressing bed using plywood boards which were cut to the shape of the beam cross-section with holes occurring on a 50 mm (2 in) grid spacing at possible strand locations, as shown in Figure 3.3. Since the prestressing bed was approximately 40 m (130 ft) long and the 12.2 m (40 ft) beams would be brought to the lab and tested in pairs, it was desirable to cast two beams at a time. Therefore, with the prestressing strand running the entire length of

the bed, the plywood boards used to align the strands served as end forms for two beams, with one board placed at each end of each beam.

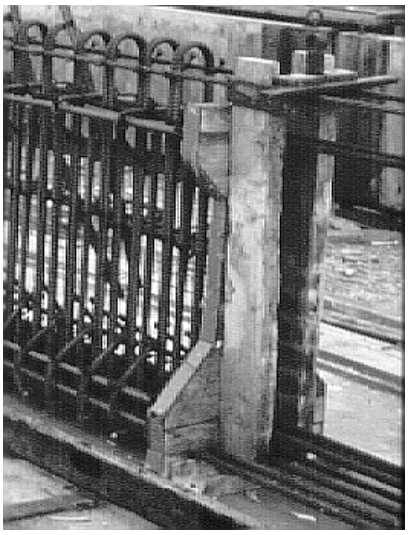

Figure 3.3- Plywood End Forms Serve as Strand Placement Guide

Next, the strands were tensioned according to the designed amounts shown in Table 3.1. Since the large bulkhead, used by Texas Concrete for some pretensioning applications, was not accessible by the prestressing bed, it was not possible to tension the strands simultaneously. Therefore, each strand was tensioned separately using a calibrated hydraulic ram. After a strand was tensioned it was anchored using one-way chucks, as demonstrated in Figure 3.4. Also visible in Figure 3.4 are the two extra strands that were tensioned above the top of the beam to enable easier placement of shear reinforcement.

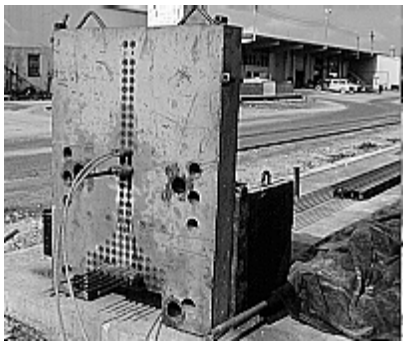

Figure 3.4- Strand Anchorage after Tensioning

After the strands were tensioned, the vertical mild steel shear reinforcement was placed according to the details shown in Figure 3.2 and pictured in Figure 3.5. The placement of H-bars is also visible in Figure 3.5, which only occurs at one end of one beam in each pair.

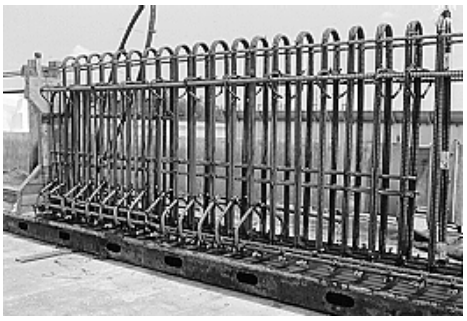

Figure 3.5- Shear reinforcement in the End Region of the Beam

After the shear reinforcement was placed, some internal strain gauges installed on short pieces of reinforcement were placed at the center of gravity of the prestressing strand. These internal strain gauges were anchored to the vertical shear reinforcement, as shown in Figure 3.6, and were used to confirm estimated losses which occur in the prestressing strand over time.

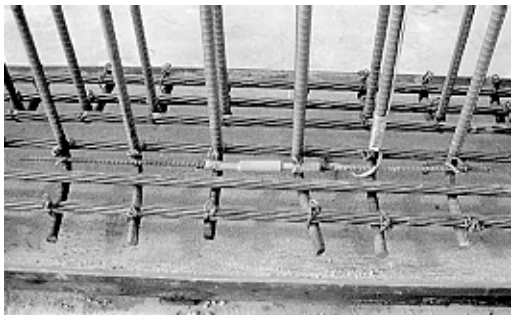

Figure 3.6- Placement of Internal Strain Gauges

Before the steel side forms could be placed, the dust was removed from the forms using compressed air. Then, the forms were lubricated with oil, as shown in Figure 3.7, being careful not to oil the reinforcing steel. Once the forms had been oiled, the steel side forms for the exterior of the concrete beams were placed and anchored, as shown in Figures 3.8 and 3.9, respectively.

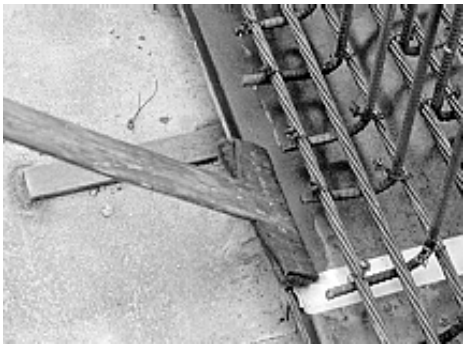

Figure 3.7- Oiling of the Bottom Form

Figure 3.8- Placement of the Steel Side Forms

Figure 3.9- Anchoring of the Steel Side Forms

After the steel forms were firmly in place, the concrete was placed, finished, and covered to allow for proper curing of the concrete. The concrete placement can be seen in Figure 3.10 and the covered beams can be seen in Figure 3.11.

Figure 3.10- Concrete Placement

Figure 3.11- Curing of Concrete Beams

The next day, after the beam had reached sufficient strength according to the f'_{ci} previously discussed in Section 3.3.1.1, the beams were uncovered and the forms were removed. The concrete beams were then ready to be instrumented to obtain transfer length data, which will be discussed in Chapter 4.

3.5 RELEASE OF PRESTRESS

After the beams were instrumented and the first set of measurements was taken, as described in Chapter Four, the prestress in the strands was released. As shown in Figure 3.12, flame-cutting was used to release the prestressing force. When strands are flame-cut, normal practice is to cut the strands at one end, the live end, and then, after the prestressing force has been released, the strands are cut at the other end, the dead end. However, for this project an attempt was made to gain consistent transfer lengths at both ends of each beam by simultaneously cutting the strands at three locations: at both ends of the prestressing bed and in between the two beams. Due to human error, however, the strands were not cut at *exactly* the same time in the three locations. Therefore, the transfer lengths vary from end to end as seen in Chapter Four.

Figure 3.12- Release of Prestress by Flame-Cutting

After the strands were cut, measurements were taken again according to Chapter Four. Once all the measurements had been completed, the beams were transported to another location at Texas Concrete to await transportation to Ferguson Laboratory.

3.6 PREPARATION AND PLACING OF THE CONCRETE DECK

The beams were transported to Ferguson Laboratory at J. J. Pickle Research Campus in Austin, TX, from Victoria, TX, to undergo the second stage of testing. In order to perform the development testing, however, it was necessary to first complete the

designed cross-section, by casting a concrete deck which would act composite with the concrete beam. The deck details can be found in Section 3.2.2 and 3.3.1.2 and development length testing is discussed in Chapter Five.

3.6.1 Preparation for the Concrete Deck

Due to space requirements in the lab and the extensive formwork system, it was only possible to cast one concrete deck at a time. The deck forms were plywood and the formwork supports, bracing, and guardrails were a combination of wood 51 x 102 mm (2 x 4 in) and 102 x 102 mm (4 x 4 in) pieces [for actual dimensions of wood members subtract 12.7 mm (½ in) from the nominal dimension].

The deck preparation process is best described by a list of events, which is supplemented by pictures. Therefore, a list of the preparation steps is followed by some photographs:

1. Formwork supports were placed
2. Deck forms were placed and leveled on the supports
3. Deck forms bolted together on each side of the beam
4. Steel strapping used to secure each side of the deck forms together
5. Deck forms were cleaned and joints sealed with silicon
6. Deck forms oiled to prevent the absorption of water from the concrete
7. Steel reinforcement cage placed and tied one layer at a time
8. Formwork supports braced
9. Guardrails placed
10. Concrete beam shored

Figure 3.13 shows the result of Steps 1-3. Figure 3.14 shows the results of Steps 4-7. Figure 3.15 shows how the beam was shored.

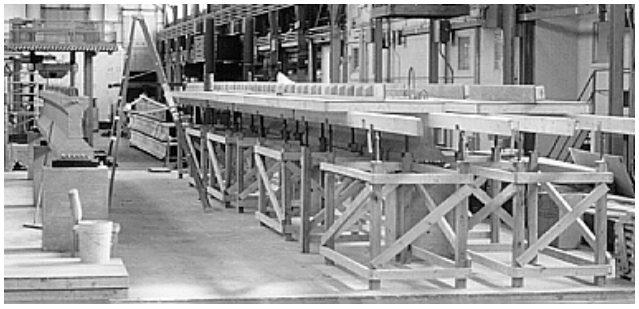

Figure 3.13- Placement of Deck Forms

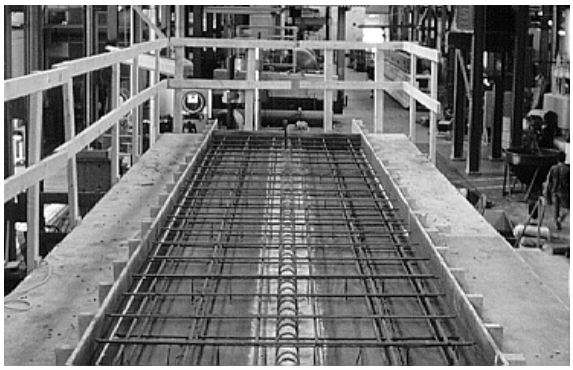

Figure 3.14- Placement of Steel Cage

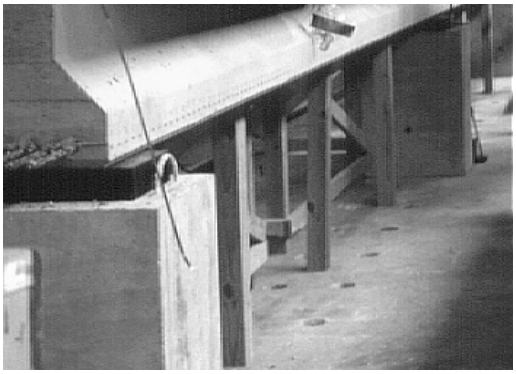

Figure 3.16- Placement of Shores

3.6.2 Placing of the Concrete Deck

Once the concrete beam was shored, the concrete deck could be placed. As discussed in Section 3.3.1.2, the concrete for the deck was ordered from Capitol Aggregates to arrive on the scheduled casting day. The concrete truck was brought into the lab and a slump test was performed. If the slump was not between 89 and 140 mm (3.5 and 5.5 inches), water was added to the concrete in the truck. Then, the slump was tested again, and if correct, the concrete was placed.

The concrete was carried up to the slab by means of a concrete bucket and the overhead crane in the lab, as shown in Figure 3.17. The concrete was then placed, spread, and vibrated, as shown in Figure 3.17. Next, the concrete surface was leveled and pushed forward using a wood 2 x 4 as a screed, also shown in Figure 3.17. Once all the concrete was placed, the surface was bull-floated (Figure 3.18) and finished with trowels (Figure 3.19). This created a relatively smooth surface, facilitating the surface preparation to be performed later for mounting the concrete surface strain gauges used during testing. Finally, when the concrete surface was dry enough, the slab was covered with plastic to allow the concrete to cure properly.

Figure 3.17- Transportation, Placement, and Vibration, and Screeding of Concrete

Figure 3.18- Bull-floating of Concrete Deck

Figure 3.19- Finishing of Concrete Surface

As discussed in Section 3.3.1.2, concrete cylinders were made at the same time as the each concrete deck and were covered at the same time as the deck, to simulate similar curing conditions. Once the concrete deck had reached a sufficient compressive strength, the forms were stripped and the process was repeated for the concrete deck of the second beam of the pair.

CHAPTER FOUR

TRANSFER LENGTH TESTING

4.1 INTRODUCTION

After the concrete beams were cast in Victoria as described in Chapter Three, the beams were instrumented to obtain transfer length data. This includes instrumentation to read both the surface strains at the center of gravity of the bottom strands and the strand pull-in at release. The instrumentation was used to take readings both on the day of the release of the prestress and at a later date after the placement of the concrete deck, which allowed the observation of possible long term effects on the transfer length. This chapter describes the preparation for and execution of this transfer length testing, as well as the test results.

4.2 TRANSFER LENGTH INSTRUMENTATION AND MEASUREMENTS

In this section, the different types of measurements, and related instrumentation, for transfer length will be discussed. These measurements include the concrete surface strains and draw-in of the strands to determine the transfer length, and internal strains to determine prestress losses.

4.2.1 The DEMEC Mechanical Strain Gauge System

The DEMEC Mechanical Strain Gauge System was chosen for the measurement of transfer length because several projects at Ferguson Laboratory in Austin, TX, have shown it to be a reliable and reasonably accurate method [6,16,28,33,42,44], with an accuracy of ±25 microstrains [6].

4.2.1.1 Instrumentation

Transfer length was measured using a device called a DEMEC gauge, which had a gauge length of approximately 200 mm (7.87 in), and precisely machined metal discs, 6.3 mm (0.25 in) in diameter, with a hole made especially for the DEMEC gauge. As

shown in Figure 4.1 and Figure 4.2, the metal discs were placed every 50 mm (1.97 in), starting at 25 mm (1 in), for approximately 1.8m (5.8 ft), 1.4m (4.5ft) for the M0BX pair of beams, on each side of each end of each beam. Furthermore, the discs were set on the surface of the concrete along the projected center of gravity of the bottom pretensioning strands with a fast setting two-part epoxy, as shown in Figure 4.2.

The first four discs of each group of points were placed on marks made at a ruler measurement. The remaining DEMEC points, however, were placed by measuring the distance and setting the points with a standard placement bar that was supplied by the gauge manufacturer. This ensured that all points were consistently approximately 200 mm (7.87 in) apart. In order to further ensure a consistent distance between DEMEC points, the points were set in groups of four, only after the epoxy at the previous four points had sufficiently hardened.

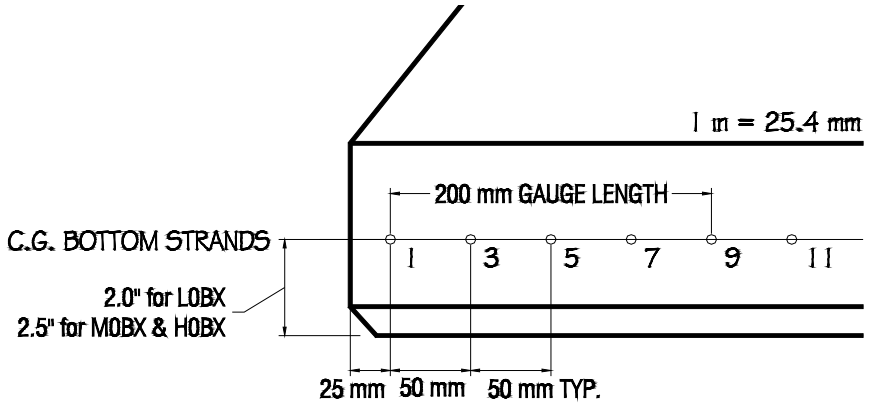

Figure 4.1- Diagram of DEMEC Point Locations

Figure 4.2- Demec Points Placed Along One Side of One End of One Beam

4.2.1.2 Measurements

After the epoxy at all the points had sufficiently set, and prior to the release of the prestress in the strands, the first set of readings was taken with the DEMEC gauge. As shown in Figure 4.3, readings were taken between each set of points approximately 200 mm (7.87 in) apart, moving progressively from the first point at the end of the beam to the next points mounted as shown in Figure 4.2 until all intervals had a measurement.

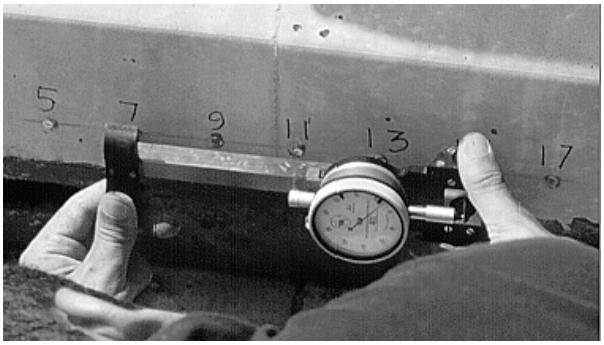

Figure 4.3- Measurements with DEMEC Gauge

For each set of points, two readings were taken, which were required to be no more than 2 tick marks apart, to assure the accuracy of the measurement. Each tick mark was equivalent to a distance of 0.002 mm (0.051 in), or approximately 16 microstrains.

Once the prestress in the strands was released, the distance between each set of DEMEC points was read again, in the same manner, by the same person. The difference of the distance between the points was calculated as the second set of readings was performed. If the second set of readings did not seem to correspond with the trend of the previous readings in the transfer zone, or along the plateau, then the set of points was read again. Sometimes, however, the values on the plateau did not follow a trend because of shrinkage cracks.

All of the values were recorded on data sheets and later put into a spreadsheet which converted the readings to values of strain. Each gauge had a unique gauge factor which was used in that conversion. The method of data reduction is discussed in Section 4.3.

4.2.2 Draw-in Instrumentation and Measurements

The first attempt at draw-in measurements was a system successfully used for the transfer length testing in TxDOT Project 589 [42]. The L0BX beams were instrumented with clamps, and the distance from the clamp to the face of the beam was recorded before and after the release of the prestressing force. This was accomplished using a micrometer with an accuracy of 0.001 mm (0.0004 in).

However, since the stress in the strands in the beams for Project 589 was released slowly, no damage to the location of the draw-in devices was encountered. In this project, though, the strands were flame-cut, which disrupted the draw-in devices, causing them to rotate from their original location. Since the distance to the face of the concrete was no longer being measured from the same location, the draw-in measurements were rendered invalid. This measurement system and the rotation of the draw-in devices can be seen in Figure 4.4.

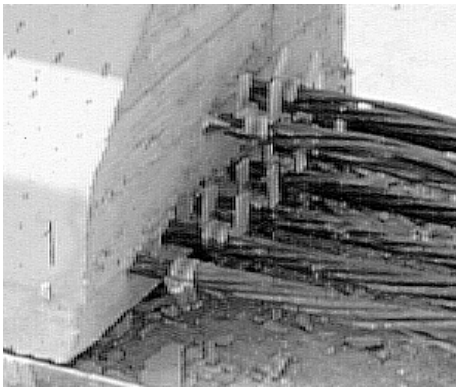

Figure 4.4- Draw-in Devices

For the M0BX pair of beams, a modification was made to the system to attempt to prevent the jarring of the devices from the cutting of the strands. This modification was the placement of an additional clamp around the strand at a location closer to the location of the cutting of the strands. Although the extra clamp did help tame the behavior of the strands to some degree, most of the draw-in devices were still jarred from their original positions.

Lastly, for the H0BX pair of beams, the draw-in devices were not used at all. A new system was attempted, using electrical tape wrapped around the strand near the end of the beam and a clamp wrapped around the strand near the cutting location, as shown in Figure 4.5. A mark was made on the electrical tape with a paint pen. Then, a steel ruler was lined up with the mark, and the distance to the face of the concrete was measured to the nearest 0.254 mm (0.01 in) both before and after the release of the prestress. This measurement technique proved to be more effective than the previous method, but problems were still encountered. It seems that the electrical tape did not bond sufficiently to the strands in certain cases, and therefore, was slightly altered from its original position when the strands were cut.

Figure 4.5- Draw-in Measurements Using Tape System

The draw-in measurement system received one final alteration, which was and will be implemented on the rest of the beams in the research program. Instead of relying on the position of the tape for the measurement location, tape was placed around the strand and the strand was spray painted. The tape was then removed, and a straight line existed on the strand, which would not be altered by the twisting of the strands. Alignment marks for the ruler were then made directly on the strand, and measurements made before and after release with a steel ruler.

4.2.3 Internal Strain Gauges

Internal strain gauges were placed in each beam to observe prestress losses over time. The gauges were bonded to pieces of reinforcing steel with a small diameter. These pieces of steel were then tied to the vertical reinforcement cage at the center of gravity of the top and bottom strands at several locations in the beam. An example of an internal strain gauge was shown in Chapter Three in Figure 3.6.

Measurements were taken before and after release of the prestressing force, and at several other key times before development length testing of the specimen.

4.3 REDUCTION OF TRANSFER DATA

DEMEC readings were taken on every face of every end of every beam in order to obtain the most accurate strain profile for each beam end. Also, by averaging the measurements on both faces, it was possible to reduce the effects on the transfer length due to temperature which caused the some of the beams to bend. or bow, out-of-line.

Before the measurements from the two sides were averaged, however, it was necessary to smooth the data from one face. This process is diagrammed in Figure 4.5. First, the two readings taken from one set of DEMEC points was averaged for both the initial and final readings. Then, the difference between the two averages was multiplied by the applicable gauge factor to produce a differential strain. Since this differential strain is merely an average strain over the measured distance, the differential strain was assigned to the midpoint of the distance between the points (See Step 1 in Figure 4.5). This assignment also served to simplify calculations. Once the differential strains had been calculated and assigned to their respective points, the variability in the data was reduced by a technique called "smoothing," as diagrammed by Step 2 in Figure 4.5 and illustrated by Figure 4.6. Smoothing is performed by averaging a number of data points in an overlapping manner. For this project, the results over three gauge lengths are averaged by use of the following equation [6]:

$$Strain_i = \frac{Strain_{i-1} + Strain_i + Strain_{i+1}}{3} \qquad (4)$$

Therefore, as a result of this smoothing technique, even though the first DEMEC point is the first data point is only 25 mm (1 in) from the beam end, the first data point occurs at 175 mm (6.91 in) from the beam end.

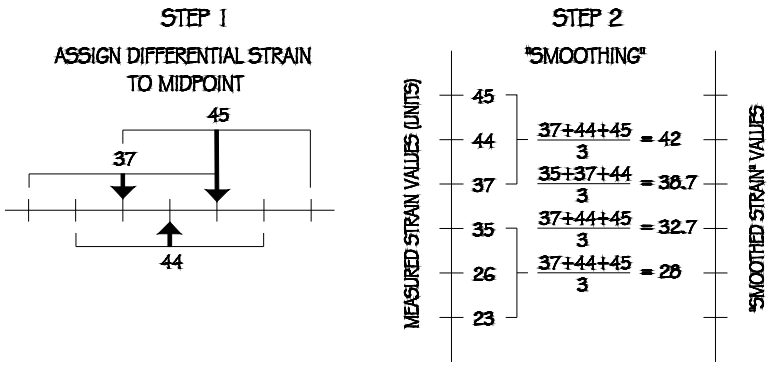

Figure 4.5- Diagram of Smoothing Technique [6]

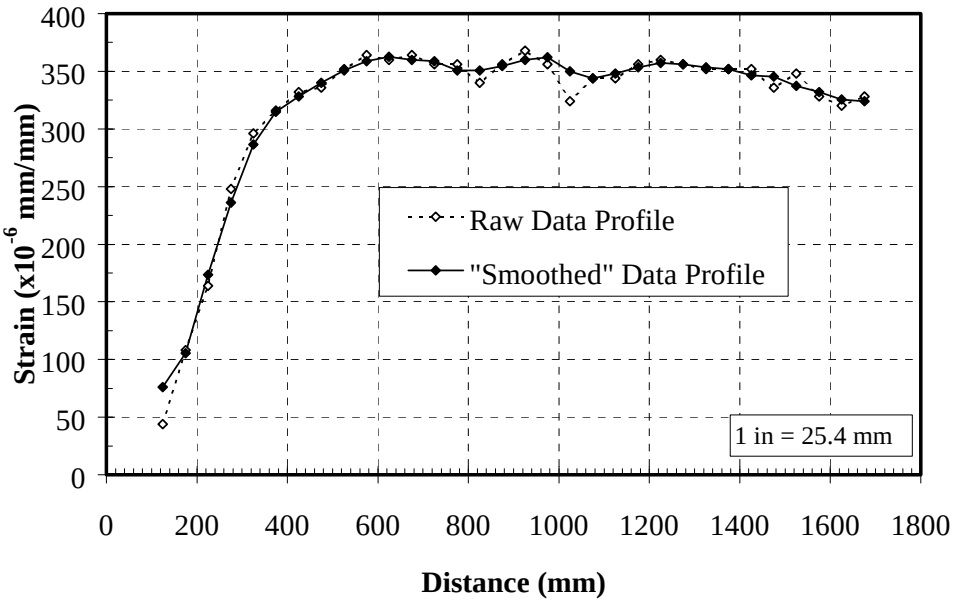

Figure 4.6- Effect of the Smoothing Technique on a Typical Strain Profile

Once the data from each face had been properly smoothed, the data at corresponding points from both faces of one end were averaged to obtain the strain profiles located in Appendix D. This process was performed on the data recorded to

produce strain profiles corresponding to “after release of the prestress” and “after the placement of the concrete deck.”

4.4 DETERMINATION OF TRANSFER LENGTH

The transfer length results recorded in the literature must be carefully considered because there are several methods of calculating the transfer length. Methods which have been used are the 100% Average Maximum Strain [23,28], 95% Average Maximum Strain [6,26], Slope-Intercept [27,29], and Draw-in and Initial Prestress [6,33]. The transfer lengths for this study were calculated using the latter1 three methods. However, reliable results were not obtained by the Draw-in and Initial Prestress Method because of the problems encountered with the instrumentation, as described in Section 4.2.2.

4.4.1 95% Average Maximum Strain Method

4.4.1.1 Definition of the Method

The *95% Average Maximum Strain Method* defines the transfer length as the intersection of the smoothed strain profile with a line corresponding to 95% of the average maximum strain.

4.4.1.2 Discussion of the Method

As discussed by Buckner [36], the 95% Average Maximum Strain Method provides reasonable compensation for various effects on the transfer length, including shear lag and beam weight. Therefore, it appears that this method, while not exact, gives at least a conservative value for the transfer length.

4.4.1.3 Execution of the Method

From the smoothed strain profile, the points on the strain plateau, corresponding to the fully effective prestress, are determined and used to calculate an average maximum value of strain. Since the strain profile is not exactly bilinear, due to effects mentioned in Section 4.4.1.2, points near the beginning and the end of the plateau are eliminated from

this average. Figure 4.7 shows an example of a transfer length determined by this method.

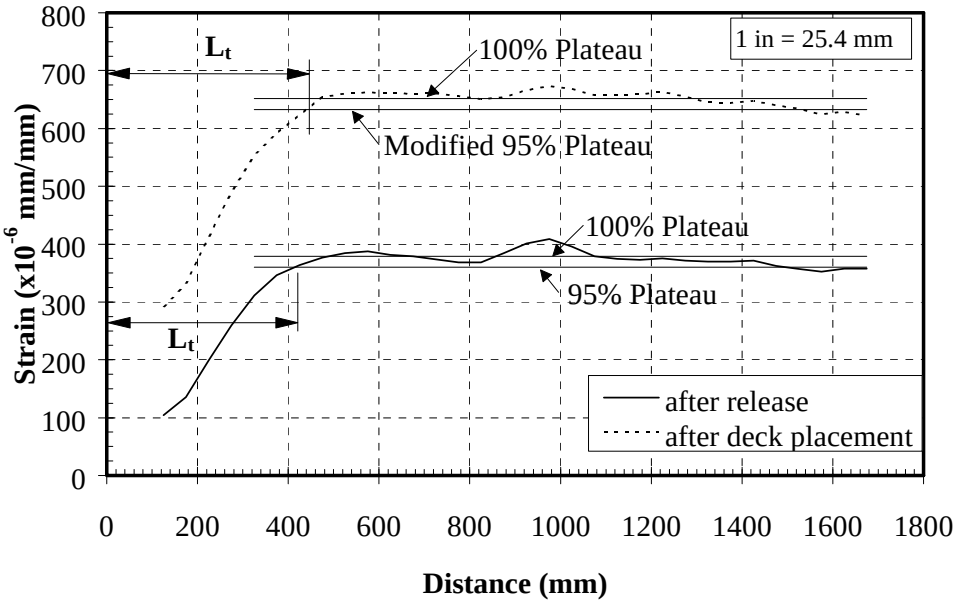

Figure 4.7- Transfer Length Based on the 95% Ave. Max. Strain Method

4.4.1.4 Alteration of the Method for Long-Term Effects

The effects on the transfer length over time are due primarily to an increase in strains due to creep and shrinkage. Therefore, the entire strain profile is raised, with the rate of change of the strain increasing through the transfer zone until the difference in strain levels off at a higher strain value along the strain plateau. This effect can be seen in Figure 4.7.

Since 95% of a higher value yields a larger number, the transfer length based on 95% of the average maximum strain after release can not be compared to a transfer length calculated from 95% of the long-term (after deck placement) average maximum strain.

Therefore, the 95% Average Maximum Strain Method was slightly altered for long-term transfer length calculations to fix the bias due to a higher strain plateau.

First, the difference between the value of the 100% plateau and the 95% plateau of the "after release" strain profile is calculated. Then, this value is subtracted from the value of the 100% Plateau of the long-term profile. A line is draw corresponding to the new value. The location where this new "95%" line intersects the long-term strain profile is the recorded value for transfer length, as shown in Figure 4.7.

4.4.2 Slope-Intercept Method

4.4.2.1 Definition of the Method

The *Slope-Intercept Method* defines the transfer length as the intersection of the estimated slope of the strain profile in the transfer zone with a line corresponding to the value of the average maximum strain.

4.4.2.2 Discussion of the Method

This method is even less certain than the 95% Average Maximum Strain Method because an additional subjective judgment is introduced into the determination of the transfer length. That is, in order to determine the slope of the strain profile in the transfer zone, the number of points to be included must be determined. It is believed that as more strain values are included from the beam end, the transfer length can increase by approximately 10%.

Therefore, the Slope-Intercept Method is not used independently. It is used for comparison with the transfer length values determined from the 95% Method and for comparison with the literature which used the Slope-Intercept Method to determine transfer length. Also, the Slope-Intercept Method is used to verify the apparent trends related to transfer length found with the 95% Method.

4.4.2.3 Execution of Method

Execution of the slope-intercept method also begins with the smoothed strain profile. Then, a line corresponding to the value of the average maximum strain and the apparent slope of the curve in the transfer zone are drawn. The place of intersection is the recorded transfer length, as illustrated in Figure 4.8.

As previously discussed, the strain profile is not exactly bilinear. Therefore, in the determination of the slope, the points located in the region where the profile starts to curve over and upward towards the strain plateau must be eliminated from both the calculation of the average maximum strain and the slope of the varying strain region.

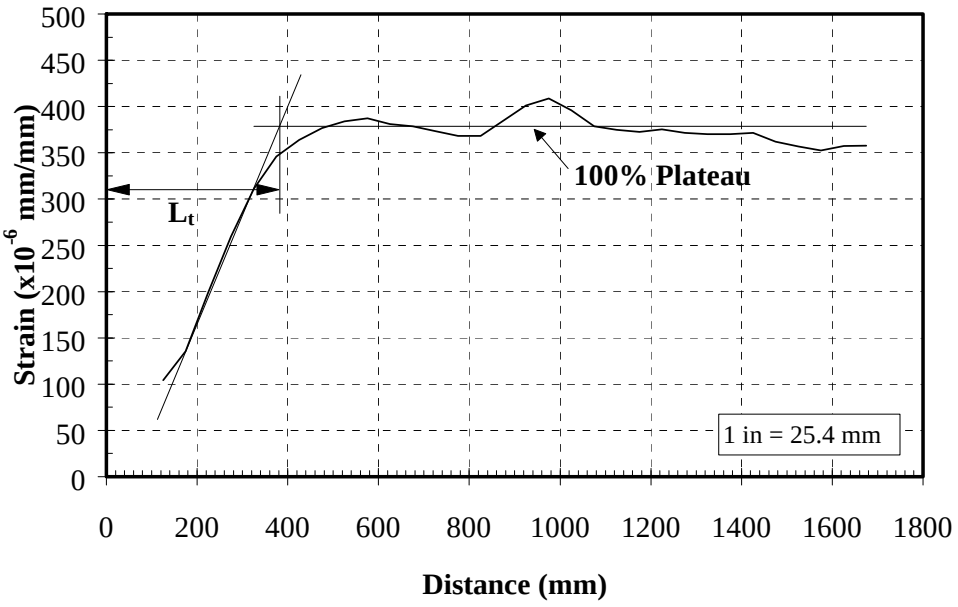

Figure 4.8- Transfer Length Determined by the Slope-Intercept Method

4.4.3 Draw-in and Initial Prestress Method

The transfer length can also be determined using the measured draw-in distance of the strands and the initial prestress (f_{si}) in the strands. The draw-in distance of the

strands must first be corrected, however, by subtracting the contribution to the draw-in distance by elastic shortening. Elastic shortening (ES) can be determined by using Equation 5. Then, using the corrected draw-in distance, per Equation 6, the transfer length can be calculated by Equation 7 [34]:

$$ES = \frac{(f_{si})(Free\ Length)}{E_{ps}} \qquad (5)$$

$$Draw-in = (Measured\ Draw-in) - ES \qquad (6)$$

$$L_t = \frac{\alpha(Draw-in)}{\varepsilon_{si}} \qquad (7)$$

The α in Equation 6 is a constant based on the shape of the bond stress distribution present in the transfer zone. The constant α is equal to 2 when the bond stress distribution is constant, resulting in a perfectly linear strain profile in the transfer zone, and $\alpha = 3$ when the bond stresses are linear, resulting in a parabolic strain profile. Polish researchers, however, found through transfer length testing that the strain profiles in the transfer zone were somewhere in between linear and parabolic, with $\alpha = 2.86$ [45] and $\alpha = 2.46$ [46].

4.4 TRANSFER LENGTH TEST RESULTS

4.4.1- Results from 95% Plateau and Slope-Intercept Methods

The transfer length test results are summarized in Table 4.1 and the actual strain profiles for each beam end are presented in Appendix D. For the sake of clarity, only the transfer length corresponding to the 95% Plateau Method is shown on the plots in Appendix D. The results given in Table 4.1 will be discussed and compared with current code equations and previous research results in Chapter Seven.

Table 4.1- Transfer Length Results

			95% Method		Slope-Intercept Method	
Beam End	f'_{ci} **MPa (psi)**	f'_c **MPa (psi)**	**After Release**	**After Deck Placement**	**After Release**	**After Deck Placement**
L0B0A-1	29.2	45.0	540 mm	680 mm	485 mm	560 mm
L0B0B-2	29.2	45.0	475 mm	640 mm	475 mm	540 mm
L0B1A-3	29.2	45.0	515 mm	660 mm	525 mm	580 mm
L0B1B-4	29.2	45.0	455 mm	715 mm	385 mm	500 mm
Mean	***29.2 (4240)***	***45.0 (6520)***	***496 mm (19.5 in)***	***674 mm (26.5 in)***	***468 mm (18.4 in)***	***545 mm (21.5 in)***
M0B0A-1	45.6	74.0	490 mm	610 mm	425 mm	480 mm
M0B0B-2	45.6	74.0	545 mm*	605 mm*	570 mm*	605 mm*
M0B1A-3	45.6	74.0	515 mm	520 mm	460 mm	470 mm
M0B1B-4	45.6	74.0	480 mm	505 mm	480 mm	520 mm
Mean	***45.6 (6610)***	***74.0 (10730)***	***495 mm (19.5 in)***	***545 mm (21.5 in)***	***455 mm (17.9 in)***	***490 mm (19.3 in)***
H0B0A-1	76.2	87.8	435 mm	425 mm	380 mm	415 mm
H0B0B-2	76.2	87.8	415 mm	440 mm	385 mm	390 mm
H0B1A-3	76.2	87.8	450 mm	455 mm	415 mm	455 mm
H0B1B-4	76.2	87.8	405 mm	480 mm*	365 mm	390 mm*
Mean	***76.2 (11,060)***	***87.8 (12,730)***	***426 mm (16.8 in)***	***440 mm (17.3 in)***	***386 mm (15.2 in)***	***420 mm (16.5 in)***

Notes: (*) indicates the number was eliminated from the mean calculation because the transfer length was based on data from only one face of the beam.

1 in =25.4 mm

1 psi = 6894.8 Pa

4.4.2 Results from the Draw-in and Initial Prestress Method

The draw-in data for the L0BX, M0BX, and H0BX beams is not very reliable due to problems with the methods used to obtain measurements. Therefore, the results of the calculated transfer length based on draw-in and initial prestress are very limited. The measured end slips are shown in bar charts in Appendix E, and the transfer lengths based on the retrievable data are given in Table 4.2 and 4.3.

As apparent by the strain profiles presented in Appendix D, the strain profile in the transfer zone for the tests in this test series was neither completely linear ($\alpha = 2$), nor completely parabolic ($\alpha = 3$). For this reason, Table 4.2 presents the transfer length calculations for both extreme cases. Then, in the last column of Table 4.2, the experimentally determined value for α is presented, using the transfer length data presented in Table 4.1

Table 4.2- End Slip Test Results at Release

Beam End	**Measured End Slip**	**Actual End Slip (Eq. 6)**	**L_t (Eq. 7, α=2)**	**L_t (Eq. 7, α=3)**	**Calculated α**
L0B0A-1	1.70 mm	1.27 mm	358 mm	310 mm	3.01
L0B0B-2	2.11 mm	1.65 mm	467 mm	546 mm	2.04
L0B1A-3	----	----	----	----	----
L0B1B-4	1.63 mm	1.17 mm	328 mm	490 mm	2.77
Mean	***1.80 mm (0.071 in)***	***1.37 mm (0.054 in)***	***384 mm (15.1 in)***	***526 mm (20.7 in)***	***2.61***
M0B0A-1	2.01 mm	1.73 mm	485 mm	729 mm	2.02
M0B0B-2	2.72 mm	2.41 mm	678 mm	1016 mm	1.61*
M0B1A-3	2.24 mm	2.01 mm	566 mm	851 mm	1.81
M0B1B-4	2.39 mm	2.03 mm	572 mm	859 mm	1.68
Mean	***2.34 mm (0.092 in)***	***2.05 mm (0.081 in)***	***575 mm (22.6 in)***	***864 mm (34.0 in)***	***1.84***
H0B0A-1	1.12 mm	0.94 mm	264 mm	404 mm	3.31
H0B0B-2	1.58 mm	1.37 mm	389 mm	584 mm	2.14
H0B1A-3	1.02 mm	0.81 mm	226 mm	340 mm	3.97
H0B1B-4	0.71 mm	0.56 mm	160 mm	239 mm	5.07
Mean	***1.12 mm (0.044 in)***	***0.91 mm (0.036 in)***	***259 mm (10.2 in)***	***392 mm (15.4 in)***	***3.62***

Notes: (*) indicates the number was eliminated from the mean calculation because the transfer length was based on data from only one face of the beam.

ε_{si} = 0.007232 (L0BX, M0BX), 0.007105 (H0BX)
1 in =25.4 mm

Table 4.3- End Slip Test Results after Deck Placement

Beam End	**Measured End Slip**	**Actual End Slip (Eq. 6)**	**ε_s**	**L_t (Eq. 7, α=2)**	**L_t (Eq. 7, α=3)**	**α**
M0B0A-1	2.49 mm (0.098) in	2.21 mm (0.087 in)	0.006333	706 mm (27.8 in)	1063 mm (41.8 in)	1.73
M0B0B-2	2.92 mm (0.115 in)	2.59 mm (0.102 in)	0.006333	820 mm (32.3 in)	1230 mm (48.4 in)	1.48*
M0B1A-3	2.65 mm (0.104 in)	2.44 mm (0.096 in)	0.006333	767 mm (30.2 in)	1150 mm (45.3 in)	1.36
M0B1B-4	2.59 mm (0.102 in)	2.26 mm (0.089 in)	0.006333	712 mm (28.0 in)	1068 mm (42.0 in)	1.42
Mean	***2.66 mm (0.105 in)***	***2.37 mm (0.094 in)***		***751 mm (29.6 in)***	***1127 mm (44.4 in)***	***1.50***
H0B0A-1	1.52 mm (0.060 in)	1.35 mm (0.053 in)	0.006627	407 mm (16.0 in)	610 mm (24.0 in)	2.09
H0B0B-2	2.03 mm (0.080 in)	1.70 mm (0.067 in)	0.006627	512 mm (20.1 in)	768 mm (30.2 in)	1.71
H0B1A-3	1.57 mm (0.062 in)	1.37 mm (0.054 in)	0.006601	414 mm (16.3 in)	621 mm (24.4 in)	2.21
H0B1B-4	1.52 mm (0.060 in)	1.37 mm (0.054 in)	0.006601	415 mm (16.3 in)	623 mm (24.5 in)	2.32*
Mean	***1.66 mm (0.066 in)***	***1.45 mm (0.057 in)***		***436 mm (17.2 in)***	***655 mm (25.8 in)***	***2.00***

Notes: (*) indicates the number was eliminated from the mean calculation because the transfer length was based on data from only one face of the beam.
No long term readings taken for the L0BX beam pair
The long term readings for the M0BX beam pair are very questionable
1 in =25.4 mm

CHAPTER FIVE

DEVELOPMENT LENGTH TESTING

5.1 INTRODUCTION

After the measurements had been completed in Victoria, as discussed in Chapter Four, the concrete beams were shipped, one pair at a time, to Ferguson Laboratory at the J. J. Pickle Research Campus of The University of Texas at Austin. The pair of beams was brought into the lab and then set on the pedestals and bearing pads, which were already prepared and placed prior to the arrival of the beams. Once the beams were in place, complete with concrete decks per Section 3.6, the specimens were prepared for development length testing. Preparation involved determining the location of the load points, and placing and hooking up the instrumentation to the data acquisition system at the end to be tested. Therefore, this chapter describes the preparation for and execution of the development length testing, and presents the test results.

5.2 TEST SETUP

As discussed in Chapter Two, the length of each beam was designed to allow for two development length tests, one at each end. Therefore, the reinforced concrete pedestals and neoprene bearing pads were placed for each test to create a 6.1 m (20 ft) simply-supported test region, with the remaining length of the beam cantilevered. The bearing pads were 279 x 559 mm (11 x 22 in), and were placed such that the center-of-bearing of the outside pad was 152 mm (6 in) from the beam end and 6.1 m (20 ft) from the center-of-bearing of the other pad.

The next part of the setup involved the placement of the load points and spreader beam. The distance between load points was 914 mm (3 ft) and the distance between the outside load point and the end of the beam was equivalent to the embedment length. The embedment length for the first test was determined by calculating the development length which would be required by the AASHTO specifications. If the test with this embedment length resulted in a bond failure, the embedment length was increased for the next test. If

a flexural failure occurred, the length was decreased. In this manner it was possible to indirectly determine the development length. In other words, the embedment length was altered in subsequent tests to determine the length which defined the boundary between bond and flexural failure.

The final test of each pair of beams *always* contained the longitudinal shear reinforcement. Therefore, due to the presence of the H-bars, the embedment length was determined in a slightly different manner. In order to make conclusions regarding the effect of the H-bars on beam behavior, the embedment length was set at the same length as the previous embedment length closest to bond failure. As can be observed from Table 5.1, each pair of beams utilized the same set of embedment lengths, which aided the comparison of the test results from each beam pair. Figure 5.1 shows the typical test setup with the sketch showing each of the lengths tabulated in Table 5.1.

Table 5.1- Development Length Test Setup Parameters

Test I.D.	**Embed. Length (L_e) m *(in)***	**Supported Length (L_s) m *(in)***	**Overhang Length (L_o) m *(in)***	**Cantilever Length (L_c) m *(in)***	**Ram Location (a) m *(in)***	**Distance b/t Load Points (L_{lp}) m *(in)***
L0B0A-1	2.44 *(96)*	6.10 *(240)*	0.152 *(6)*	5.94 *(234)*	0.43 *(16.88)*	0.91 *(36)*
L0B0B-2	1.83 *(72)*	"	"	"	0.31 *(12.31)*	"
L0B0A-3	1.37 *(54)*	"	"	"	0.23 *(8.88)*	"
L0B0B-4	1.37 *(54)*	"	"	"	0.23 *(8.88)*	"
M0B0A-1	2.44 *(96)*	6.10 *(240)*	0.152 *(6)*	5.94 *(234)*	0.42 *(16.63)*	0.91 *(36)*
M0B0B-2	1.83 *(72)*	"	"	"	0.31 *(12.25)*	"
M0B0A-3	1.37 *(54)*	"	"	"	0.23 *(8.88)*	"
M0B0B-4	1.37 *(54)*	"	"	"	0.23 *(8.88)*	"

Note: Table 5.1 continued on next page

Table 5.1 (continued)- Development Length Test Setup Parameters

Test I.D.	Embed. Length (L_e) m *(in)*	Supported Length (L_s) m *(in)*	Overhang Length (L_o) m *(in)*	Cantilever Length (L_c) m *(in)*	Ram Location (a) m *(in)*	Distance b/t Load Points (L_{lp}) m *(in)*
H0B0A-1	2.44 *(96)*	6.10 *(240)*	0.152 *(6)*	5.94 *(234)*	0.42 *(16.63)*	0.91 *(36)*
H0B0B-2	1.83 *(72)*	"	"	"	0.29 *(11.38)*	"
H0B0A-3	1.37 *(54)*	"	"	"	0.23 *(9.00)*	"
H0B0B-4	1.37 *(54)*	"	"	"	0.23 *(9.00)*	"

Finally, once the position of the load points was determined, and the spreader beam centered and set evenly across the load points, the location of the hydraulic ram was set. Due to statics, the ram was not located at the center of the load points, but off-center, in order to create the desired constant *applied* moment region between the load points.

The test setup is illustrated in Figure 5.1 and 5.2.

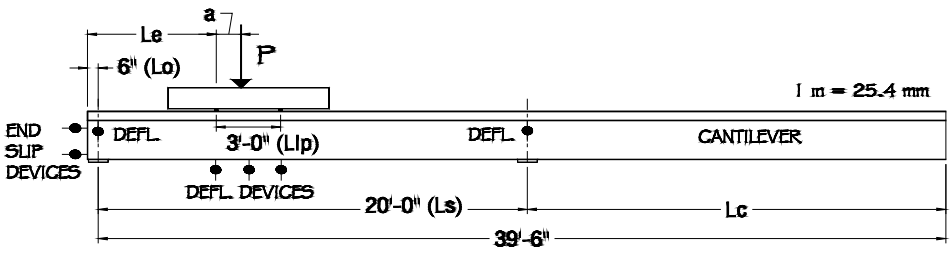

Figure 5.1- Diagram of a Typical Test Setup

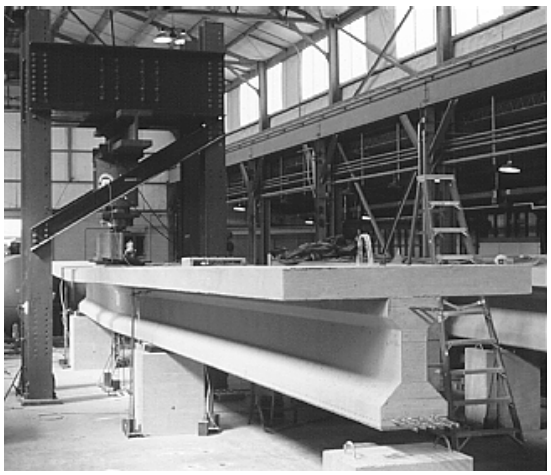

Figure 5.2- Overview of Test Setup

5.3 INSTRUMENTATION FOR DEVELOPMENT LENGTH TESTING

Prior to each development length test, instrumentation was placed to record the following measurements:

1. Applied load
2. Beam deflection
3. Vertical and horizontal support deflection
4. Strand end slip
5. Concrete deck top fiber strain

The sections that follow include a description of the measurement devices used and a picture to enhance that description. Most of the instrumentation used during the development length testing was monitored electronically through the data acquisition system briefly described in Section 5.3.5. However, manual measurement devices were also installed in critical locations in case of electronic failure.

5.3.1 Applied Load Instrumentation

The load was applied by a 4.45 MPa (1000 kip) capacity hydraulic ram. The load was then measured electronically through the pressure gauge on the pump and a load cell attached to the hydraulic ram. The load was calculated by the data acquisition system for both devices by converting the change in voltages to force. Furthermore, the load cell was attached to a plotter; therefore, providing the necessary load data for the load-deflection plot.

5.3.2 Deflection Instrumentation

The beam deflection was measured by linear potentiometers, a piano wire system, and a dial gauge. Linear potentiometers were placed under both load points and under the center of the load points on glass slides, to ensure the presence of a uniform surface. The linear potentiometer at the center of the load points was used to monitor the approximate deflection during the test and was electronically connected to the plotter, to provide the deflection input for the load-deflection curve.

Linear potentiometers were also located on either side of each support under the slab near the beam to measure the vertical support movement. Although the bearing pads were designed to contribute very little to the vertical deflection of the beam, small deflections still occurred. Therefore, the measured support deflections were used to calculate a *real* deflection at critical times by subtracting the correct proportion of each support deflection from the deflection at the center of the load points. The location of the vertical deflection devices is indicated in Figures 5.1, 5.3a, and 5.3b.

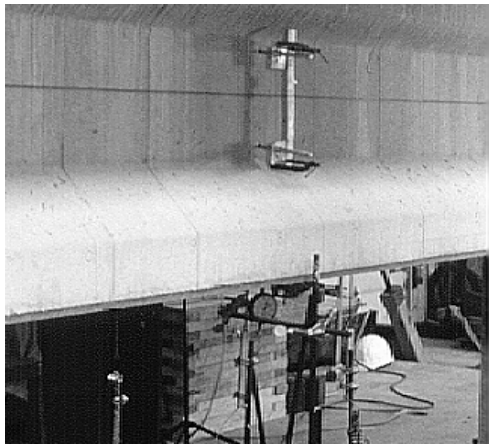

Figure 5.3a- Linear Potentiometers and Piano Wire Deflection System

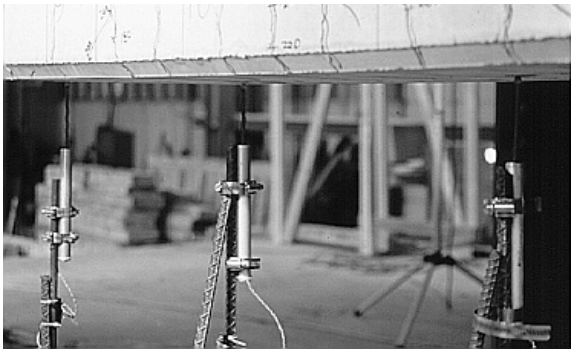

Figure 5.3b- Linear Potentiometers

This calculated *real* deflection was then compared to the installed manual deflection measurement piano wire system, as shown in Figure 5.3a. The piano wire system consisted of a wire and a steel ruler with an accuracy of 0.25mm (0.01 in). The wire spanned the test length at the center of the beam, and the ruler was located at the center of the load points on the beam web. As the beam deflected the change in distance of the piano wire on the ruler was measured and recorded. The piano wire system was usually within 0.51 mm (0.02 in) of the calculated real deflections of the electronic system.

Finally, a dial gauge was placed under the beam at the center of the load points for redundancy. This ensured that if a problem with the center potentiometer occurred, a real deflection could still be calculated. The dial gauge also proved to be useful when problems occurred with the plotter during the deflection controlled part of the development length test.

Horizontal deflection of the bearing pads was also measured using linear potentiometers. The bearing pads were designed with several steel reinforcement plates to force deflection primarily in the horizontal direction by shear. Therefore, a linear potentiometer measuring the movement of a bearing pad can be seen in Figure 5.4.

5.3.3 Strand End Slip Instrumentation

The instrumentation for this project also involved linear potentiometers to electronically measure end slip of the strands, as shown in Figure 5.4. The location of the potentiometers was such that they were securely set in place, but with enough distance remaining to allow for a large amount of slip. Glass slides were used to create a uniform surface for the linear pots. The relative end slip was recorded and printed by the data acquisition system, and therefore, monitored at each load step. The end slip of the strands for each test can be seen in Appendix E.

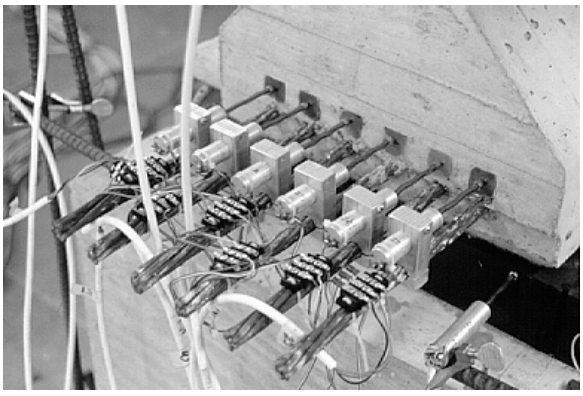

Figure 5.4- End Slip Potentiometers

5.3.4 Concrete Deck Top Fiber Strain Instrumentation

The top fiber strains of the concrete deck were measured in the constant moment region of each test using both Electric Resistance Strain Gauges (ERSG's) and the DEMEC Mechanical Strain Gauge system. The ERSG's were strategically placed in eight locations on the surface of the concrete, with the location of half of the gauges visible in Figure 5.5. The DEMEC system was implemented by centering the target points about the locations of the two ERSG's closest to the edge of the slab, and were used primarily in case of electronic difficulties. The location and implementation of the DEMEC system during development length testing can be seen in Figure 5.6 and was done in accordance with Section 4.2.1.

The top fiber strains were measured to aid the determination of the test end, which occurred when the strains reached a maximum plateau. These maximum values of strain usually occurred at the gauges located closest to the supports. Also, the measurement of the surface strains enabled the calculation of strand elongation to be made using strain compatibility.

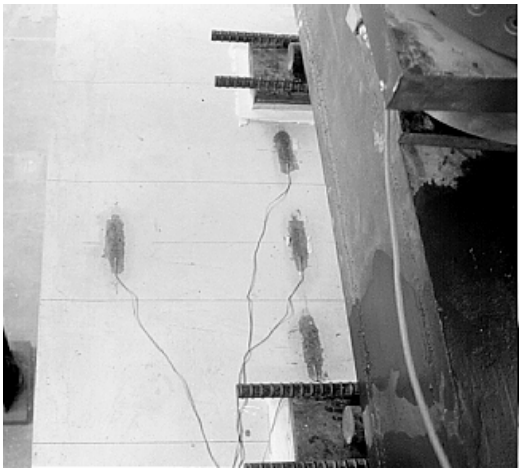

Figure 5.5- Location of Half of the Electronic Resistance Strain Gauges (ERSG's)

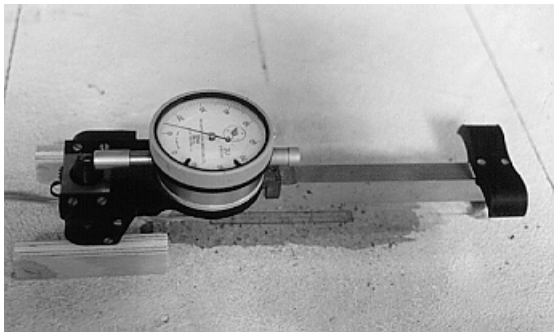

Figure 5.6- Location and Implementation of the DEMEC Strain Gauge System

5.3.5 Data Acquisition System

The data acquisition system was composed of 2 voltage sources, 1 quarter bridge box, 2 full bridge boxes, 1 IBM personal computer, and 1 Hewlett Packard scanner, partially shown in Figure 5.7. The scanner read the voltages of each piece of instrumentation through the recording of data from individual channels. These voltages were then converted to engineering units by the HPDAS2 conversion program, written by Alex Tahmassebi. The data was later converted to a spreadsheet format.

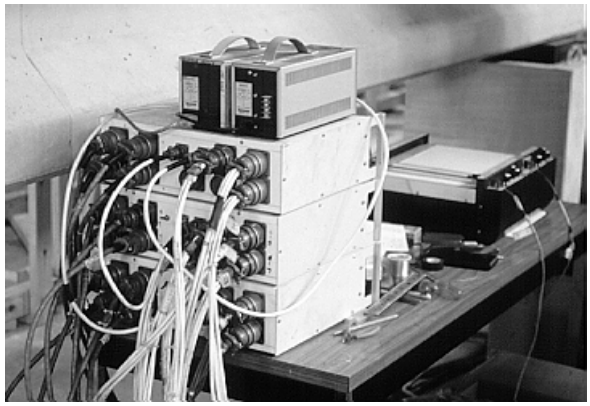

Figure 5.7- Data Acquisition System

5.4 TEST PROCEDURE

Once the instrumentation was properly installed and before any load was applied, initial readings were recorded from each piece of instrumentation described in Section 5.3.

Each development length test proceeded by loading the test specimen in increments. The end of each of these increments was determined by observing the pen location on the load-deflection curve created by the plotter. At first, along the steeper portion of the curve, the load steps were measured in small increments of load. Then, as the rate of change of the deflection became greater than the rate of change of the load, the test was controlled by increments of deflection.

At the end of each load step, measurements were recorded and significant behavior noted. Also, cracks were marked after each load step occurring at and after first flexural cracking. As the cracks propagated into the slab, the cracks were then used to monitor the neutral axis depth. Also, as the cracks began to open, crack width measurements were taken at several selected positions along the beam.

The end of each test was defined by either a flexural or bond failure. A flexural failure occurred with both the observation of the ultimate flexural capacity and ductile behavior of the specimen. Ductile behavior was observed if the strains in the steel reached or exceeded the required total value of 0.035. In several cases, flexural failure also resulted in a compression failure (i.e. spalling), of the concrete deck. Bond failure was defined as a sudden loss of beam capacity due to a general slip of the strand relative to the concrete.

After failure had occurred, the beam was unloaded in one final step. Upon completion of unloading, measurements were taken one last time.

5.4 DEVELOPMENT LENGTH TEST RESULTS

This section presents the test results from the development length testing of the L0BX, M0BX, and H0BX specimens. The following results will be presented in subsequent sections:

1. Failure Type
2. Critical Applied Loads, Net Deflection, and Maximum Moment
3. Approximate Maximum Strand Elongation
4. Strand End Slip
5. Cracking Pattern

Discussion of these test results in relationship to expected results and previous research can be found in Section 7.2.

5.4.1 Failure Type

The first results that are important to present are the failure types for each test. As discussed in Section 5.2, each failure mode can be classified as flexural or bond. The criteria for flexural failure are the achievement of the ultimate moment capacity and ductile behavior. Ductile behavior is confirmed by ensuring the bottom row of prestressing strands reached a total of 3.5% strain.

Although small amounts of end slip occurred during some of the tests, as shown in Table 5.4, *all failures were classified as flexural*. As indicated by Table 5.3, the test specimens all showed sufficient ductility, and none of the specimens saw a significant drop in capacity due to end slip, as would be indicative of a bond failure. Spalling of the concrete occurred at failure in several of the tests: L0B1A-3, L0B1B-4, M0B0A-1, M0B0B-2, M0B1A-3, M0B1B-4, H0B0A-1, H0B0B-2, H0B1A-3, H0B1B-4. A typical photograph of spalling, which occurred in the M0B1B-4 test, is shown in Figure 5.8.

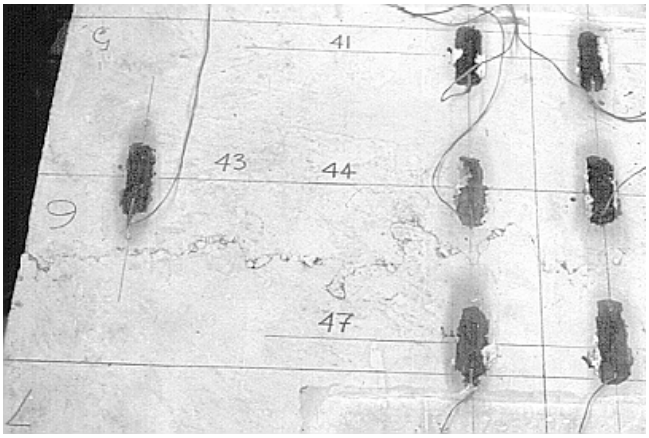

Figure 5.8- Typical Flexural Failure Resulting in Spalling of the Concrete Deck

5.4.2 Critical Applied Loads, Net Deflection, and Maximum Moment

This section presents the values of the critical applied loads, net deflection, and the maximum total moment in Table 5.2. The load values include first flexural cracking (P_{cr}), first shear cracking in both the right and left shear span (P_{sc1} and P_{sc2}), and the maximum applied load (P_u). None of these loads presented, however, include the self weight of the test specimen or the weight of the spreader beam.

Unlike the load values, the maximum moment values ($M_{u,total}$) in Table 5.2 *do* include the weight of the test specimen. Also, these maximum moments always occurred near one of the support locations, and inside of the constant moment region.

The net deflection of the beam, as discussed in Section 5.3.2, is the difference between the deflection measured by the potentiometer located at the center of the load points and a deflection resulting from a function of the support deflections. The residual deflection for each test is also listed in Table 5.2

Table 5.2- Critical Loads, Deflections, and Maximum Moment

Test I.D.	**P_{cr}** **kN** ***(kips)***	**P_{sc1}** **kN** ***(kips)***	**P_{sc2}** **kN** ***(kips)***	**P_u** **kN** ***(kips)***	**$M_{u,total}$** **kN-m** ***(kip-ft)***	**Δ_u** **mm** ***(in)***	**Δ_r** **mm** ***(in)***
L0B0A-1	752 *(169)*	801 *(180)*	890 *(200)*	1190 *(267)*	1478 *(1090)*	67.6 *(2.66)*	24.6 *(0.97)*
L0B0B-2	841 *(189)*	716 *(161)*	1116 *(251)*	1383 *(311)*	1546 *(1140)*	63.5 *(2.50)*	23.1 *(0.91)*
L0B0A-3	1032 *(232)*	672 *(151)*	1655 *(372)*	1664 *(374)*	1546 *(1140)*	53.1 *(2.09)*	19.3 *(0.76)*
L0B0B-4	1027 *(231)*	672 *(151)*	1579 *(355)*	1690 *(380)*	1573 *(1160)*	51.3 *(2.02)*	20.1 *(0.79)*
M0B0A-1	983 *(221)*	1032 *(232)*	1406 *(316)*	1508 *(339)*	1898 *(1400)*	61.2 *(2.41)*	22.1 *(0.87)*
M0B0B-2	1112 *(250)*	939 *(211)*	1704 *(383)*	1704 *(383)*	1912 *(1410)*	58.4 *(2.30)*	21.6 *(0.85)*
M0B0A-3	1383 *(311)*	898 *(202)*	NC	2046 *(460)*	1898 *(1400)*	34.5 *(1.36)*	8.6 *(0.34)*
M0B0B-4	1374 *(309)*	939 *(211)*	1966 *(442)*	2108 *(474)*	1952 *(1440)*	39.4 *(1.55)*	13.2 *(0.52)*
H0B0A-1	987 *(222)*	987 *(222)*	1290 *(290)*	1517 *(341)*	1898 *(1400)*	70.6 *(2.78)*	27.9 *(1.10)*
H0B0B-2	1112 *(250)*	903 *(203)*	1664 *(374)*	1739 *(391)*	1966 *(1450)*	59.7 *(2.35)*	21.1 *(0.83)*
H0B0A-3	1357 *(305)*	894 *(201)*	NC	2077 *(467)*	1925 *(1420)*	42.9 *(1.69)*	12.7 *(0.50)*
H0B0B-4	1299 *(292)*	939 *(211)*	2002 *(450)*	2099 *(472)*	1952 *(1440)*	43.9 *(1.73)*	14.7 *(0.58)*

Note: NC means cracking did not occur at any load

5.4.3 Approximate Maximum Strand Elongation

The approximate maximum strand elongation is reported in Table 5.3. The strand elongation was calculated using the maximum top fiber strain measured per Section 5.3.4, the measured final neutral axis depth (c), and the given material properties. The maximum top fiber strain and the final neutral axis depth are also listed in Table 5.3.

Table 5.3- Final Top Fiber Strain, Neutral Axis Depth, and Strand Elongation

Test I.D.	**Maximum Top Fiber Strain** $\times 10^{-6}$ **mm/mm or in/in**	**Final Neutral Axis Depth (c)** **mm *(in)***	**Maximum Strand Elongation** **%**
L0B0A-1	2948	63.5 *(2.50)*	4.19
L0B0B-2	2916	63.5 *(2.50)*	4.15
L0B0A-3	2778	50.8 *(2.00)*	4.89
L0B0B-4	3395	50.8 *(2.00)*	5.83
M0B0A-1	3298	55.9 *(2.20)*	5.11
M0B0B-2	3219	63.5 *(2.50)*	4.44
M0B0A-3	2992	43.2 *(1.70)*	5.97
M0B0B-4	2937	57.2 *(2.25)*	4.52
H0B0A-1	3332	57.2 *(2.25)*	5.07
H0B0B-2	2757	54.6 *(2.15)*	4.49
H0B0A-3	3708	50.8 *(2.00)*	6.21
H0B0B-4	3103	54.6 *(2.15)*	4.96

5.4.4 Strand End Slip

Even though all of the test specimens failed in flexure, some specimens did contain strands which experienced small amounts of slip. Therefore, the maximum amount of slip and the load at which first slipping occurred is recorded in Table 5.4. Since the L0BX pair of beams only contained one row of strands, values are only

recorded for that row. Row A is the bottom row of strands and row B is the next to the bottom row of strands.

Strand end slip was measured according to Section 5.3.3 and is plotted in Appendix E.

Table 5.4- End Slip Results

Test I.D.	**$P_{slip,b}$** **kN *(kips)***	**Maximum End Slip (Row B)*** **mm *(in)***	**$P_{slip,a}$** **kN *(kips)***	**Maximum End Slip (Row A)*** **mm *(in)***
L0B0A-1	----	----	NS	0.000
L0B0B-2	----	----	NS	0.000
L0B0A-3	----	----	1.29 *(291)*	0.178 *(0.007)*
L0B0B-4	----	----	1.38 *(311)*	0.102 *(0.004)*
M0B0A-1	NS	0.000	NS	0.000
M0B0B-2	NS	0.000	NS	0.000
M0B0A-3	1.33 *(300)*	0.457 *(0.018)*	1.69 *(381)*	0.203 *(0.008)*
M0B0B-4	1.42 *(320)*	0.356 *(0.014)*	NS	0.000
H0B0A-1	NS	0.000	NS	0.000
H0B0B-2	NS	0.000	NS	0.000
H0B0A-3	1.69 *(381)*	0.432 *(0.017)*	1.61 *(361)*	0.051 *(0.002)*
H0B0B-4	1.76 *(395)*	0.432 *(0.017)*	NS	0.000

Note: (*)See Figure 3.1 for location of Row A and Row B strands at 51 and 102 mm (2 and 4 in), respectively, from the bottom fiber.

NS means no significant slip occurred in any strand in the row.

5.4.5 Cracking Patterns

Sketches of the crack patterns on each face, at the maximum applied load of each test, are presented in Appendix G. Critical cracking loads are listed in Table 5.2 and the maximum crack width and its location are listed for each test in Table 5.5.

As apparent from Table 5.5, due to the presence of H-bars, the fourth test of each beam pair yielded a maximum crack width at a distance farther from the beam end than the maximum crack width location of the third test. In other words, the presence of the maximum crack width was moved to a location farther from the transfer zone due to the presence of the longitudinal shear reinforcement. Also, it should be noted that the widths of the cracks occurring in the beam along the region containing the longitudinal shear reinforcement remained smaller than the cracks outside of this region.

Table 5.5- Maximum Crack Widths and Crack Widths within the H-bar Zone

Test I.D.	**Maximum Crack Width mm *(in)***	**Location of Maximum Crack Width from End of Beam m *(in)***
L0B0A-1	3.5 *(0.14)*	2.59 *(102)*
L0B0B-2	4.0 *(0.16)*	2.69 *(106)*
L0B0A-3	4.0 *(0.16)*	1.47 *(58)*
L0B0B-4	6.5 *(0.26)*	2.44 *(96)*
M0B0A-1	4.0 *(0.16)*	2.59 *(102)*
M0B0B-2	4.5 *(0.18)*	2.54 *(100)*
M0B0A-3	3.0 *(0.12)*	1.72 and 1.37 *(69 and 54)*
M0B0B-4	4.1 *(0.16)*	2.18 *(86)*
H0B0A-1	4.0 *(0.16)*	3.25 *(128)*
H0B0B-2	3.0 *(0.12)*	2.46, 1.98, and 1.72 *(97, 78,and 69)*
H0B0A-3	3.0 *(0.12)*	2.29, 1.80, and 1.47 *(90, 71, and 58)*
H0B0B-4	5.0 *(0.20)*	2.24 *(88)*

CHAPTER SIX

STRAND PULL-OUT

6.1 INTRODUCTION

As discussed in the literature review section, pull-out testing was developed in 1974 by Concrete Technology under the direction of Saad Moustafa to determine a qualitative idea of the bond performance for a particular combination of steel prestressing strand and concrete mix. At this time, the test embedment length was standardized and a benchmark for an acceptable pull-out capacity was established for 13 mm (0.5 in) diameter prestressing strand [38].

The standard embedment length (l_{pe}) remains acceptable today, but some uncertainty has arisen regarding the validity of using the same embedment length for both the 12.7 mm (0.5 in) and the 15.2 mm (0.6 in) diameter strand. Therefore, the data presented in this section gives insight into the determination of a standard embedment length for pull-out tests performed on 15.2 mm (0.6 in) diameter strand.

6.2 PREPARATION AND TESTING OF THE PULL-OUT BLOCK

6.2.1 Preparation of the Pull-Out Block

On the day that each pair of beams was cast in Victoria, Texas, at Texas Concrete, a pull-out block was prepared with the same concrete and prestressing strand study, three total pull-out blocks were prepared and cast: one on July 1, July 5, and October 2, 1996. Each pullout block was 914x610x610 mm *(36x24x24 in)* and contained seven-wire 15.2 mm (0.6 in) diameter bright prestressing strand and normal strength, middle strength, or high strength concrete, respective to the previous dates. Figure 6.1 shows the details of the test block.

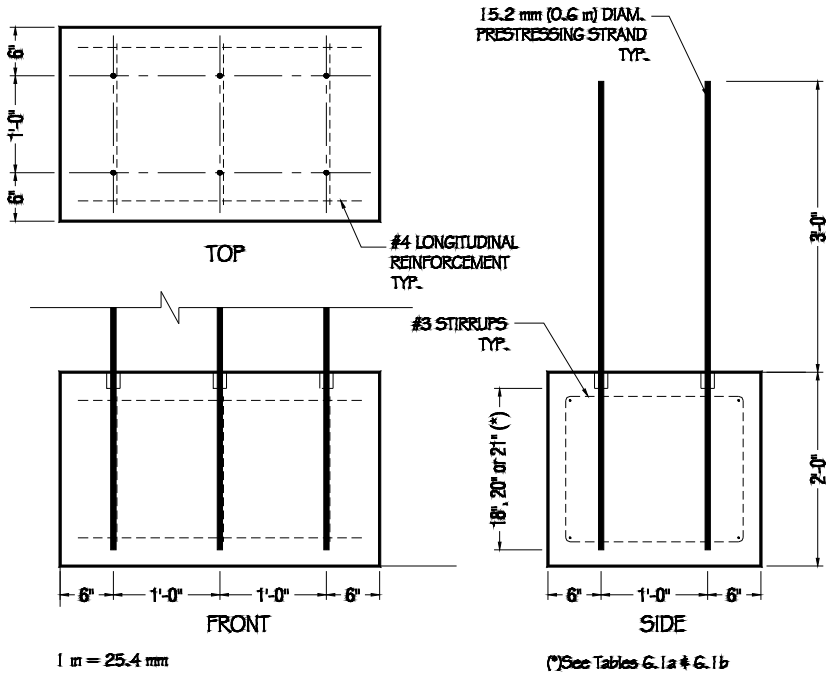

Figure 6.1- Details of Pull-Out Block

In the preparation of the pull-out block, it was necessary to first place the required mild steel reinforcement and the six samples of the prestressing strand to be tested. For a previously defined embedment length (l_e), the prestressing strand was left uncovered, while the remaining strand was covered with a plastic coating to prevent bonding with the concrete, as shown in Figure 6.2. Then, after the strand was placed and properly coated, the forms for the block were placed and the concrete was cast, as shown in Figures 6.2 and 6.3. Finally, the concrete was finished, as shown in Figure 6.4, and covered in order to cure with the respective concrete beams.

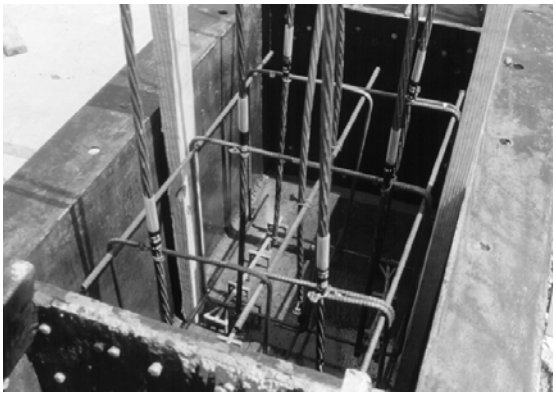

Figure 6.2- Steel Cage and Prestressing Strand in Pull-Out Block

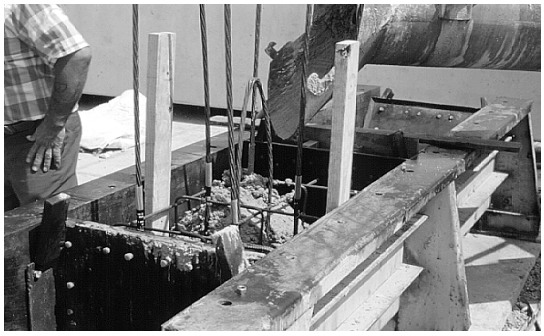

Figure 6.3- Concrete is Placed in the Pull-Out Block

Figure 6.4- Finished Concrete Pull-Out Block

6.2.2 Testing of the Pull-Out Block

On the date of transfer, the pull-out block was uncovered with the beams, and subsequently set aside. Then, if possible, on the day the beams were three days old, the pull-out tests were performed in Victoria, Texas. A picture of the test set-up can be seen in Figure 6.5 and a description follows the figure.

Figure 6.5- Pull-Out Block Testing Configuration

First, the extra plastic coating around the each strand was cut down as far as possible to the concrete block and was removed. Then, in consecutive order, a steel stand, load cell, and one-way hydraulic ram were placed and centered around the strand to be tested, as shown in Figure 6.5. Next, a small steel plate was placed on top of the ram and a chuck was set on the strand approximately one finger's width above the plate, for ease of removal after testing.

After each component of the test set-up was in place, the electric and hydraulic equipment was properly connected. The hydraulic ram was connected to the pump, and

the load cell was connected to the voltage source and the multi-meter being used to measure the voltage output. Then, the strand was pre-loaded to approximately 3.5 MPa (500 psi) to set the chuck and make final preparations for testing. A clear reference mark was then made on the prestressing strand in order to measure slipping of the strand during the test.

Next, the strand was loaded at a constant rate of approximately 6.9 kPa (1 psi) per second. This rate was previously determined according to the testing procedure specified by PCI and was specific to the particular hydraulic ram used for the test. The strand was loaded until one of three events occurred: any or all of the seven strand wires fractured, the strand could no longer sustain the maximum load, or the strand surpassed f_{pu} = 1.86 Gpa (270 ksi). An example of strand fracture is shown in Figure 6.6.

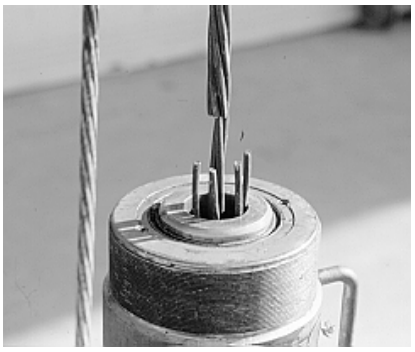

Figure 6.6- An Example of Strand Fracture

Measurements were taken at important events during the load cycle. The loading was continuous and the measurements were recorded as loading was continued at a constant rate. At the point the slipping of the strand seemed apparent, a voltage reading was taken. A voltage reading was also taken at the point of strand fracture, or if the strand did not fracture, the peak voltage was recorded along with the slip distance of the strand at that voltage. For the case in which fracture did not occur, after the strand had reached the maximum load and the hydraulic pressure was released, it was common for a

sudden, definable amount of slip to occur. Therefore, these final slip distances were also recorded.

6.3 TEST RESULTS

The test results for each pull-out block are summarized in Table 6.1a and Table 6.1b, in metric and English units, respectively, Chapter 7 discusses the test results, and conclusions are made in Chapter 8. Each strand tested in a pull-out block is identified by the related pair of beams and the order in which is was tested. For example, the first strand tested in the pull-out block for the normal, medium, and high strength concrete beams would be identified as L0BX-1, M0BX-1, and H0BX-1, respectively.

As is evident from Tables 6.1a and 6.1b, different embedment lengths (l_{pe}) were tested to see if a significant difference occurred in the test results at these different lengths of the 15.2 mm (0.6 in) diameter strand, and therefore, to see if the standard embedment length of 457 mm (18 in) used for pull-out tests with the 13 mm (0.5 in) diameter strand can be used for the 15.2 mm (0.6 in) diameter strand as well. Another pertinent fact to Tables 6.1 and 6.2 is that the concrete compressive strength (f'_c) reported is based on the strength of the cylinders cured with the respective beams and tested on the day of the pull-out test. Finally, the failure types listed in Tables 6.1a and 6.1b are described in Table 6.2.

Table 6.1a- Pull-out Test Data Summary in Metric Units

Specimen I.D.	Embed. Length l_e (cm)	f'_c .... (MPa)	Strand Surface Condition	Peak Load (N)	Peak Stress (GPa)	Pull-out Length at Peak Load (cm)	Failure Type
L0BX-1	53.3	36.2	Bright	262	1.87	2.5	PO
L0BX-2	53.3	36.2	Bright	251	1.79	2.5	PO
L0BX-3	53.3	36.2	Bright	247	1.77	2.2	PO
L0BX-4	53.3	36.2	Bright	253	1.81	2.2	F2
L0BX-5	53.3	36.2	Bright	254	1.81	3.2	PO
L0BX-6	53.3	36.2	Bright	266	1.90	1.9	F4
M0BX-1	45.7	53.8	Bright	262	1.87	1.3	N
M0BX-2	45.7	53.8	Bright	263	1.88	0.6	N
M0BX-3	50.8	53.8	Bright	259	1.85	0.5	F1
M0BX-4	50.8	53.8	Bright	261	1.87	0.5	N
M0BX-5	50.8	53.8	Bright	271	1.94	0.6	F2
H0BX-1	45.7	76.3	Bright	243	1.74	—	PO/S
H0BX-2	45.7	76.3	Bright	241	1.72	2.2	PO/S
H0BX-3	45.7	76.3	Bright	257	1.83	1.9	PO/S
H0BX-4	50.8	76.3	Bright	272	1.94	1.6	F4
H0BX-5	50.8	76.3	Bright	261	1.87	3.2	PO/S
H0BX-6	50.8	76.3	Bright	267	1.91	2.5	PO/S

Table 6.1b- Pull-out Test Data Summary in English Units

Specimen I.D.	Embed. Length l_e (in)	f'_c (psi)	Strand Surface Condition	Peak Load (kips)	Peak Stress (ksi)	Pull-out Length at Peak Load (in)	Failure Type
L0BX-1	21	5250	Bright	58.9	271	1	PO
L0BX-2	21	5250	Bright	56.5	260	1	PO
L0BX-3	21	5250	Bright	55.6	256	7/8	PO
L0BX-4	21	5250	Bright	56.8	262	7/8	F2
L0BX-5	21	5250	Bright	57.0	263	1-1/4	PO
L0BX-6	21	5250	Bright	59.9	276	3/4	F4
M0BX-1	18	7800	Bright	58.9	271	1/2	N
M0BX-2	18	7800	Bright	59.2	273	1/4	N
M0BX-3	20	7800	Bright	58.2	268	3/16	F1
M0BX-4	20	7800	Bright	58.7	271	3/16	N
M0BX-5	20	7800	Bright	60.9	281	1/4	F2
H0BX-1	18	11070	Bright	54.6	252	—	PO/S
H0BX-2	18	11070	Bright	54.1	249	7/8	PO/S
H0BX-3	18	11070	Bright	57.7	266	3/4	PO/S
H0BX-4	20	11070	Bright	61.1	282	5/8	F4
H0BX-5	20	11070	Bright	58.7	271	1-1/4	PO/S
H0BX-6	20	11070	Bright	60.1	277	1	PO/S

Table 6.2- Description of the Pull-Out Test Failure Types

Failure Type	Description
F#	Fracture of # of wires in strand
N	Ceased above nominal f_{pu}
PO	Gradual pull-out
PO/S	Gradual pull-out followed by sudden slip of ~3/8” after peak load achieved

It is important to note that these test results only include the pull-out blocks related to the beams containing fully bonded bright strand. Therefore, these test results and any related conclusions should be compared with the comprehensive test results to be presented in the dissertation by Robbie Barnes upon completion of this research program.

CHAPTER SEVEN

DISCUSSION OF TEST RESULTS

7.1 TRANSFER LENGTH TESTING

7.1.1 Comparison of Test Results within the Test Program

This section contains a comparison and discussion of the transfer length results within the test program. Specifically, the variables of interest in this transfer length study are the effects of time and the concrete strength.

The first variable considered is the effect of time on the transfer length. The age of the concrete at transfer was approximately 24 hours for all the beams, and the age of the concrete at the long term transfer length measurements was 18, 22, 60, 62, 15, and 19 days for L0B0, L0B1, M0B0, M0B1, H0B0, and H0B1, respectively. Table 7.1 shows the normalized values of the "after deck placement" transfer length to the "after release" transfer length. Normalized values were calculated for each end of each beam using the data from Tables 4.1, 4.2, and 4.3. However, for simplicity, only the average, minimum, and maximum normalized values are recorded in Tables 7.1a, 7.1b, and 7.1c. It should be noted that in all cases, with one exception, the transfer length measured after the deck placement was longer than the transfer length measured after the release of the prestress.

It is also important to mention that the long term transfer length was measured after the beams had been moved to Ferguson Laboratory and the test specimen had been completed with the placement of a composite concrete deck.

Table 7.1a- Effect of Time on Transfer Length Results for 95 % Method

Beam I.D.	f'_{ci} MPa *(psi)*	f'_c MPa *(psi)*	Average $L_{t,DP}/L_{t,R}$	Minimum $L_{t,DP}/L_{t,R}$	Maximum $L_{t,DP}/L_{t,R}$
L0BX	29.2 *(4240)*	45.0 *(6520)*	674/496=1.36	680/540=1.26	715/455=1.57
M0BX	45.6 *(6610)*	74.0 *(10,730)*	545/495=1.10	520/515=1.01	610/490=1.24
H0BX	76.2 *(11,060)*	87.8 *(12,730)*	440/426=1.03	425/435=0.98	480/405=1.19

Notes: $L_{t,DP}$ *is defined as the transfer length after deck placement*

$L_{t,R}$ *is defined as the transfer length after release of the prestress*

Table 7.1b- Effect of Time on Transfer Length Results for Slope-Intercept Method

Beam I.D.	f'_{ci} MPa *(psi)*	f'_c MPa *(psi)*	Average $L_{t,DP}/L_{t,R}$	Minimum $L_{t,DP}/L_{t,R}$	Maximum $L_{t,DP}/L_{t,R}$
L0BX	29.2 *(4240)*	45.0 *(6520)*	545/468=1.16	580/525=1.10	500/385=1.30
M0BX	45.6 *(6610)*	74.0 *(10,730)*	490/455=1.08	470/460=1.02	480/425=1.13
H0BX	76.2 *(11,060)*	87.8 *(12,730)*	420/386=1.09	390/385=1.01	455/415=1.10

Notes: $L_{t,DP}$ *is defined as the transfer length after deck placement*

$L_{t,R}$ *is defined as the transfer length after release of the prestress*

Table 7.1c- Effect of Time on Transfer Length Results for Draw-In Method

Beam I.D.	f'_{ci} MPa *(psi)*	f'_c MPa *(psi)*	Average $L_{t,DP}/L_{t,R}$	Minimum $L_{t,DP}/L_{t,R}$	Maximum $L_{t,DP}/L_{t,R}$
L0BX	29.2 *(4240)*	45.0 *(6520)*	----	----	----
M0BX	45.6 *(6610)*	74.0 *(10,730)*	751/575=1.31	820/678=1.21	706/485=1.46
H0BX	76.2 *(11,060)*	87.8 *(12,730)*	436/259=1.68	511/389=1.31	----

Notes: $L_{t,DP}$ *is defined as the transfer length after deck placement*

$L_{t,R}$ *is defined as the transfer length after release of the prestress*

From the normalized results presented in Table 7.1, first of all, it seems that time does affect transfer length. Also, it seems that the effect of time on the transfer length

decreases with an increase in concrete strength. For example, the change in transfer length over time in the normal strength concrete beams was over 25%, while the average percent change in the transfer length of the medium and high strength concrete beams was not quite as significant, with a percent change of only 10% and 3%, respectively.

The effect of concrete strength on the transfer length results of the test specimens is further presented in Figure 7.1and Table 7.2. Figure 7.1 is a graphical representation of the effects of concrete strength on the transfer length. The values recorded in Table 7.2 are the average transfer length values presented in Tables 4.1, 4.2, and 4.3 normalized to the respective average transfer length of the normal strength beams (L0BX). Also, for simplicity, the concrete strengths are not listed again, but are listed in Table 4.1.

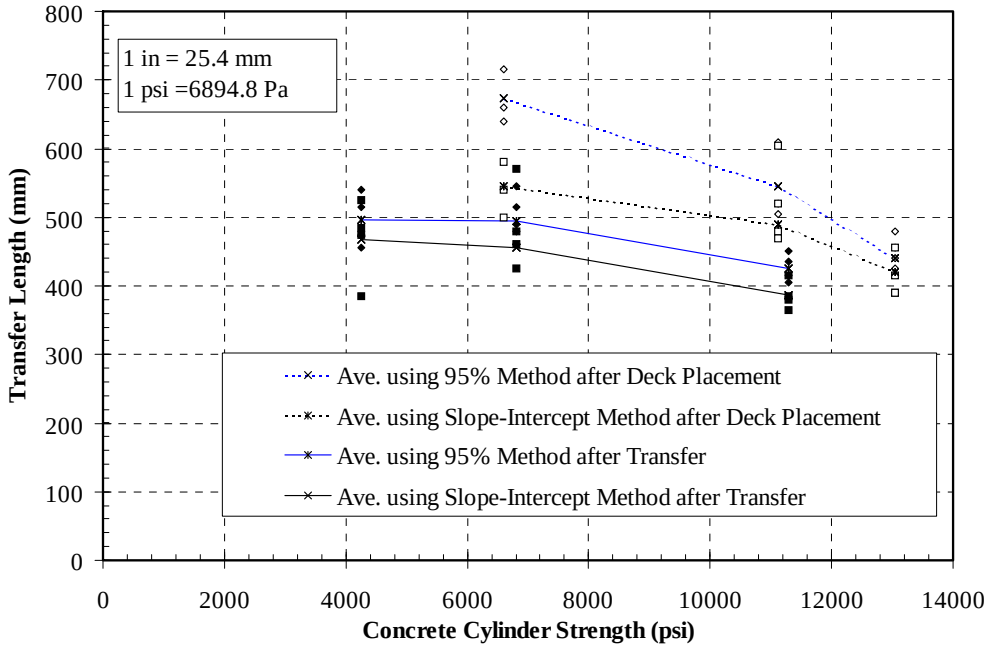

Figure 7.1- Transfer Length Results vs. Concrete Cylinder Strength

Table 7.2a- Effect of Concrete Strength on Ave.Transfer Length Results for 95% Method

Beam I.D.	f'_{ci} MPa *(psi)*	f'_c MPa *(psi)*	After Release	After Deck Placement
L0BX	29.2 *(4240)*	45.0 *(6520)*	496/496*=1.00	674/674*=1.00
M0BX	45.6 *(6610)*	74.0 *(10,730)*	495/496=1.00	545/674=0.81
H0BX	76.2 *(11,060)*	87.8 *(12,730)*	426/496=0.86	440/674=0.65

Notes: (*)496mm and 674mm are the average transfer lengths for the L0BX beam pair

Table 7.2b- Effect of Concrete Strength on Ave. Transfer Length Results for Slope-Intercept Method

Beam I.D.	f'_{ci} MPa *(psi)*	f'_c MPa *(psi)*	After Release	After Deck Placement
L0BX	29.2 *(4240)*	45.0 *(6520)*	468/468*=1.00	545/545*=1.00
M0BX	45.6 *(6610)*	74.0 *(10,730)*	455/468=0.81	490/545=0.90
H0BX	76.2 *(11,060)*	87.8 *(12,730)*	386/468=0.65	420/545=0.77

Notes: (*)468mm and 545mm are the average transfer lengths for the L0BX beam pair

Table 7.2c- Effect of Concrete Strength on Ave. Transfer Length Results for Draw-In Method

Beam I.D.	f'_{ci} MPa *(psi)*	f'_c MPa *(psi)*	After Release	After Deck Placement
L0BX	29.2 *(4240)*	45.0 *(6520)*	384/384*=1.00	----
M0BX	45.6 *(6610)*	74.0 *(10,730)*	575/384=1.50	----
H0BX	76.2 *(11,060)*	87.8 *(12,730)*	259/384=0.67	----

Notes: (*)384mm is the average transfer lengths for the L0BX beam pair

Figure 7.1 and Tables 7.2a, 7.2b, and 7.2c seem to indicate that as the concrete strength increases, the transfer length decreases, although in varying degrees. It appears that the higher the concrete strength, the greater the effect on the transfer length.

The effects of time and concrete strength on the transfer lengths found using the draw-in method are listed solely for information and are disregarded from any conclusions due to the uncertainty of the reliability of the results. Also, the results from the slope-intercept method are used solely to confirm trends; and therefore, are not used in any numerical comparisons regarding transfer length, per the discussion in Section 4.4.2.

7.1.2 Comparison of Transfer Length to Suggested Equations

The next important level of discussion is a comparison of the transfer length results to the existing and suggested equations for transfer length. For simplicity, only the transfer length results using the 95% Method will be used in the comparison presented in Sections 7.1.2 and 7.1.3. However, for reference, the transfer length results determined using the Slope-Intercept Method and draw-in measurements are presented in Tables 4.1 and 4.2. Since several equations exist, only the calculated transfer lengths from the various equations are listed in Table 7.3. The actual equations are listed in Table 2.1 and a summary of the average transfer length results are listed in Table 7.4.

Table 7.3- Calculated Transfer Lengths Using Suggested Equations

Author(s) of Equation(s)	**Calculated Transfer Length (L0BX)**	**Calculated Transfer Length (M0BX)**	**Calculated Transfer Length (H0BX)**
ACI 318/ AASHTO	[eq1)]798 mm (31.4 in) [eq2)]762 mm (30.0 in)	[eq1)]767 mm (30.2 in) [eq2)]762 mm (30.0 in)	[eq1)]767 mm (30.2 in) [eq2)]762 mm (30.0 in)
Martin & Scott	1219 mm (48.0 in)	1219 mm (48.0 in)	1219 mm (48.0 in)
Zia & Mostafa	963 mm (37.9 in)	574 mm (22.6 in)	297 mm (11.7 in)
Cousins, Johnston, & Zia	1359 mm (53.5 in)	1097 mm (43.2 in)	861 mm (33.9 in)
Russell & Burns	1196 mm (47.1 in)	1151 mm (45.3in)	1151 mm (45.3in)
Mitchell et. al.	855 mm (33.6 in)	684 mm (26.9 in)	529 mm (20.8 in)
Burdette, Deatherage, & Chew	1016 mm (40.0 in)	1016 mm (40.0 in)	1016 mm (40.0 in)
Buckner (FHWA)	[eq1)]750 mm (29.5in) [eq2)]1016 mm (40.0 in)	[eq1)]576 mm (22.7 in) [eq2)]1016 mm (40.0 in)	[eq1)]523 mm (21.2 in) [eq2)]1016 mm (40.0 in)

Notes to Table 7.3:

f'_{ci} and E_c values used in the equations from the beam cured cylinders

f_{si} = 200 ksi

f_{se} = 157 ksi (L0BX), 151 ksi (M0BX, H0BX)

f_{se} calculated by estimating losses per AASHTO Code [cc] per Section 9.16.

B = 300 psi/in

U't = 6.7

1 in = 25.4 mm

1 psi = 6894.8 Pa

Table 7.4- Average Transfer Length Results for This Study

Beam I.D.	***f'ci***	**Method**	**Type of Cross-Section**	**Ave. L_t After Transfer**	**Ave. L_t After Deck Placement**
Ave L_t for. L0BX	29.2 MPa (4240 psi)	95%	AASHTO Type I	496 mm (19.5 in)	674 mm (26.5 in)
Ave L_t for. M0BX	45.6 MPa (6610 psi)	95%	AASHTO Type I	495 mm (19.5 in)	545 mm (21.5 in)
Ave L_t for. H0BX	76.3 MPa (11,060 psi)	95%	AASHTO Type I	426 mm (16.8 in)	440 mm (17.3 in)

The current code equations give conservative results compared to the measured transfer lengths resulting from this study. As shown in Table 7.3, the transfer length from AASHTO is 762 mm (30 in), while the average values measured were within the range 426 mm (16.8 in) to 674 mm (26.5 in). When the ACI equation is compared with the experimental results, the minimum and maximum error are 12% and 44%, respectively. The minimum error occurs with the long term, normal strength transfer length measurement and the maximum error occurs with the transfer length measurement after release of the highest strength beams.

A comparison of the experimental transfer length results of this study and the transfer lengths calculated from several of the previous equations is shown in Figure 7.2 using data from Table 7.3. In Figure 7.2, the beam identification with a -R and a -DP refer to the transfer length results immediately after the release of the prestress and after the deck placement, respectively. It appears that the equation developed by Mitchell et. al. [y] seems to fit the trend of the test results the best and also remains adequately conservative for both short term and long term transfer lengths. It is based both on the initial prestress in the strand (f_{si}) and the strength of the concrete at release (f_{ci}).

The equations fsi*db/3 and 80*db seem to be over conservative for the transfer length results of this study, as shown in Figure 7.2.

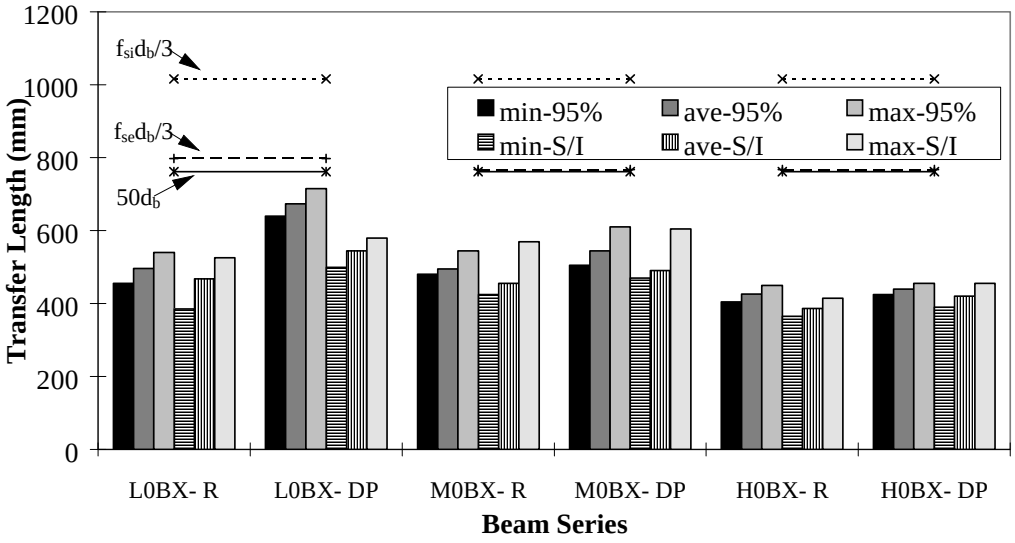

Figure 7.2- Comparison of Test Results with Selected Equations

7.1.3 Comparison of Test Results with Previous Literature

The last level of discussion of transfer length is a comparison of the results from this test program to the results of other test programs. However, only the transfer length results from previous literature which correspond to specimens containing 15.2 mm (0.6 in) diameter, Grade 270, prestressing strand, and concrete strengths equivalent to the those used in this test program will be compared with the test results of this study. A summary of these relevant results is listed in Table 7.5.

Table 7.5- Summary of Transfer Length Results from Previous Literature

Researchers	**f'_{ci}**	**Type of Cross-Section**	**Method**	**Average Lt**
Unay, Russell & Burns [6,16]	26.5 MPa *(3850 psi)*	prism (4x5 in)	95%	1.2 m *(47.0 in)*
	31.2 MPa *(4530 psi)*	prism (5x9.5 in)	95%	1.1 m *(43.2 in)*
	30.9 MPa *(4480 psi)*	prism (5x13 in)	95%	1.2 m *(48.0 in)*
	32.1 MPa *(4660 psi)*	I-shaped	95%	813 mm *(32.0 in)*
Lane [23,36]	30.9 MPa *(4480 psi)*	prism (4.5x5 in)	95%	921 mm *(36.0 in)*
Cousins et. al. [3]	27.6 MPa *(4000 psi)*	prism (6x10 in)	100%	1.4 m *(57.0 in)*
Burdette et. al. [20,27]	27.6 MPa *(4000 psi)*	AASHTO Type I	????	610 mm *(24.0 in)*
Shaway et. al. [22]	38.9 MPa *(5640 psi)*	AASHTO Type II	100%	884 mm *(34.8 in)*
Gross [33]	48.5 MPa *(7040 psi)*	prism (14x42 in)	inspection	363 mm *(14 in)*
Cordova [42]	27.6 MPa *(4000 psi)*	Texas Type C	inspection	549 mm *(21.6 in)*

Notes: 1 in =25.4 mm

It is important to remember that the size of the specimen cross-section affects the transfer length, as well as the strand condition and concrete strength. Also, the method used to determine the transfer length varies from project to project, which can create variance in the reported transfer lengths.

It appears that the average transfer length results reported in this study, as listed in Table 7.4, are less than the average transfer lengths to date, as reported in Table 7.5, with the exception of the transfer length results reported by Gross [33]. Burdette, Deatherage, and Chew [20,27] used AASHTO Type I concrete beams to study transfer

length and reported values of transfer length using the ?? method. These results are within 25% of the values reported by this study for the equivalent strength concrete beams. Also, the results reported by Cordova for the normal strength concrete beams are within 11% of the results in this study.

7.1.4 Possible Sources of Variability and Error in the Test Results

As visible from the test results presented in Tables 4.1, 4.2, and 4.3, the transfer length varies from end to end within each pair of beams. This variability is primarily due to the *effect of flame cutting* the strands. As discussed in Chapter Three, an attempt is made to cut the strands at each end simultaneously. However, due to human error, the prestressing force was always transferred at one end before the other ends. Therefore, the end with the longest transfer length corresponds to the end at which the strands have been cut first.

Variability also exists in the draw-in results apart from the errors encountered in the *method of data collection* discussed in Section 4.2.2. As demonstrated by the limited draw-in measurements in Appendix E, the draw-in varies from strand to strand at a beam end. This is partially due to the confining effects caused by the compression in the concrete created with the cutting of each additional strand. Frequently, the strands in Row B or the outside strands in Row A experience the greatest amounts of draw-in because of less confinement.

As discussed in Chapter Four, *temperature effects* caused the beams to bow out-of-line. This source of variability was overcome by averaging the strain plateaus of both faces at each end of a beam.

Other possible sources of error include *human error* due to the uncomfortable position and weather conditions related to taking the transfer length measurements. In addition, in a few cases, the epoxy did not set properly. Therefore, it is possible that the DEMEC point moved slightly under the pressure of the gauge, causing an inconsistency between the before and after transfer readings. Care was taken, however, to minimize the occurrences of human errors.

7.2 DEVELOPMENT LENGTH TESTING

7.2.1 Predicted Results

Using the actual material properties, the ultimate total moment (M_u) for each development length was predicted. The ultimate total moment includes all moments due to applied loads, as well as the beam self weight. The analysis was completed using strain compatibility and equilibrium of forces. As presented by Collins and Mitchell [tt], a layer-by-layer evaluation of the section forces was implemented in the analysis. The predicted and experimental ultimate moments, as well as the ratio of the experimental ultimate moment to the predicted value are given in Table 7.6.

As shown in Table 7.6, the experimental values yielded a moment between 3% and 8% higher than the values predicted from the strain compatibility. Furthermore, it should be noted that the predicted strains in the strand were also lower than the experimental values.

If the guaranteed strength of strand (f_{pu} = 270 ksi) were used rather than the actual strength from tests of strand samples, the predicted ultimate moment values would be slightly less than the values given in Table 7.6.

Table 7.6- Comparison of Predicted to Experimental Ultimate Moments (M_u)

Test I.D.	Predicted Mu kN-m *(k-ft)*	Experimental Mu kN-m *(k-ft)*	Predicted/Experimental
L0B0A-1	1430 *(1055)*	1478 *(1090)*	1.03
L0B0B-2	1430 *(1055)*	1546 *(1140)*	1.08
L0B1A-3	1430 *(1055)*	1546 *(1140)*	1.07
L0B1B-4	1430 *(1055)*	1573 *(1160)*	1.08
M0B0A-1	1803 *(1330)*	1898 *(1400)*	1.05
M0B0B-2	1805 *(1331)*	1912 *(1410)*	1.06
M0B1A-3	1807 *(1333)*	1898 *(1400)*	1.05
M0B1B-4	1809 *(1334)*	1952 *(1440)*	1.07
H0B0A-1	1809 *(1334)*	1898 *(1400)*	1.08
H0B0B-2	1810 *(1335)*	1966 *(1450)*	1.08
H0B1A-3	1811 *(1336)*	1925 *(1420)*	1.06
H0B1B-4	1813 *(1337)*	1952 *(1440)*	1.07

7.2.2 Comparison of Test Results within the Test Program

In this section, a general discussion of the development length test results is given. Then, the test results related to each pair of beams will be compared. Finally, a comparison of the test results from different pairs of beams will be given.

7.2.2.1 General Discussion of Development Length Test Results

Since all of the tests resulted in flexural failures, an exact development length cannot be specified from the test results. Development length tests were performed at 2.44, 1.83, 1.37 m (96, 72, and 54 in). Tests under 1.37 m (54 in) would not have resulted in meaningful flexural behavior due to the shear span to depth ratio. Therefore, it is concluded that the development length for all the tests was less than 1.37 m (54 in).

Minor amounts of strand slipping was present in most of the tests with the 54 in embedment length. Therefore, a development length which provides no presence of strand slip at flexural failure exists between 1.83 and 1.37 m (72 and 54 in), but still very close to 1.37 m (54 in).

7.2.2.2 Comparison of Development Length Test Results within Beam Pairs

The first four, second four, and last four tests were performed on the normal strength concrete beams (L0BX), middle strength concrete beams (M0BX), and high strength concrete beams (H0BX), respectively, which all resulted in flexural failures. In the comparison between tests, it should be noted that the L0B0A-1 and L0B0B-2 were not taken to the point of a compression failure in the concrete deck resulting in spalling.

As seen in Table 5.2, as the embedment length was decreased, the achieved flexural cracking and ultimate load increased as expected. On the other hand, but also as expected, the load at the appearance of first shear cracking in the smallest shear spans region, located between the end of the beam and the support located at the embedment length, decreased as the embedment length decreased due to the larger shear stresses present. The appearance of the first shear cracks in the other, longer, shear span decreased with increasing load due to a decrease in shear stress. Also, greater ultimate deflections were experienced, the longer the embedment length. The presence of longitudinal reinforcement in the fourth test of each pair did not have a significant effect on the capacity of the test specimen. The presence of H-bars seemed to only slightly decrease the load at first flexural cracking and to increase the ultimate load achieved by approximately 1% to 4%.

As shown by Table 5.4, the testing of all three pair of beams resulted in no end slip at development lengths of 1.83 and 2.44 m (72 and 96 in). However, during the third test at an embedment length of 1.37 m (54 in), a very minor amount of end slip became apparent. The fourth test, which was also performed at an embedment length of 1.37 m (54 in), included the presence of H-bars and resulted in slightly less end slip in the bottom row of strands. However, the effect of the H-bars on the end slip of the next-to-

the-bottom row of strands in the M0BX and H0BX was not conclusive. The end slip in the top row of strands increased and did not change in the fourth test of the M0BX and H0BX pair of beams, respectively. In all cases, the load at which first end slip occurred seemed to either increase with the presence of the H-bars, or slip did not occur. Also, it is important to note that none of the minor end slips resulted in a reduction of flexural strength in the specimens of this study.

Finally, as shown in Table 5.5, the presence of the longitudinal reinforcement in test four of all three pair of beams caused the location of the maximum crack width to occur at a distance farther from the beam end than the location of the maximum crack width in test three at the same embedment length, without H-bars. The presence of the H-bars, however, did not prevent the cracks from propagating through the location of the prestressing strands in the transfer zone. The H-bars only seemed to control crack width.

7.2.2.2 Comparison of Development Length Test Results between Beam Pairs

Since a true bond failure was not achieved in any of the development length tests, it is not possible to make any definitive statements regarding the effects of concrete strength on the development length. From the results obtained in this portion of the research program, however, it appears that concrete strength does not have a significant effect on development length. The previous statements are based on the fact that the amounts of end slip present in tests with corresponding embedment lengths did not consistently and significantly decrease with increasing concrete strengths.

Also, since only minor amounts of slip occurred, not enough data was obtained to draw a conclusion about the effect of concrete strength on the load at which first slip occurs.

7.2.3 Comparison of Test Results to Suggested Equations

The next level of discussion regarding development length is a comparison of the test results of this study to the current and various suggested expressions for the calculation of development length. Therefore, Table 7.7 summarizes the development

lengths determined using the various expressions and Table 7.8 summarizes the development length results from this study.

It appears that the development length results obtained from this study [1.37 m (54 in)] are significantly less than the values calculated by all the suggested expressions. The most important finding from this comparison is that the current ACI [17] and AASHTO [33] expressions are conservative compared to the test results. In other words, the development length test results are approximately 50% less than the results calculated by the present code equations.

Although no indication of the development length varying with concrete strength was visible from the test results of this study, the Mitchell et. al. [29] equation seems to better approximate the development lengths found in this study than the other equations, while still remaining conservative. The development lengths from this study were 0.6, 0.75, and 0.87 times the development lengths calculated from the Mitchell et. al. equation for the L0BX, M0BX, and H0BX beams, respectively.

Table 7.7- Calculated Development Lengths Using Suggested Equations

Author(s) of Equation(s)	**Calculated Development Length (L0BX)**	**Calculated Development Length (M0BX)**	**Calculated Development Length (H0BX)**
ACI 318 [17]/ AASHTO [31]	[eq1)]2.46m (97 in) [eq2)]2.44 m (96 in)	[eq1)]2.54 mm (100 in) [eq2)]2.54 mm (100 in)	[eq1)]2.54 mm (100 in) [eq2)]2.54 mm (100 in)
Zia & Mostafa [13]	3.12 m (123 in)	2.84 m (112 in)	2.57 m (101 in)
Cousins, Johnston, & Zia [3]	4.44 m (175 in)	3.58 m (141 in)	3.15 m (124 in)
Mitchell et. al. [28]	2.29 m (90 in)	1.83 m (72 in)	1.57 m (62 in)
Burdette, Deatherage, & Chew [20,27]	3.53 m (139 in)	3.66 m (144 in)	3.66 m (144 in)
Buckner (FHWA) [36]	[eq1)]4.10 m (162 in) [eq2)]4.37 mm (172 in)	[eq1)]4.11 m (162 in) [eq2)]4.55 mm (179 in)	[eq1)]4.06 m (160 in) [eq2)]4.55 mm (179 in)

Notes: *f'_{ci} and E_c values used in the equations from the beam cured cylinders*

f_{si} = 200 ksi

f_{se} = 157 ksi (L0BX), 151 ksi (M0BX, H0BX)

f_{se} calculated by estimating losses per AASHTO Code [cc] per Section 9.16.

f_{ps} = 267 ksi

f_{pu} = 270 ksi

B = 300 psi/in

U'd = 1.32

λ = 2.0, because calculated λ is greater than 2.0

1 in = 25.4 mm

1 psi = 6894.8 Pa

Table 7.8- Development Length Results for This Study

Beam I.D.	f'_c	Type of Cross-Section	Ld
L0BX	45.0 MPa (6520 psi)	AASHTO Type I	1.37 m (<54 in)
M0BX	74.0 MPa (10,730 psi)	AASHTO Type I	1.37 m (<54 in)
H0BX	87.8 MPa (12,730 psi)	AASHTO Type I	1.37 m (<54 in)

7.2.4 Comparison of Test Results with Related Experimental Results

The last level of discussion of development length is a comparison of the results from this test program to the results of other test programs. However, only the development length results from previous literature which correspond to specimens containing 15.2 mm (0.6 in) diameter, Grade 270, prestressing strand, and concrete strengths equivalent to the those used in this test program will be compared with the test results of this study. A summary of these relevant results is listed in Table 7.4.

The development lengths from this study are less than the development lengths reported to date for 15.2 mm (0.6 in) strands. The development lengths closest to the results of this study were found by Cordova [42] through the testing of Texas Type C beams with bright 15.2 mm (0.6 in) diameter prestressing strands. Cordova [42] reported l_d < 1.83 m (72 in), which is 1.33 times the development length found in this study.

Table 7.9- Summary of Development Length Results from Previous Literature

Researchers	f'c	Type of Cross-Section	Strand Condition	Average L_d
Russell & Burns [6]	48.4 MPa (7020 psi) 43.9-51.3 MPa (6360-7440 psi)	prism I-beams	bright bright	(<78 in) (84 in)
Cousins et. al. [3]	34.5 MPa (5000 psi)	6x10	bright	3.35 m (132 in)
Burdette et. al. [20,27]	35.4-55.0 MPa (5130-7980)	AASHTO Type I	rusty	2.20 m (85 in)
Gross [33]	81.7 MPa (11,850 psi)	prism (14x42 in)	rusty	2.00 m (78 in)
Cordova [42]	48.3 MPa (7000 psi)	Texas Type C	bright	1.83 m (<72 in)

Notes: 1 in =25.4 mm

7.2.5 Possible Sources of Error in the Test Results

Only minor *equipment problems* were encountered during the development length testing. These minor problems included a few potentiometers and strain gauges which failed to give valid readings. Thankfully, the failure of these devices did not occur on a large scale and they duplicated other data readings. Therefore, when a single potentiometer or strain gauge failed, other potentiometers or strain gauges were able to be used to obtain the necessary data.

The only significant other problem encountered during development length testing was the inability to force the occurrence of a bond failure. The shortest embedment length tested was 1.37 m (54 in). Any length shorter than 1.37 m (54 in) would not have resulted in a meaningful test. The test specimen would not have behaved as a true flexural member, but more like a "deep beam." This value is shorter than other test programs have reported, thus it was not a concern with respect to safety in the current code equation. The current code equation is quite safe for development length.

7.3 STRAND PULL-OUT TESTING

7.3.1 Discussion of Pull-Out Results

The peak loads achieved in the pull-out testing ranged from 240 to 272 kN (54.1 to 61.1 kips) and are summarized in Table 7.10. All the values in this range yield a strand stress results within 8% of f_{pu} = 1.86 GPa (270 ksi) for the prestressing strand. Also, all the peak load values are above the benchmark of 160 kN (36 kips), determined by Logan in the testing of 12.7 mm (0.5 in) strand to be the benchmark for very conservative test results compared to ACI [17] provisions for transfer and development length. A plot comparing the peak loads from the pull-out tests of this study and the benchmark determined by Logan is given in Figure 7.3.

Table 7.10- Summary of the Peak Loads Achieved in Pull-Out Testing

f'_c (psi)	Embedment Length (in)	Average Peak Load (kips)	Range of Peak Loads (kips)
5250	21	57.4	55.6-59.9
7800	20	59.7	58.2-59.2
7800	18	59.0	58.2-60.9
11070	20	60.0	58.7-61.1
11070	18	55.5	54.1-57.7

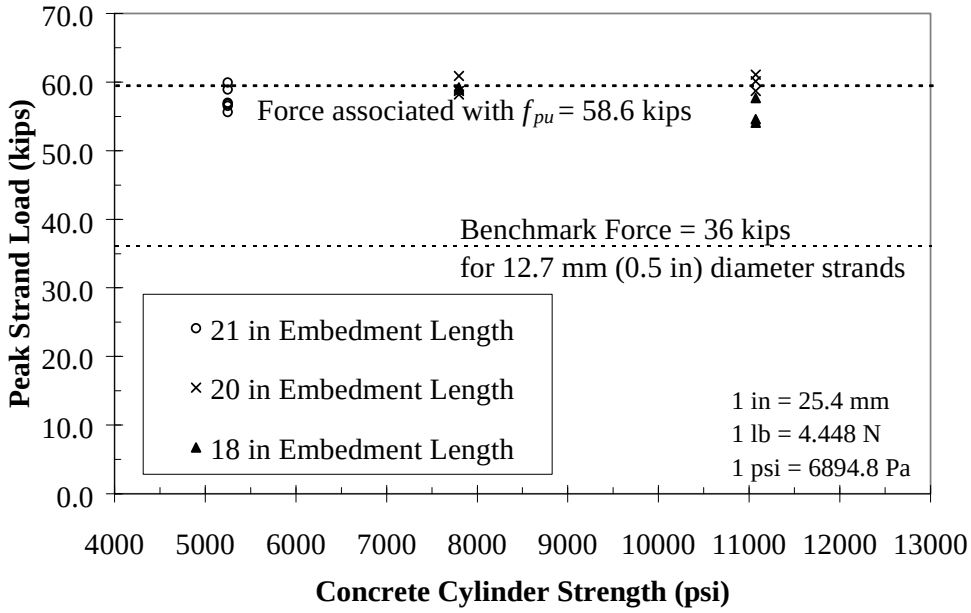

Figure 7.3- Comparison of Peak Loads to the Benchmark Determined by Logan

Since the transfer and development length results from this study are conservative compared to the ACI [17] provisions, it appears that the pull-out test results adequately indicated the satisfactory quality of bond performance to be expected between the strand and the concrete. Therefore, the test results from this study agree with the conclusion made by Logan, that the pull-out test is an "accurate predictor of the general transfer and development characteristics of the strand in pretensioned, prestressed concrete applications."

The results of pull-out tests with embedment lengths of 15.2 mm (0.6 in) diameter strand had similar peak load values for the embedment lengths 457, 508, and 533 mm (18, 20, and 21 in), as shown in Table 7.10. For this reason, it was decided that 457 mm (18 in) would be used for all future pull-out tests of 15.2 mm (0.6 in) diameter strands in this overall test program.

7.3.1 Possible Sources of Error in the Test Results

The main problem that exists in the execution of pull-out testing is *human error* in reading the important values. It is difficult to get an exact reading of the load at first slip, the peak load, and the total amount of slip because the loading is continuous and the reader must be watching the load output voltage and the strand simultaneously. Therefore, for example, when a strand first slips, the reader must look immediately at the load output voltage. Although the value recorded is close, it is not the exact measurement at first slipping because the load was continuing to increase during the time from when the reader first noticed the slipping until the load output voltage was viewed.

CHAPTER EIGHT

SUMMARY AND CONCLUSIONS

8.1 SUMMARY

In summary, the test program discussed in this thesis includes six 12.2 m (40 ft) long AASHTO Type I highway bridge girders containing 15.2 mm (0.6 in) diameter, fully bonded, Grade 270, low-relaxation prestressing strand. Each pair of beams contains concrete with a 28-day compressive strength of either 34.5-48.3 MPa (5-7 ksi), 65.5-79.3 MPa (9.5-11.5 ksi), or 89.6-103.4 MPa (13-15 ksi). The other variable in the test program is the possible presence of longitudinal shear reinforcement, which is present in only one end of each pair of beams.

The beams were cast in pairs and instrumented at Texas Concrete in Victoria, TX, for the execution of transfer length testing and subsequently delivered to Ferguson Structural Laboratory in Austin, TX, for the execution of development length testing. Each test specimen was completed at the laboratory by casting a composite concrete deck, which was designed to allow the bottom strands in the beam to reach a total strain of 0.035, 3.5%. The length of the test specimens was designed to enable two development length tests to be performed on each specimen. Pull-out testing was also included in the test program in order to determine a qualitative perspective of the expected bond performance between the concrete and the prestressing steel in the test specimens.

8.1.1 Transfer Length Testing

Transfer length testing is important both in relationship to web shear cracking and to help determine the possibility of a development anchorage failure resulting from shear or flexural cracking in the transfer zone.

Therefore, the test specimens were instrumented to determine the transfer length by measuring the concrete surface strains at the center-of-gravity of the bottom

prestressing strands using the DEMEC system, and by measuring the draw-in of the prestressing strands.

The transfer length was determined using the 95% Average Maximum Strain Method, the Slope-Intercept Method, and the Draw-In and Initial Prestress Method. However, since the 95% Method yields the most reliable results and problems were encountered with the draw-in instrumentation, as discussed in Chapter Four, the 95% Method was used for all comparisons, although the Slope-Intercept Method was used to confirm trends. A summary of the average transfer length results determined using the 95% Method is given in Table 8.1. Also, included in Table 8.1 are the average transfer lengths calculated from the draw-in, using the assumption of constant bond stresses in the transfer zone (α =2).

Table 8.1- Summary of Transfer Length Results

			95% Method		**Draw-In Method**	
Beam I.D.	**f'_{ci} (MPa)**	**f'_c (MPa)**	**After Transfer**	**After Deck Placement**	**After Transfer**	**After Deck Placement**
Ave L_t for. L0BX	29.2	45.0	496 mm (19.5 in)	674 mm (26.5 in)	384 mm (15.1 in)	----
Ave L_t for. M0BX	45.6	74.0	495 mm (19.5 in)	545 mm (21.5 in)	575 mm (22.6 in)	751 mm (29.6 in)
Ave L_t for. H0BX	76.2	87.8	426 mm (16.8 in)	440 mm (17.3 in)	259 mm (10.2 in)	436 mm (17.2 in)

Notes: 1 in =25.4 mm
1 psi = 6894.8 Pa

The bar chart discussed in Chapter Four is re-presented here in Figure 8.1 as a summary of the relationship between the experimentally determined transfer lengths and selected suggested equations for transfer length. As visible in Figure 8.1, the code equations yield conservative results for transfer length.

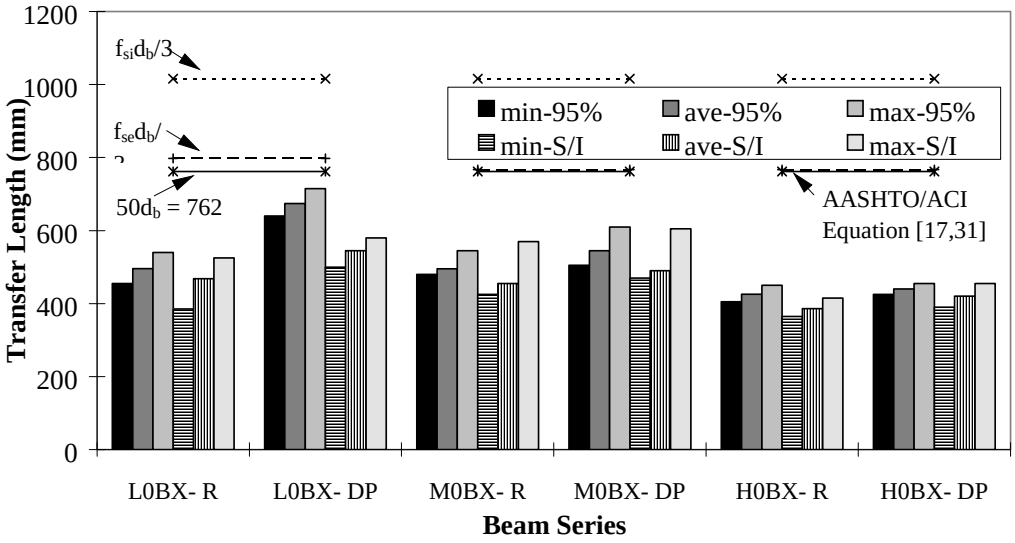

Figure 8.1- Comparison of Test Results with Selected Equations

8.1.2 Development Length Testing

Development length testing is important to determine the embedment length necessary to prevent anchorage failure of the prestressing strands. Therefore, the test specimens were tested at different embedment lengths to failure. If the test resulted in a flexural failure, the embedment length was shortened for the next test, or in a bond failure, the embedment length was increased.

The test specimens were instrumented to measure deflections in the constant moment region, at the supports, on the bearing pads. Also, instrumentation was placed to measure end slip of the strands and the applied load.

Development length tests were performed at embedment lengths of 2.44, 1.83, 1.37 m (96, 72, and 54 in) for all three pair of beams. The fourth test of each beam pair was used to determined the effect of horizontal shear reinforcement on the behavior of the test specimen. Therefore, the fourth test was conducted at the same embedment

length as the previous embedment length closest to a bond failure, which was 1.37 m (54 in) for all three pair of beams.

The development length test results were the same for all three pair of beams; that is, l_d < 1.37 m (54 in). Small amounts of end slip occurred in the tests at 1.37 m (54 in); therefore, if a flexural failure without the presence of slip is desired, the required embedment length is very close to 1.37 m (54 in).

The actual achieved ultimate total moments were between 3% and 8% higher than the ultimate moments predicted from the analysis. Also, the code equations, along with all the suggested expressions, for development length are conservative with respect to the test results. The code equations result in a development length twice the results of this study.

8.1.3 Strand Pull-Out Testing

A direct tension pull-out test is an experimental arrangement which tests the bond characteristics of seven-wire strand that is not tensioned before loading. Pull-out testing is important to obtain a qualitative understanding of the expected bond performance between a given concrete mix and steel prestressing strand.

Therefore, pull-out blocks were manufactured along with the concrete beams and were tested at a later date, according to the specified test procedure described in Chapter Six. A summary of the pull-out test results is given in Table 8.2 and is illustrated in Figure 8.2.

Table 8.2- Summary of Pull-Out Test Results

f'_c MPa *(psi)*	Embedment Length mm *(in)*	Average Peak Load N *(kips)*	Range of Peak Loads N *(kips)*
36.2 (5250)	533 *(21)*	255 *(57.4)*	247-266 *(55.6-59.9)*
53.8 *(7800)*	508 *(20)*	266 *(59.7)*	259-263 *(58.2-59.2)*
53.8 *(7800)*	457 *(18)*	262 *(59.0)*	259-271 *(58.2-60.9)*
76.3 *(11,070)*	508 *(20)*	267 *(60.0)*	261-270 *(58.7-61.1)*
76.3 *(11,070)*	457 *(18)*	247 *(55.5)*	241-257 *(54.1-57.7)*

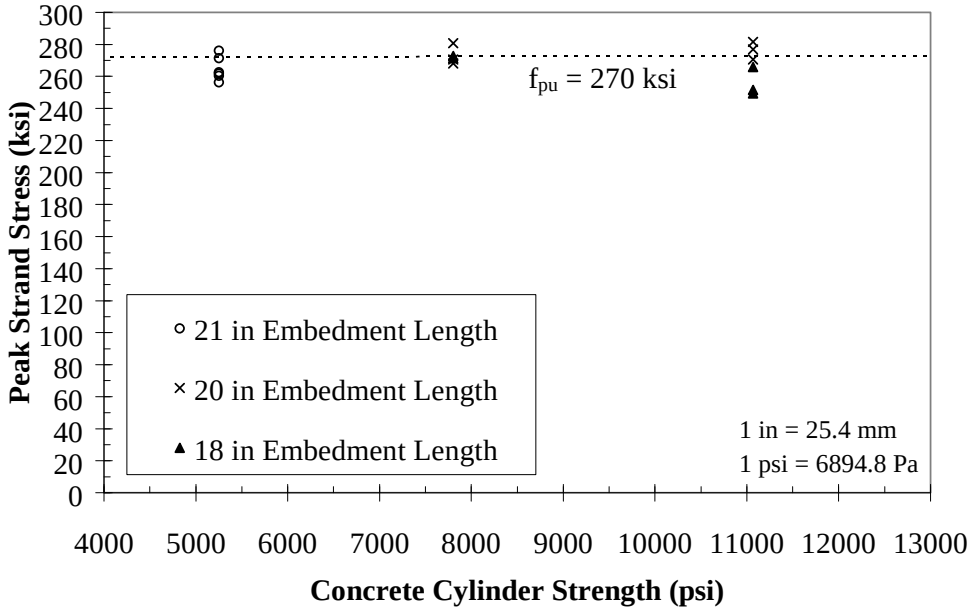

Figure 8.2- Peak Strand Stress vs. Concrete Cylinder Strength for Pull-Out Tests

8.2 CONCLUSIONS

Several conclusions, including the fact that the ACI and AASHTO equations are conservative, can be made from the results of this test program which included specimens containing bright, fully bonded 15.2 mm (0.6 in) diameter prestressing strand. These specimens provide the first portion of results to be presented in association with TxDOT Project 1388, as discussed in Sections 1.2 and 1.3. Two sets of conclusions will be presented. The first set of conclusions will be specific to the test results, and the second set will present possible trends observed in the test results. It is important to note that any visible trends are *preliminary* and should be considered in light of all the test results of the research program, which will be discussed and presented in full by Robbie Barnes at the conclusion of the project.

8.2.1 Transfer Length Testing

The following conclusions can be drawn from the transfer length test results of this test program:

1. The code equations for transfer length of $50*d_b$ and $f_{se}*d_b/3$ are *conservative*. This is a significant conclusion in light of previous research which has yielded unconservative results.
2. The transfer length at transfer and after deck placement for the *normal strength* concrete beams is 496 and 674 mm (19.5 and 26.5 in), respectively.
3. The transfer length at transfer and after deck placement for the *middle strength* concrete beams is 495 and 545 mm (19.5 and 21.5 in), respectively.
4. The transfer length at transfer and after deck placement for the *high strength* concrete beams is 426 and 440 mm (16.8 and 17.3 in), respectively.
5. The equation developed by Mitchell et. al. [29] is based on high-strength concrete material properties at release of the prestress and seems to closely fit the test results and the trends indicated by the test results, while remaining conservative.

The test results from the transfer length testing associated with this test program seem to indicate the occurrence of the following general trends:

1. Transfer length decreases with increasing concrete strengths.
2. Transfer length increases over time, but the transfer length was still well within the current AASHTO equation [31] predicted values..
3. The effect of time on the transfer length decreases as the concrete strength increases.

8.2.2 Development Length Testing

The following conclusions can be drawn from the development length test results of this test program:

1. The ACI [17] and AASHTO [31] code equations for development length are *conservative*.
2. All proposed equations for development length appear to be *conservative.*
3. Since a true bond failure did not occur it is hard to make a significant conclusion about the presence of longitudinal shear reinforcement in the test specimens. However, the following statements can be made about the effect of H-bars:
    - H-bars do not appear to reduce development length.
    - H-Bars did not appear to reduce the presence of end slip in all cases.
    - H-bars help to control crack widths, but do not prevent crack growth.
    - H-bars do not greatly affect the ultimate moment capacity. The moment capacities of specimens with H-bars was between 1% and 3% greater than the moment capacities of specimens without H-bars.

The following conclusions associated with the results of the development length portion of this test program can be made regarding the occurrence of possible trends:

1. It is not possible to make a conclusion about the effect of concrete strength on development length due to the inability to force a true bond failure. Although a minor amount of strand end slip was present in all the development length tests at 54 in without H-bars, the magnitude of the strand slip was not significant.
2. Not enough end slip data was obtained to determine the effect of concrete strength on the load at which a strand first slips.

8.2.3 Strand Pull-Out Testing

The pull-out testing performed for each pair of beams indicated that adequate bond performance was achieved, with all results within 8% of f_{pu} = 1.86 GPa (270 ksi) for the prestressing strand. This conclusion is validated by the conservative results obtained from the transfer and development length testing performed on the test specimens.

The test results indicate that the difference in the bond performance using a 457, 508, 533 mm (18, 20, or 21 in) embedment length is not significant. Therefore, for simplicity, since an 457 mm (18 in) embedment length has already been established for pull-out testing on 12.7 mm (0.5 in) diameter strand, a 457 mm (18 in) embedment length should be also be used for the 15.2 mm (0.6 in) diameter prestressing strand.

APPENDIX A

NOTATION

a	Distance from outside load point to location of hydraulic ram
A_{ps}	Area of one prestressing strand
B	Bond modulus
b	Width of the slab
c	Neutral axis
d_b	Diameter of prestressing strand
E_c	Modulus of elasticity of concrete
E_{ci}	Modulus of elasticity of concrete at transfer
E_{ps}	Modulus of elasticity of the prestressing strand
ES	Elastic shortening due to release of prestress
f'_c	Concrete compressive strength at 28 days
f'_{ci}	Concrete compressive strength at transfer
f_{ps}	Stress in strands at failure
f_{pu}	Ultimate tensile strength of strands
f_r	Modulus of rupture of concrete
f_{se}	Effective stress in prestressing strands after losses
f_{si}	Stress in strands immediately before transfer
H-bars	Longitudinal shear reinforcement in beam web
L_c	Cantilever length of test specimen
l_d	Development length of prestressing strands
L_e	Embedment length of prestressing strands
L_{lp}	Distance between load points (length of constant applied moment region)
L_o	Overhang length of test specimen at outer bearing pad
l_{pe}	Embedment length of prestressing strands in pull-out tests
L_s	Simply Supported Test Span Length

L_t	Transfer length of prestressing strands
$L_{t,DP}$	Transfer length of prestressing strands after deck placement
$L_{t,R}$	Transfer length of prestressing strands after release of prestress
$M_{u,total}$	Maximum total moment at critical section
P_{cr}	Applied load at first flexural cracking
P_{sc1}	Applied load at first shear cracking in the shortest shear span
P_{sc2}	Applied load at first shear cracking in the longest shear span
$P_{slip,a}$	Applied load at first slipping of bottom row of strands (row a)
$P_{slip,b}$	Applied load at first slipping of next to bottom row of strands (row b)
P_u	Applied load at ultimate
s	center-to-center distance between prestressing strands
U'_d	Plastic bond stress coefficient for development
U'_t	Plastic bond stress coefficient
V_{cw}	Nominal shear strength provided by concrete when diagonal cracking results from excessive principal tensile stress in web
α	Coefficient indicating shape of bond stress distribution in transfer zone 2 for a constant and 3 for a linear bond stress distribution
Δ_u	Net deflection at ultimate
Δ_r	Residual deflection
ε_s	Strain in steel at a given time
ε_{si}	Initial prestrain before release of prestress

APPENDIX B

ENGLISH - METRIC UNIT CONVERSIONS

Table B.1- English to Metric Unit Conversions

English	**Multiply by**	**= Metric**
1 psi	6894.8	Pa
1 in	2.54	cm
1 lb	4.448	N
1 oz	28.349	g
1 kip-ft	1.35596303	kN-m

APPENDIX C

MATERIAL PROPERTIES

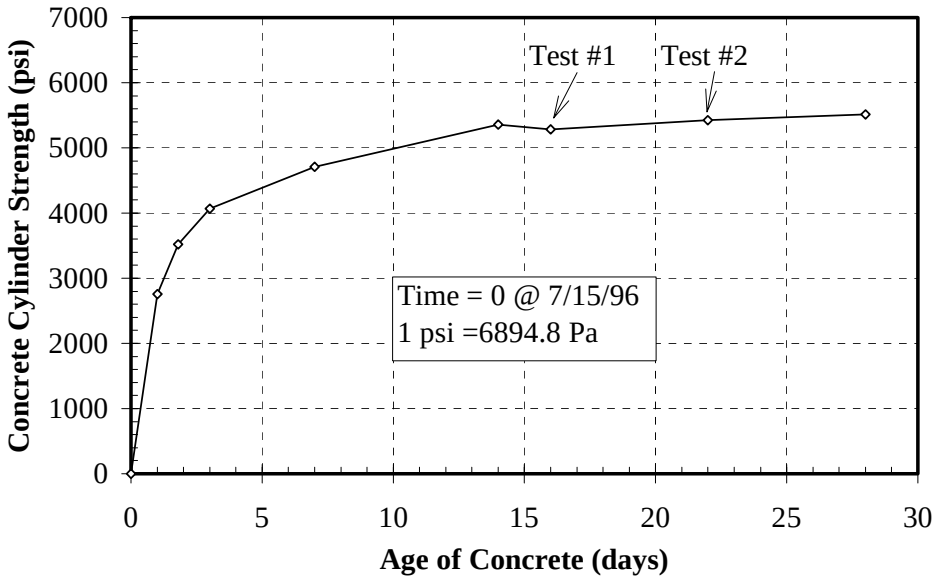

Figure C.1- Concrete Strength (f'$_c$) vs. Time for L0B0 Slab

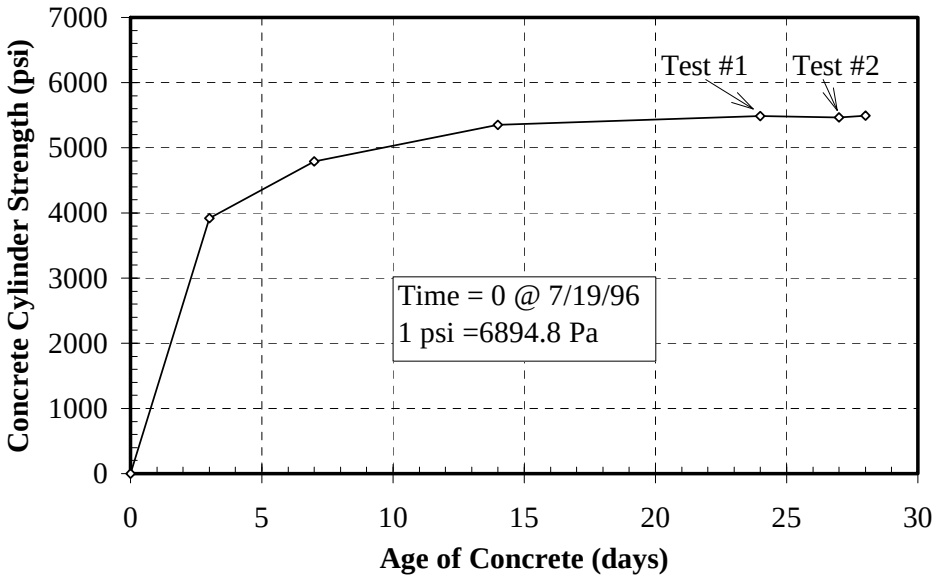

Figure C.2- Concrete Strength (f'$_c$) vs. Time for L0B1 Slab

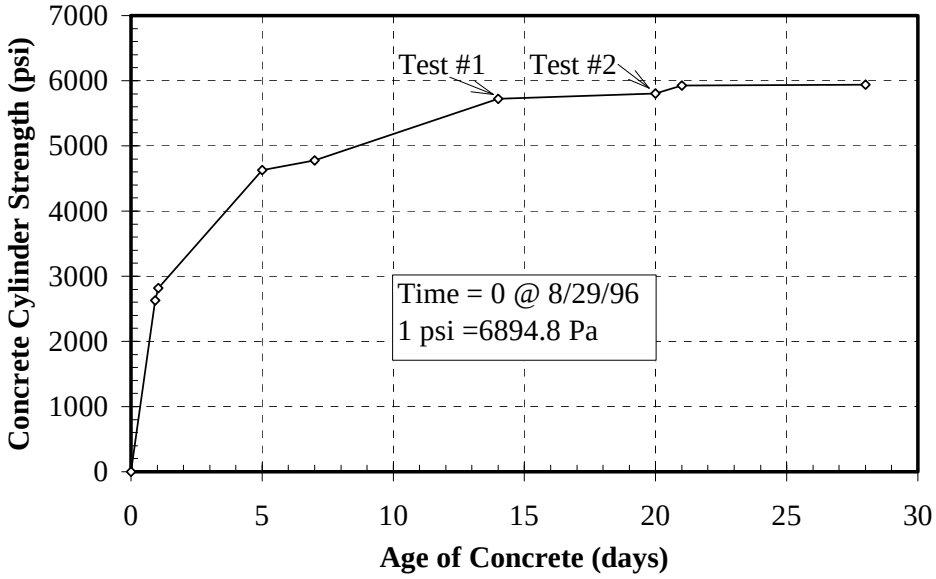

Figure C.3- Concrete Strength (f'_c) vs. Time for M0B0 Slab

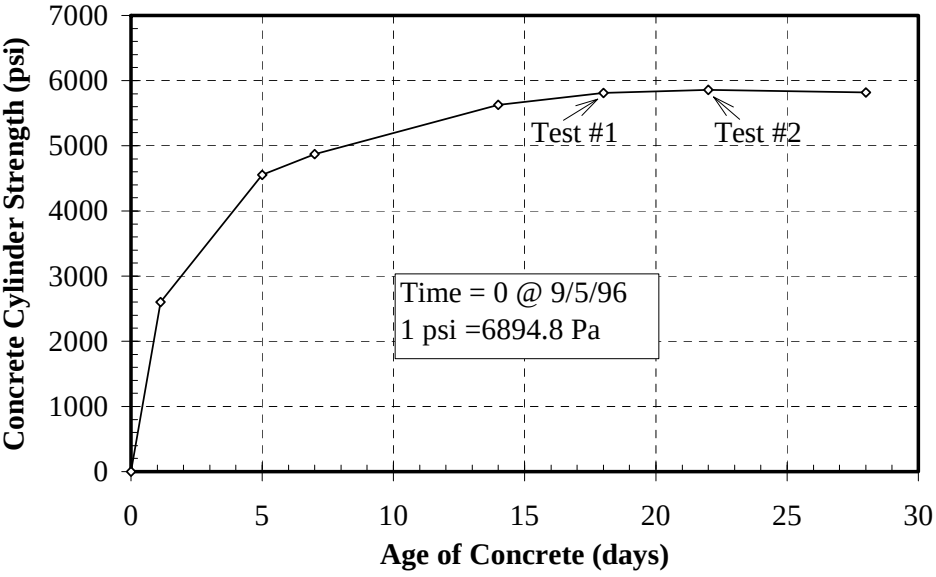

Figure C.4- Concrete Strength (f'_c) vs. Time for M0B1 Slab

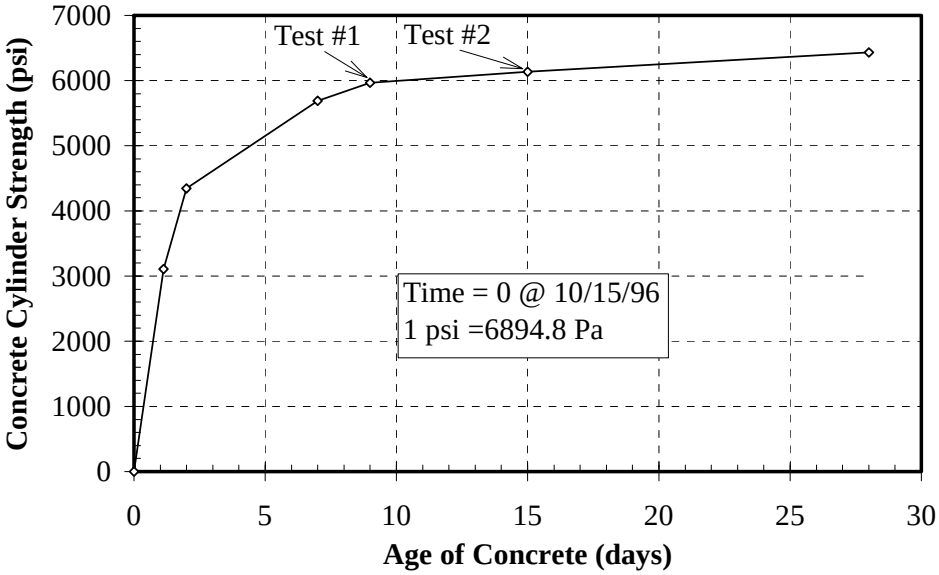

Figure C.5- Concrete Strength (f'_c) vs. Time for H0B0 Slab

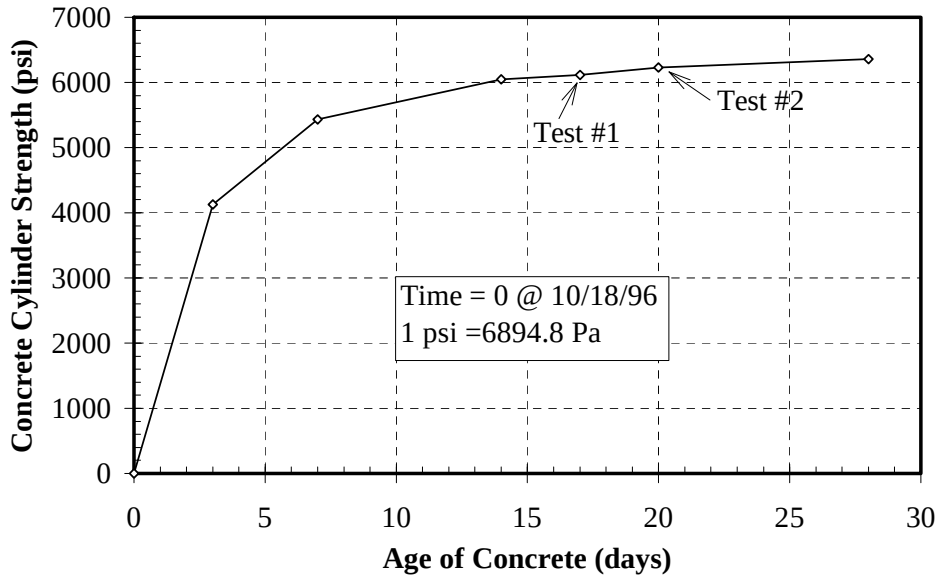

Figure C.6- Concrete Strength (f'_c) vs. Time for H0B1 Slab

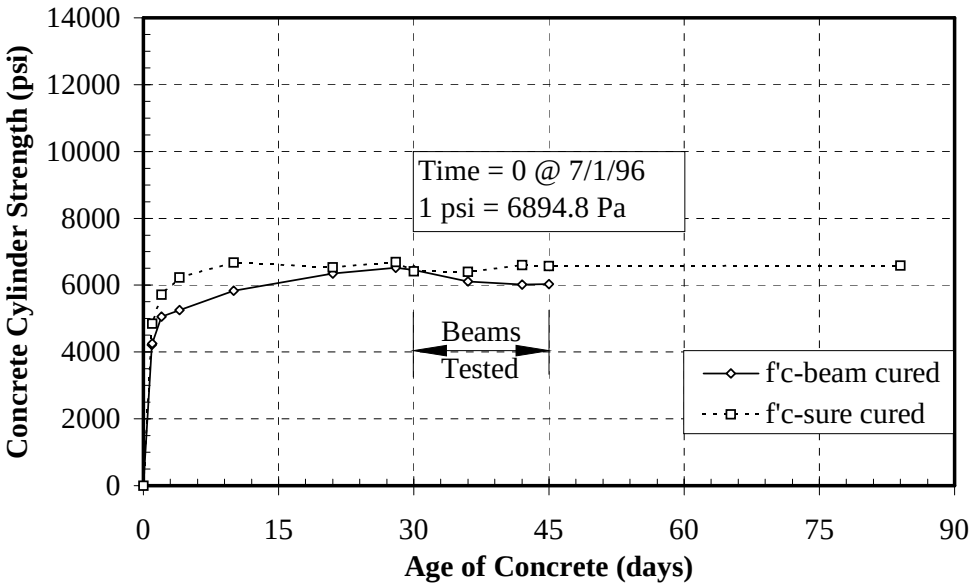

Figure C.7- Concrete Strength (f'_c) vs. Time for L0BX Beams

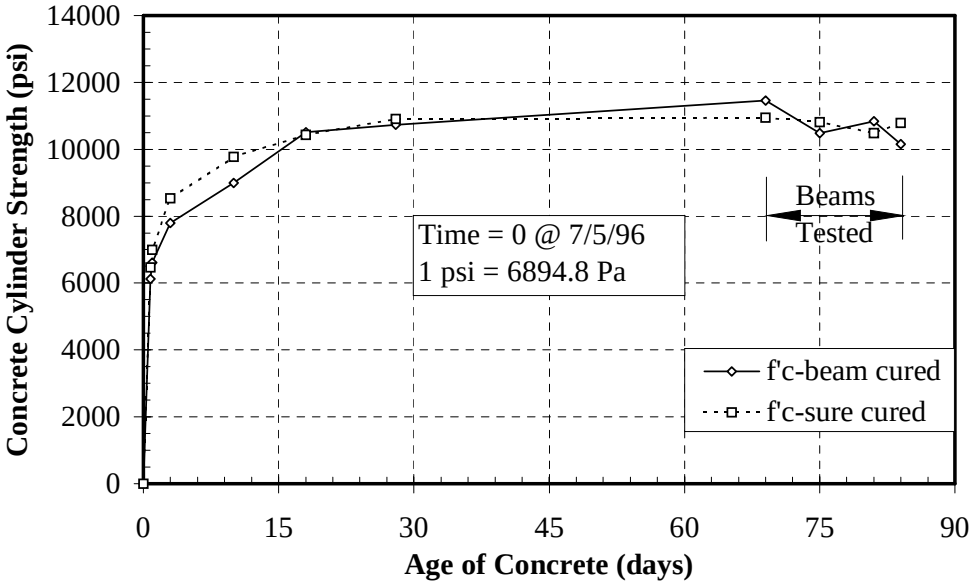

Figure C.8- Concrete Strength (f'_c) vs. Time for M0BX Beams

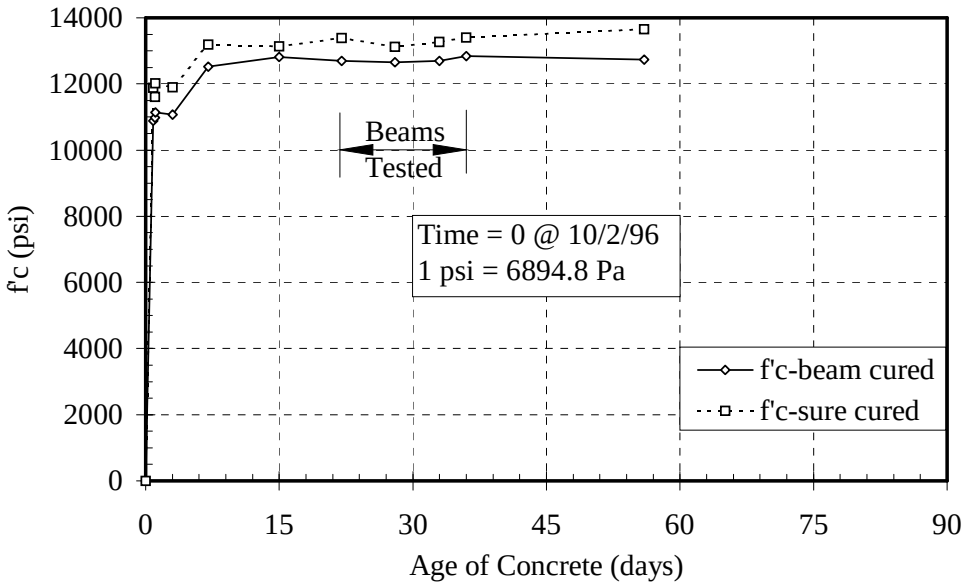

Figure C.9- Concrete Strength (f'_c) vs. Time for H0BX Beams

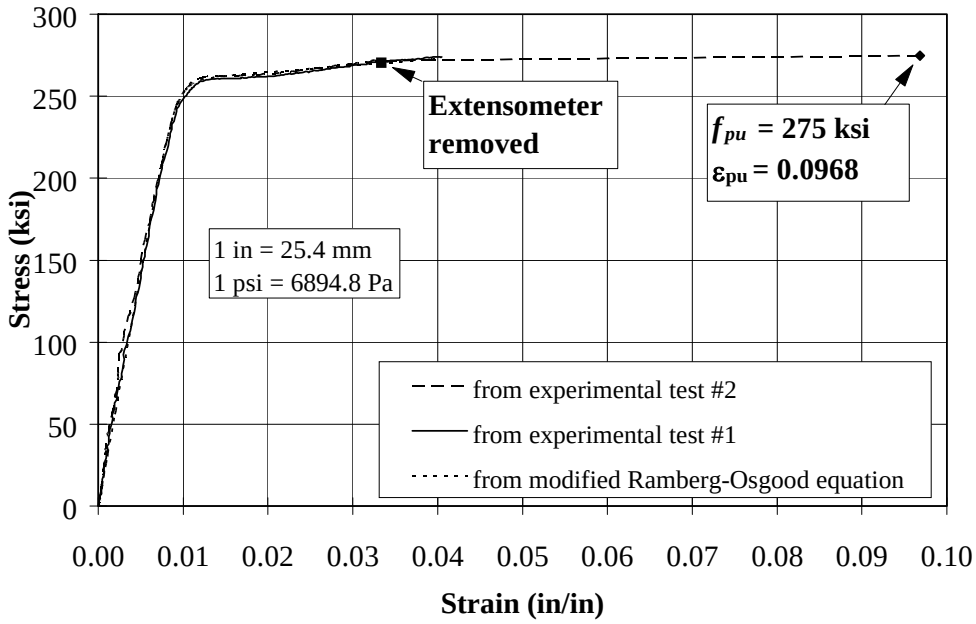

Figure C.10- Stress vs. Strain Relationship for L0BX and M0BX Beams

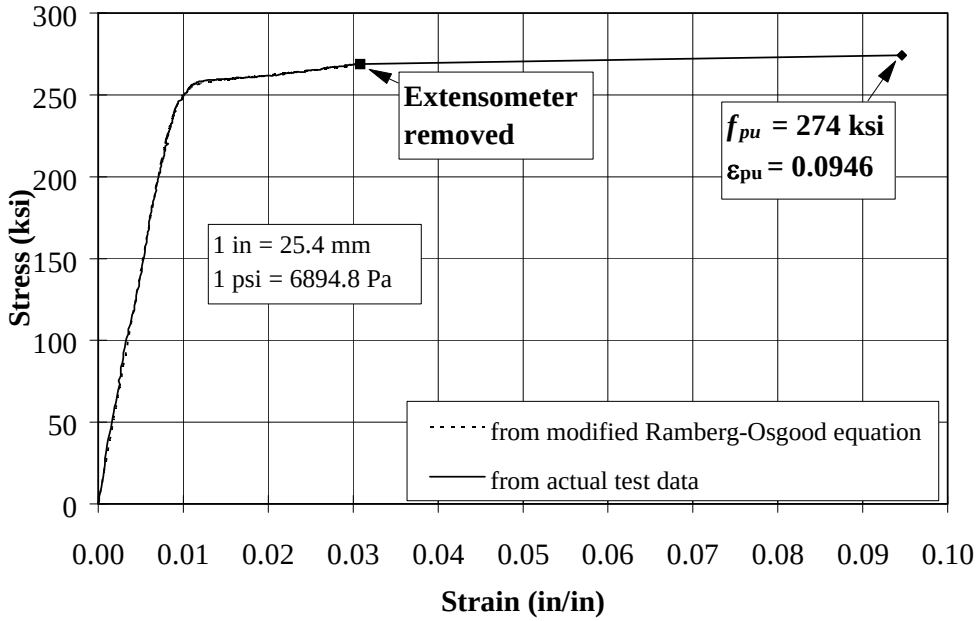

Figure C.11- Stress vs. Strain Relationship for H0BX Beams

APPENDIX D

STRAIN PROFILES
AND
TRANSFER LENGTH MEASUREMENTS

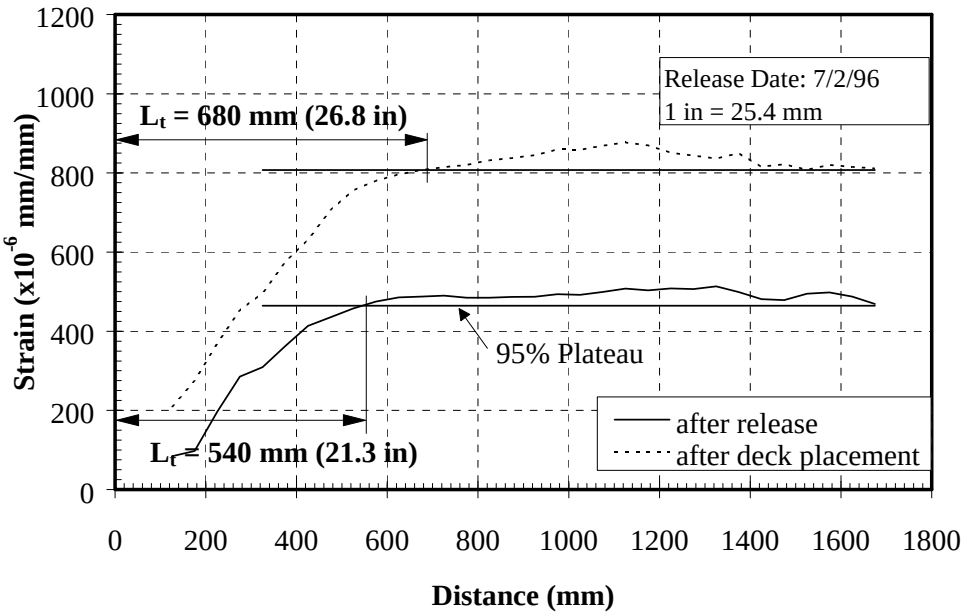

Figure D.1- Strain Profile for L0B0A-1

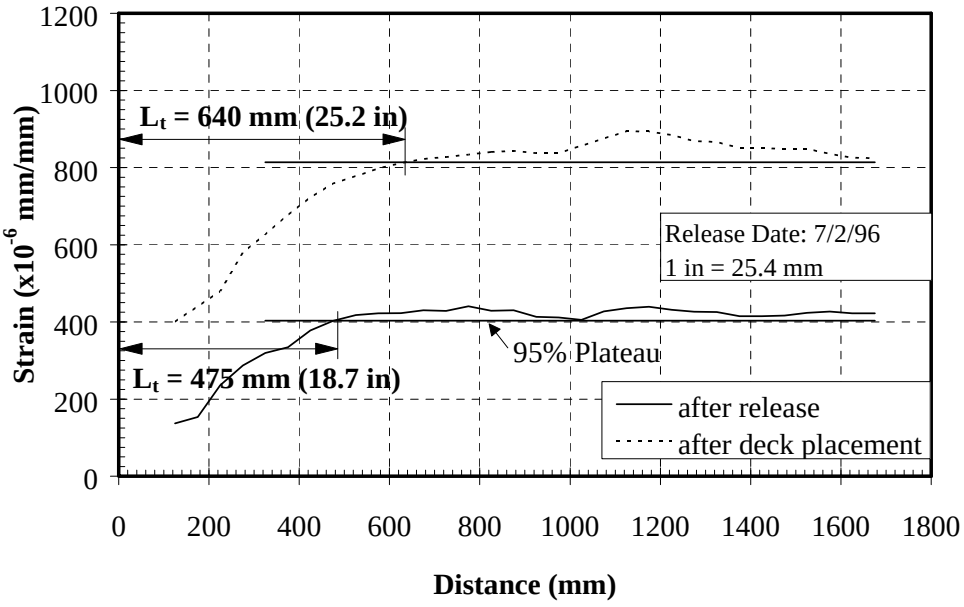

Figure D.2- Strain Profile for L0B0B-2

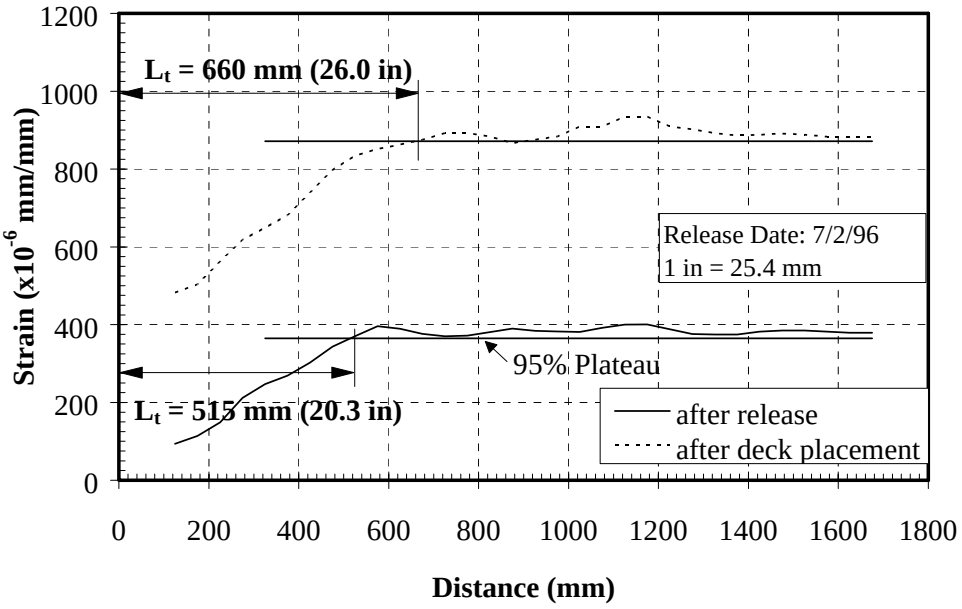

Figure D.3- Strain Profile for L0B1A-3

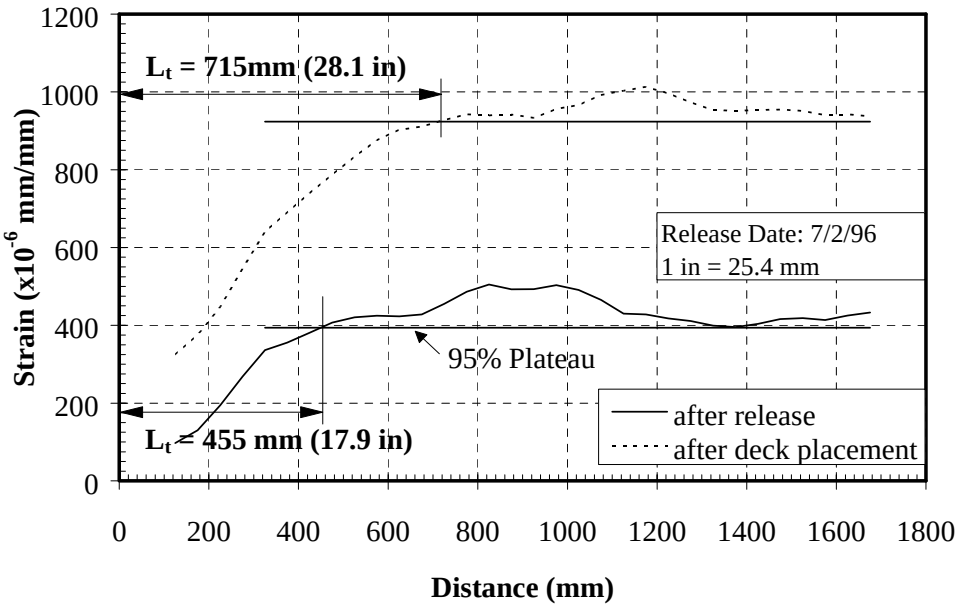

Figure D.4- Strain Profile for L0B1B-4

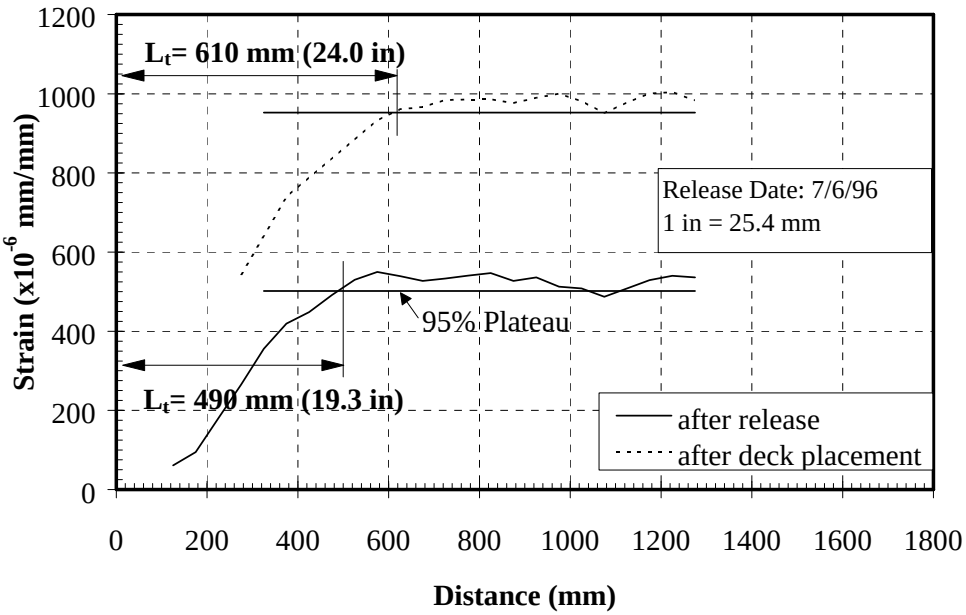

Figure D.5- Strain Profile for M0B0A-1

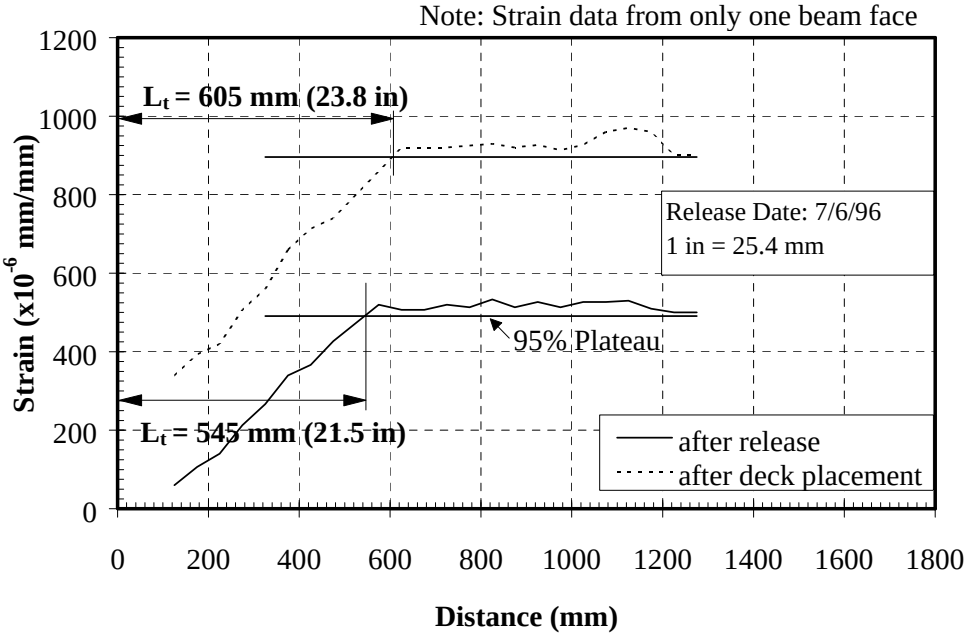

Figure D.6- Strain Profile for M0B0B-2

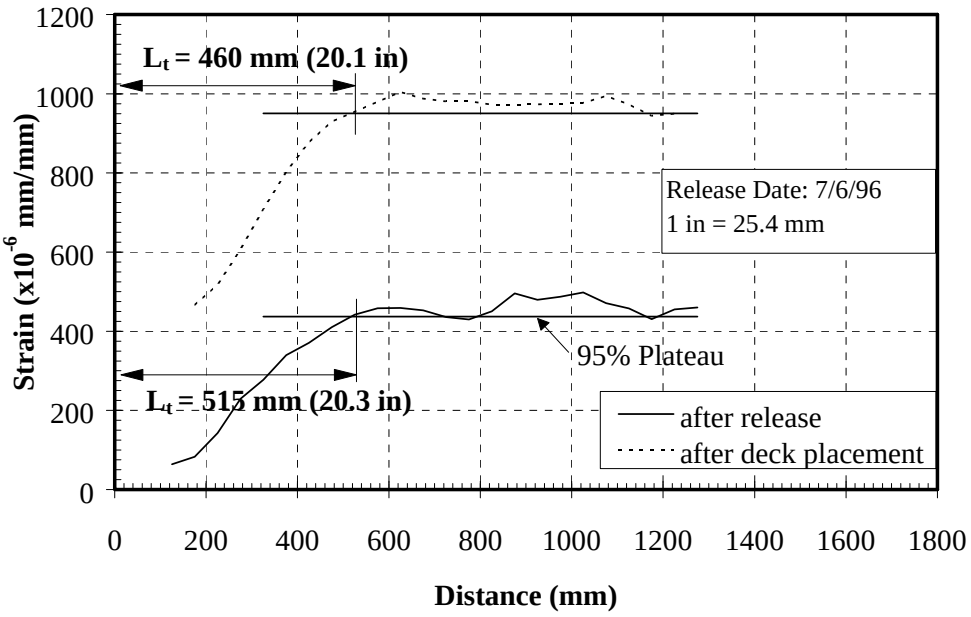

Figure D.7- Strain Profile for M0B1A-3

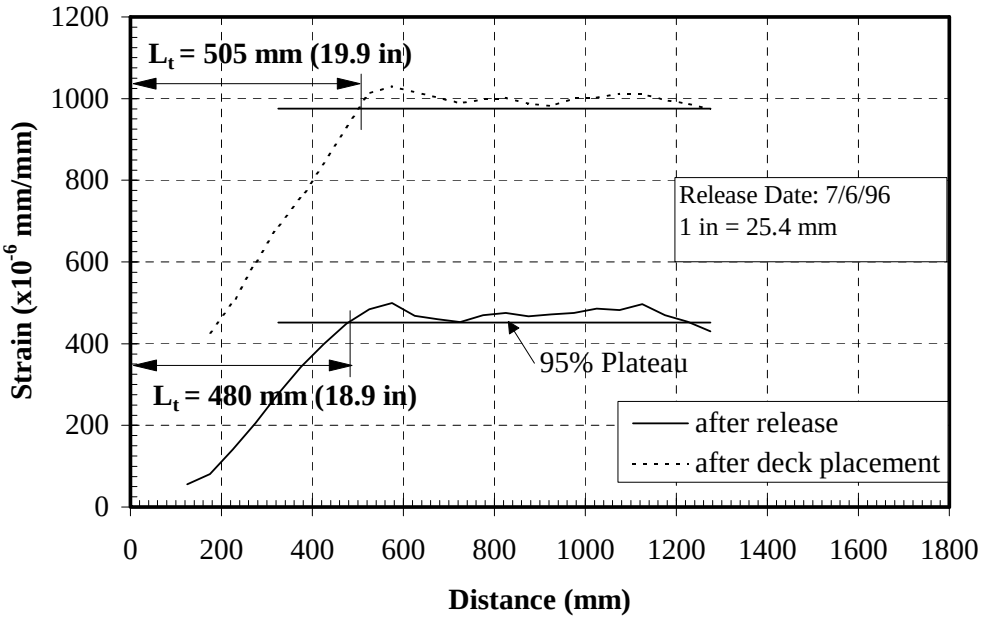

Figure D.8- Strain Profile for M0B1B-4

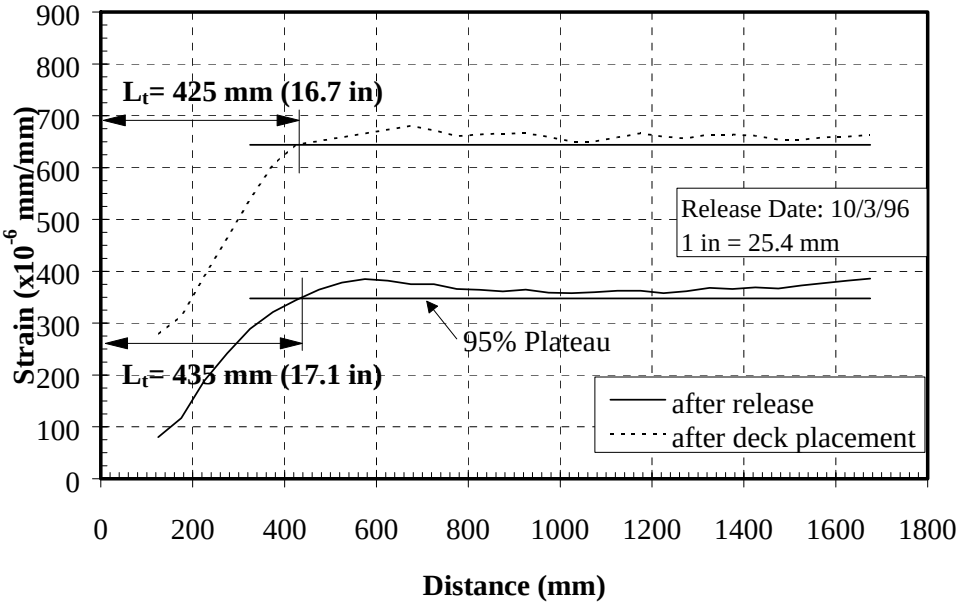

Figure D.9- Strain Profile for H0B0A-1

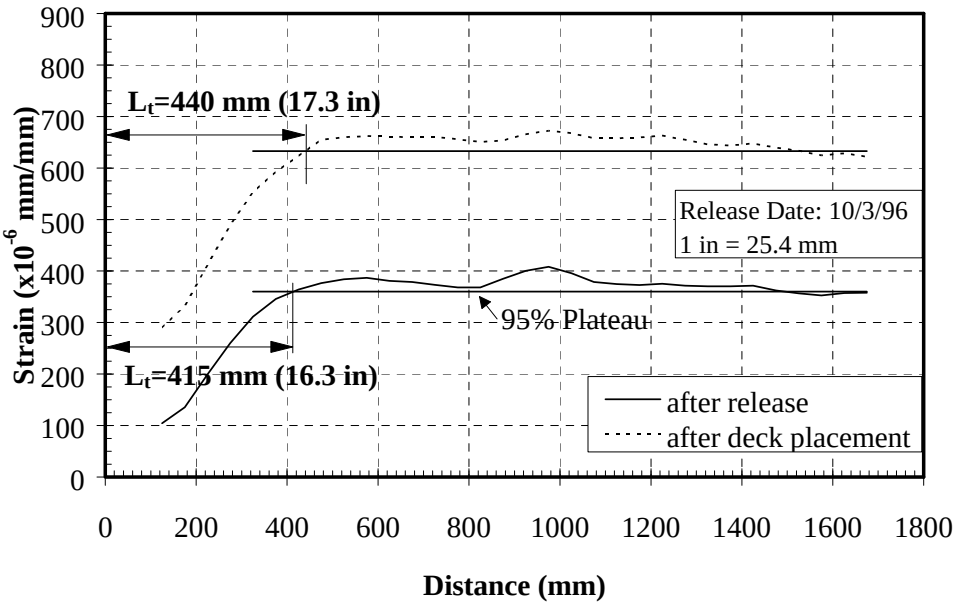

Figure D.10- Strain Profile for H0B0B-2

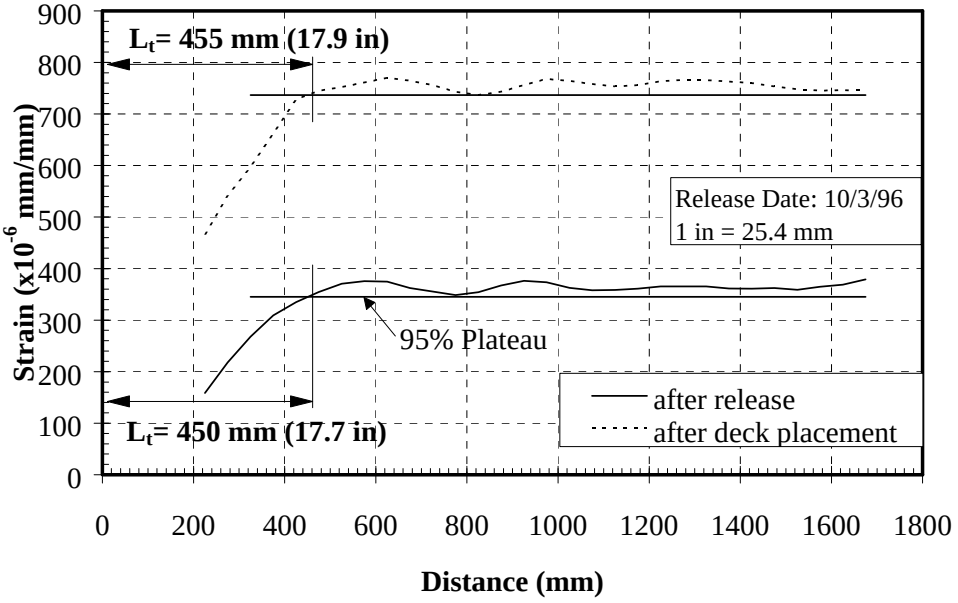

Figure D.11- Strain Profile for H0B1A-3

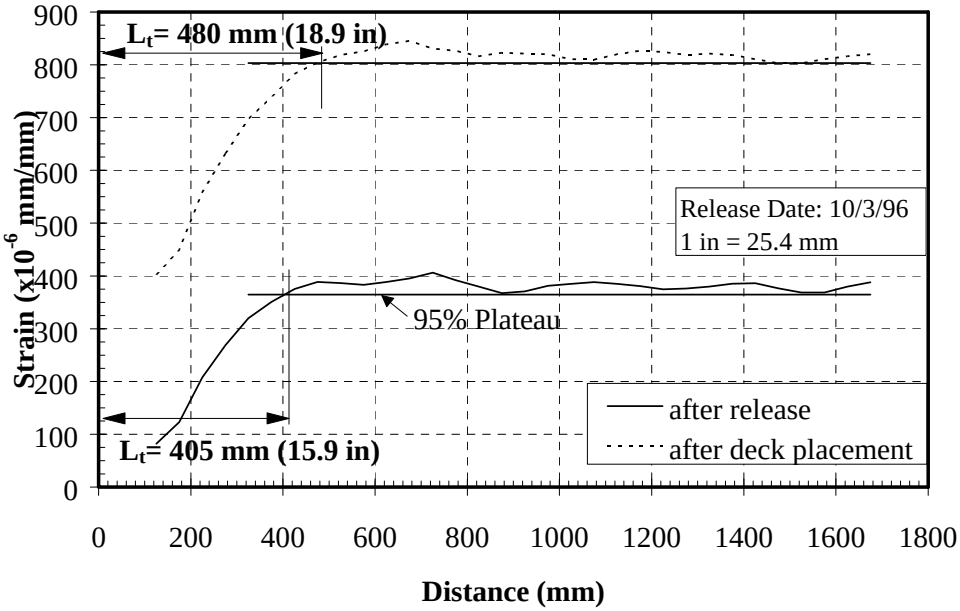

Figure D.12- Strain Profile for H0B1B-4

APPENDIX E

MEASURED DRAW-IN CHARTS

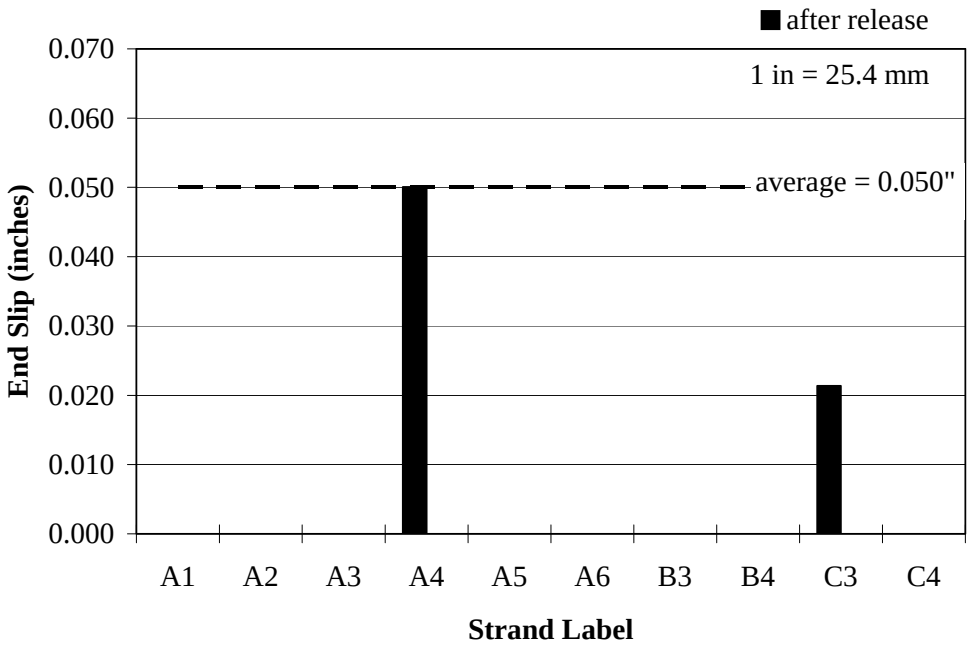

Figure E.1- Measured Draw-in Results for L0B0A-1

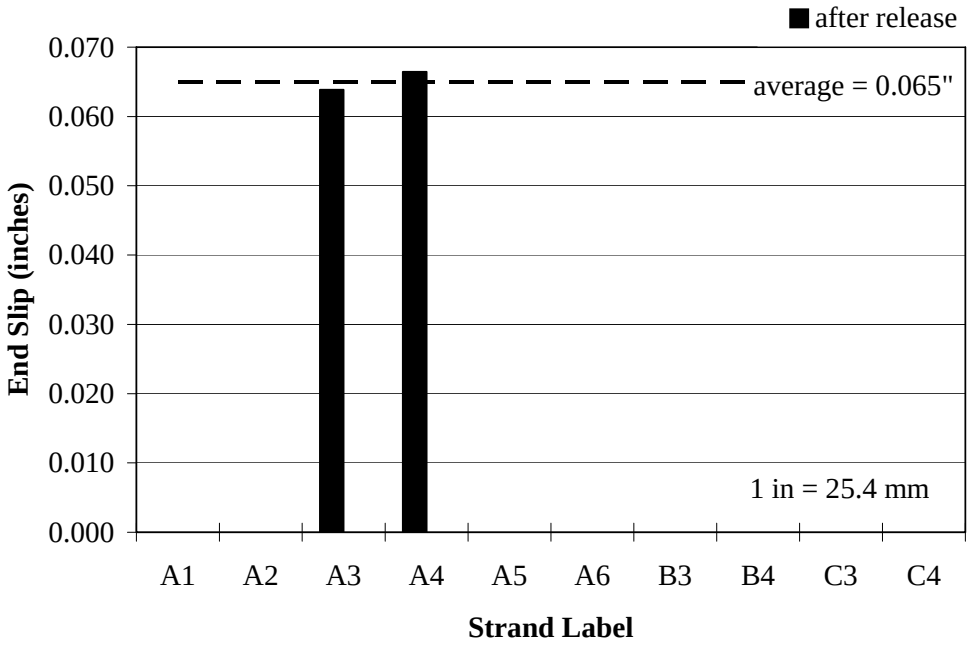

Figure E.2- Measured Draw-In Results for L0B0B-2

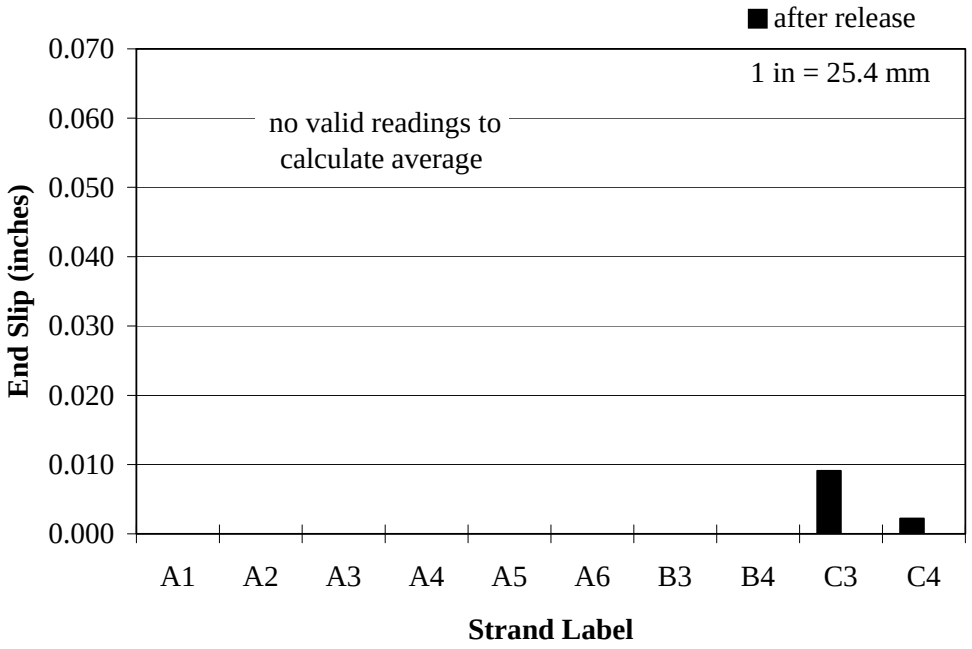

Figure E.3- Measured Draw-in Results for L0B1A-3

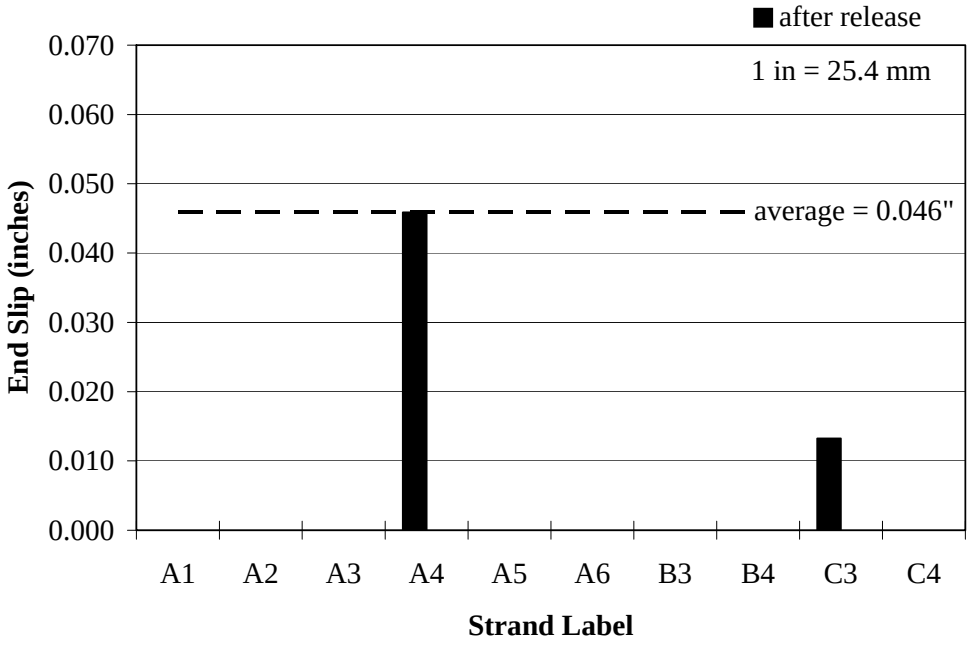

Figure E.4- Measured Draw-In Results for L0B1B-4

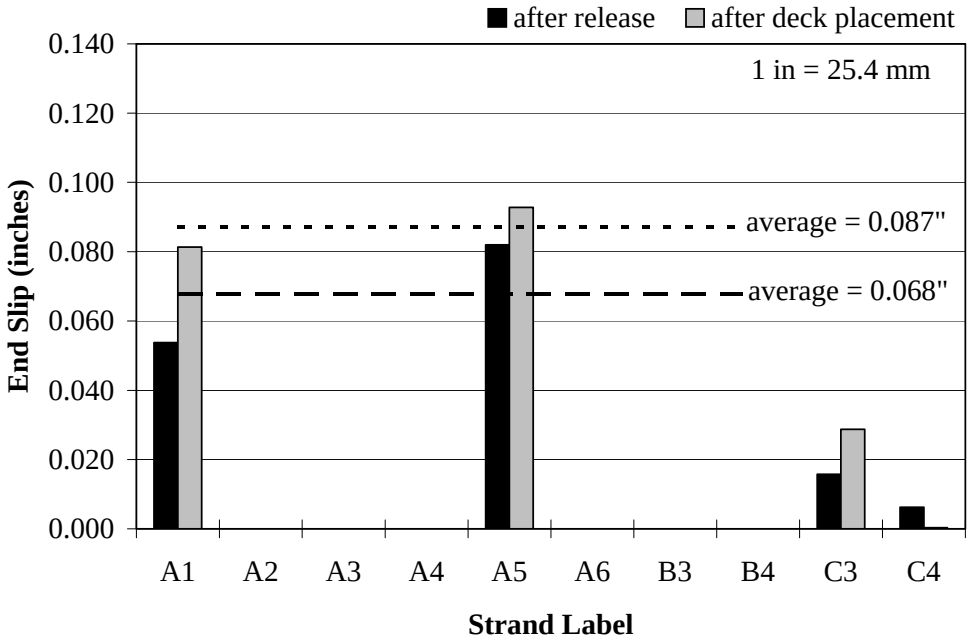

Figure E.5- Measured Draw-in Results for M0B0A-1

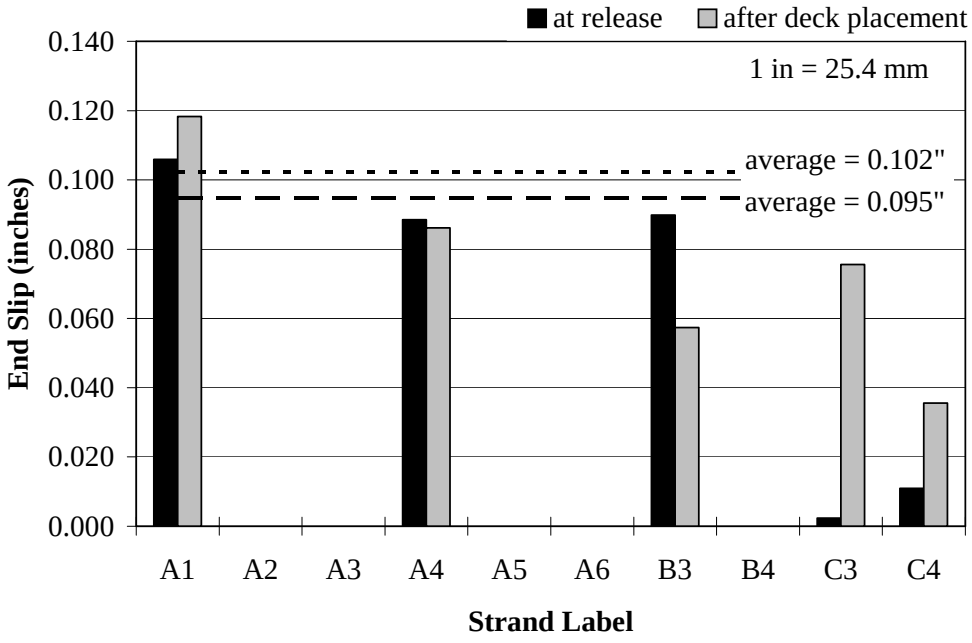

Figure E.6- Measured Draw-In Results for M0B0B-2

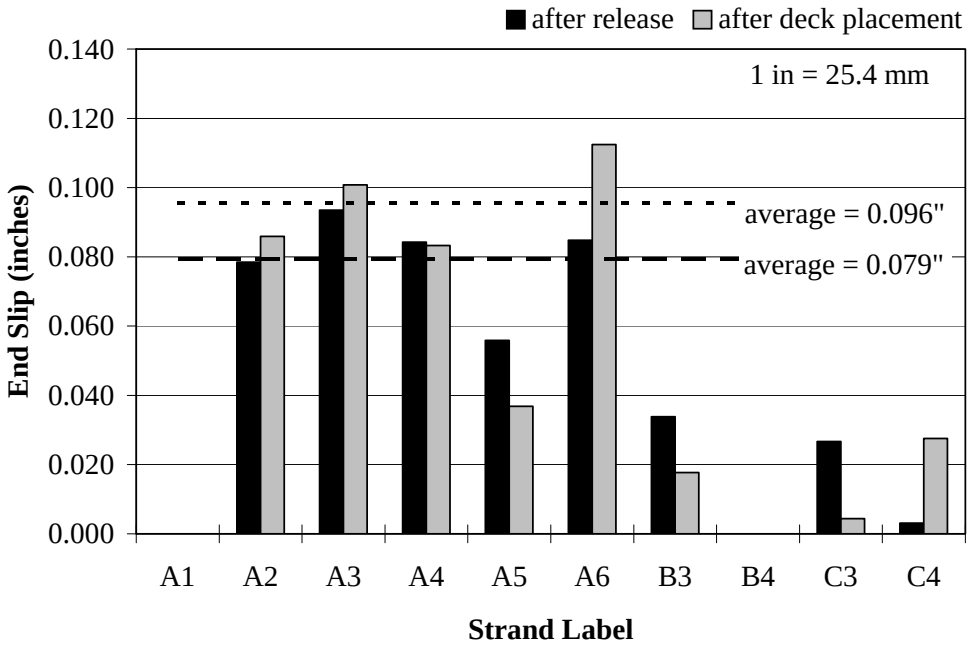

Figure E.7- Measured Draw-in Results for M0B1A-3

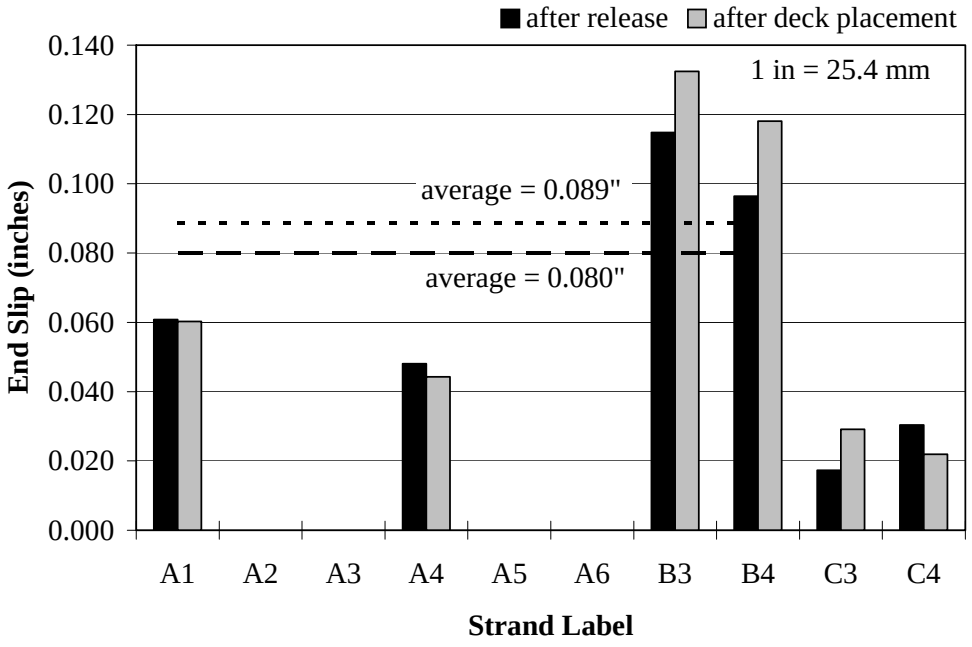

Figure E.8- Measured Draw-In Results for M0B1B-4

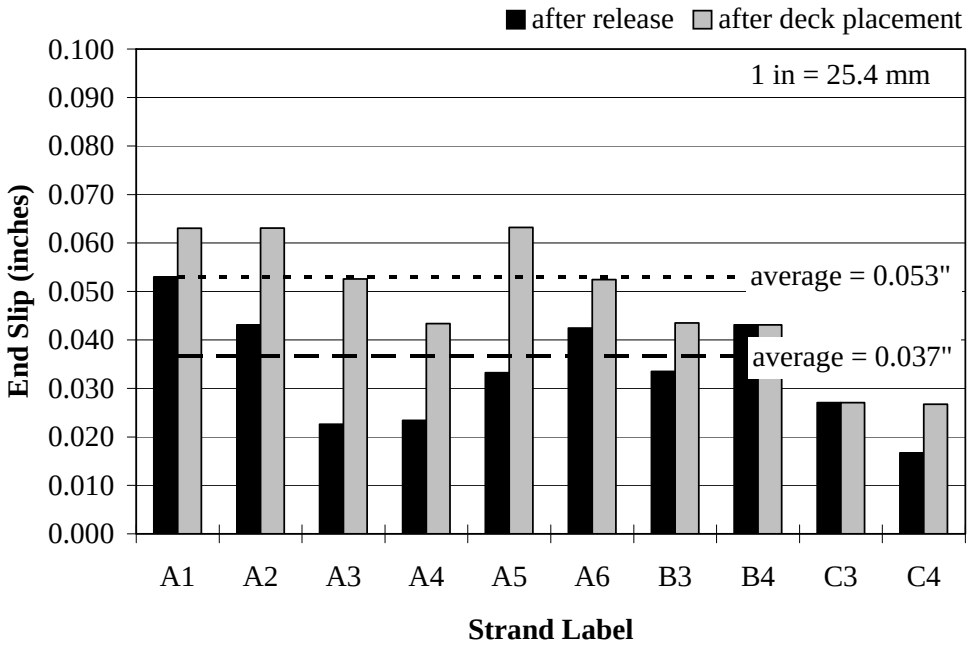

Figure E.9- Measured Draw-in Results for H0B0A-1

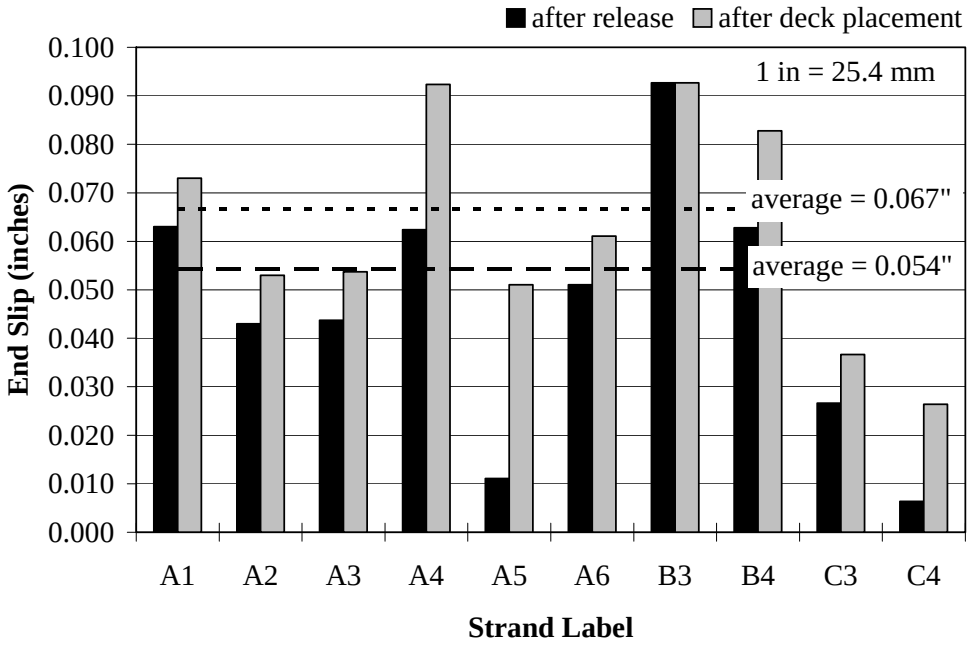

Figure E.10- Measured Draw-In Results for H0B0B-2

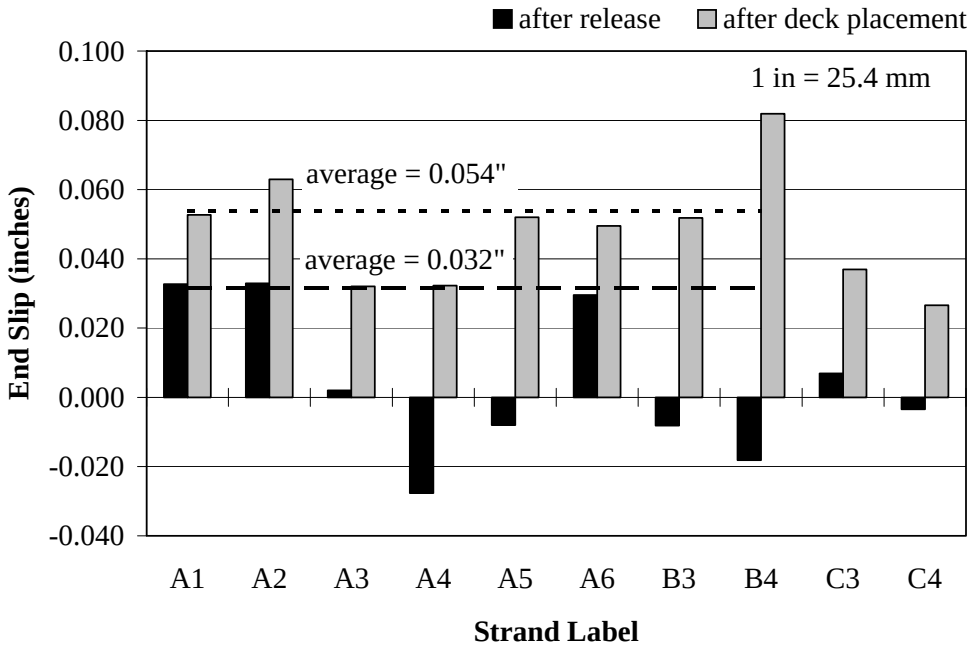

Figure E.11- Measured Draw-in Results for H0B1A-3

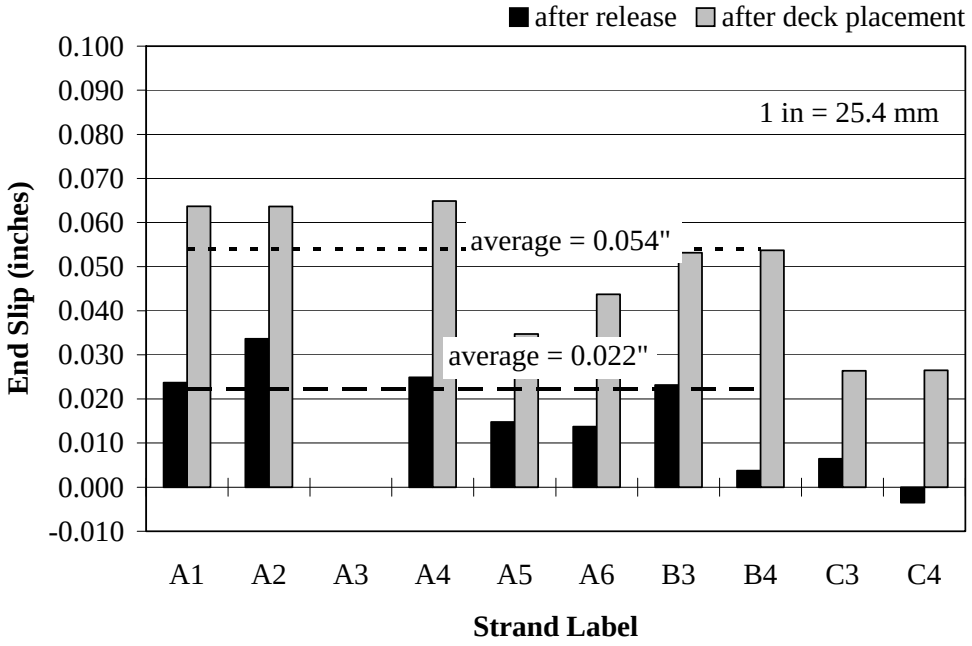

Figure E.12- Measured Draw-In Results for H0B1B-4

APPENDIX F

LOAD-DEFLECTION AND

END SLIP-DEFLECTION PLOTS

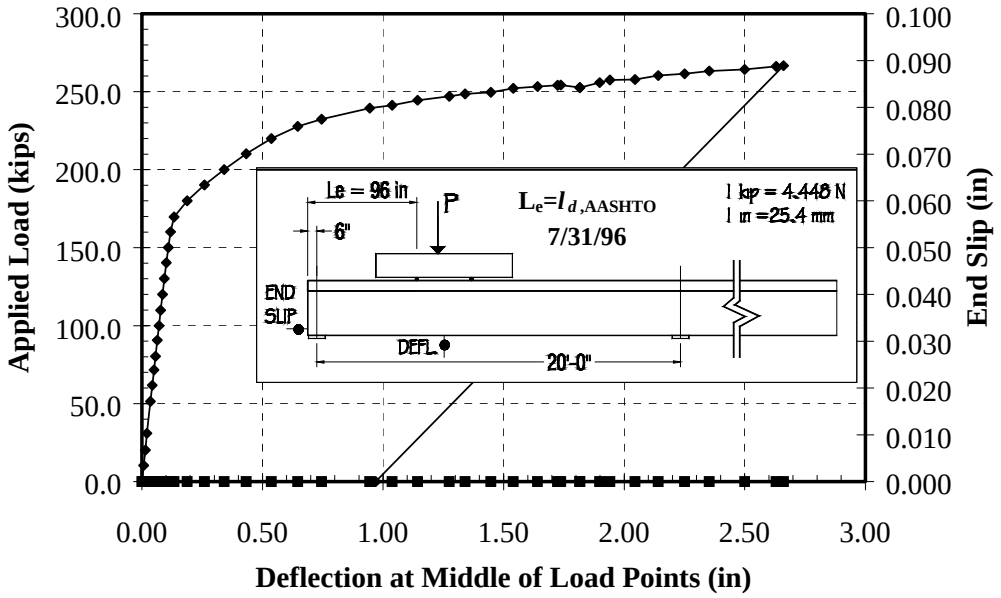

Figure F.1- Load and End Slip vs. Deflection Plot for L0B0A-1

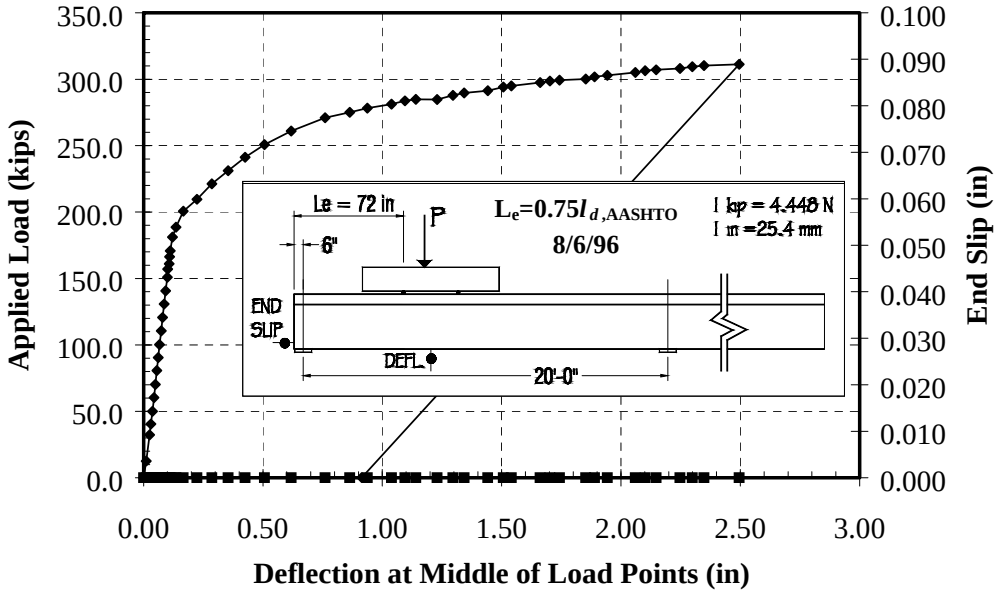

Figure F.2- Load and End Slip vs. Deflection Plot for L0B0B-2

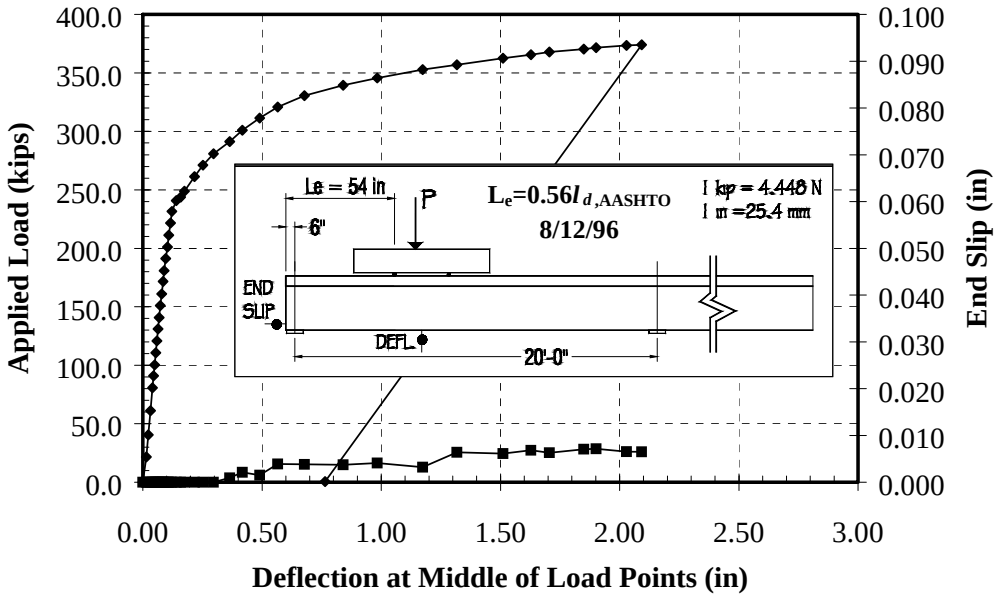

Figure F.3- Load and End Slip vs. Deflection Plot for L0B1A-3

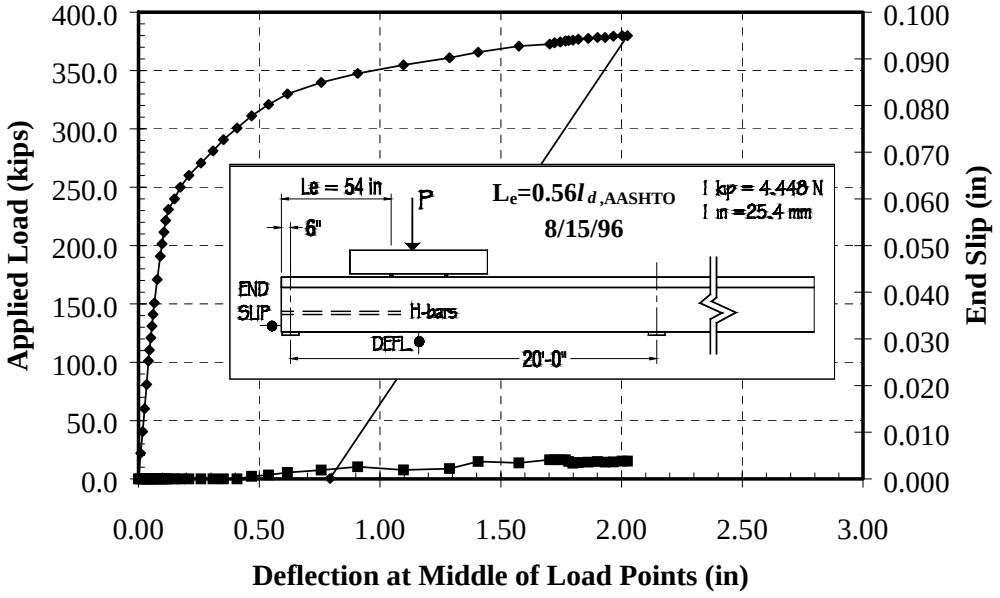

Figure F.4- Load and End Slip vs. Deflection Plot for L0B1B-4

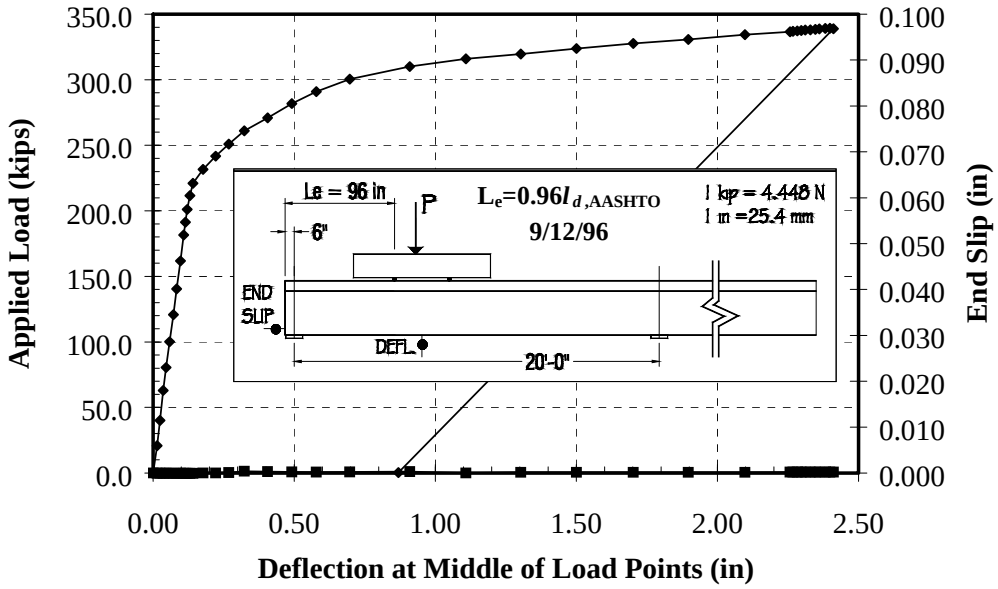

Figure F.5- Load and End Slip vs. Deflection Plot for M0B0A-1

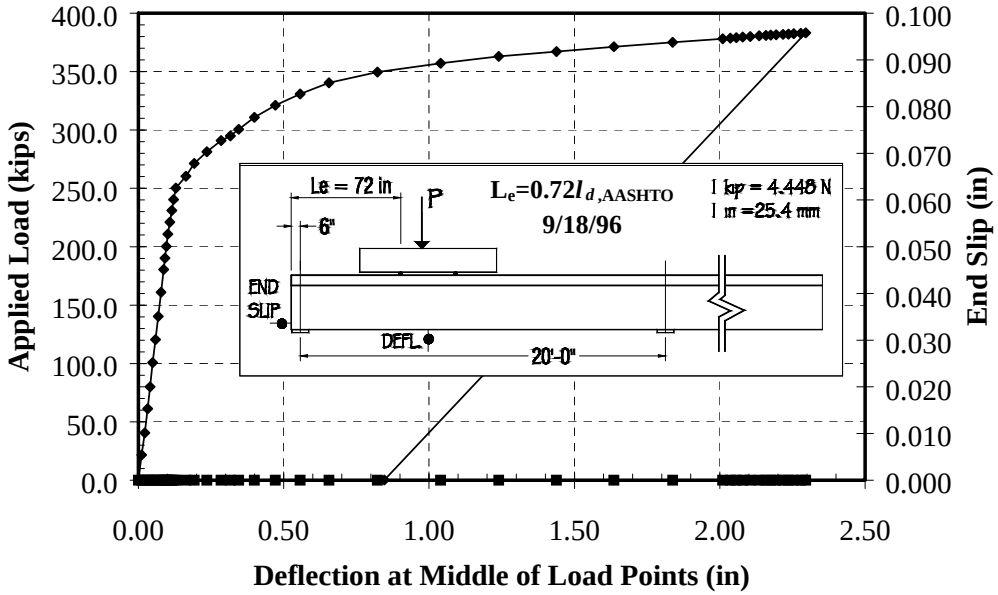

Figure F.6- Load and End Slip vs. Deflection Plot for M0B0B-2

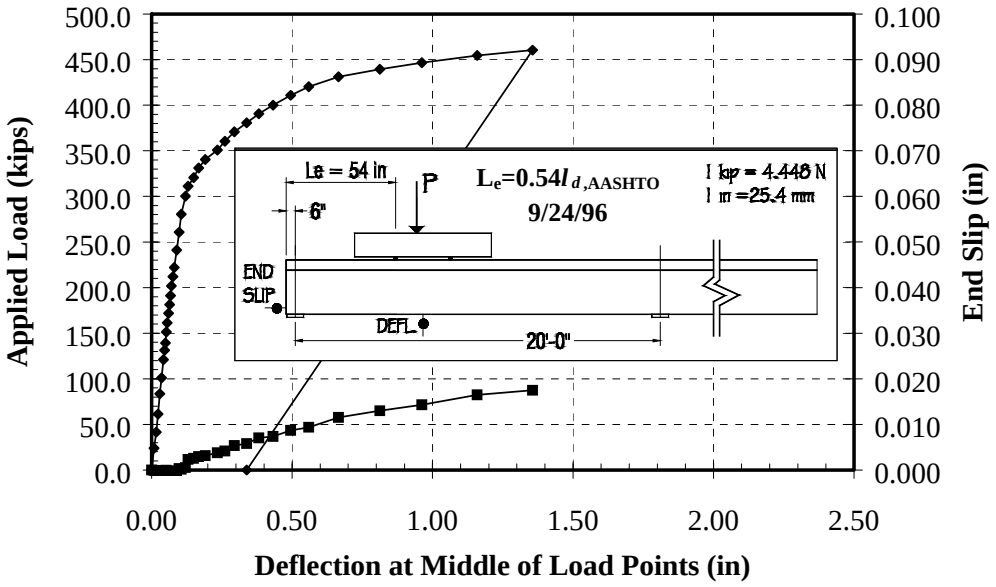

Figure F.7- Load and End Slip vs. Deflection Plot for M0B1A-3

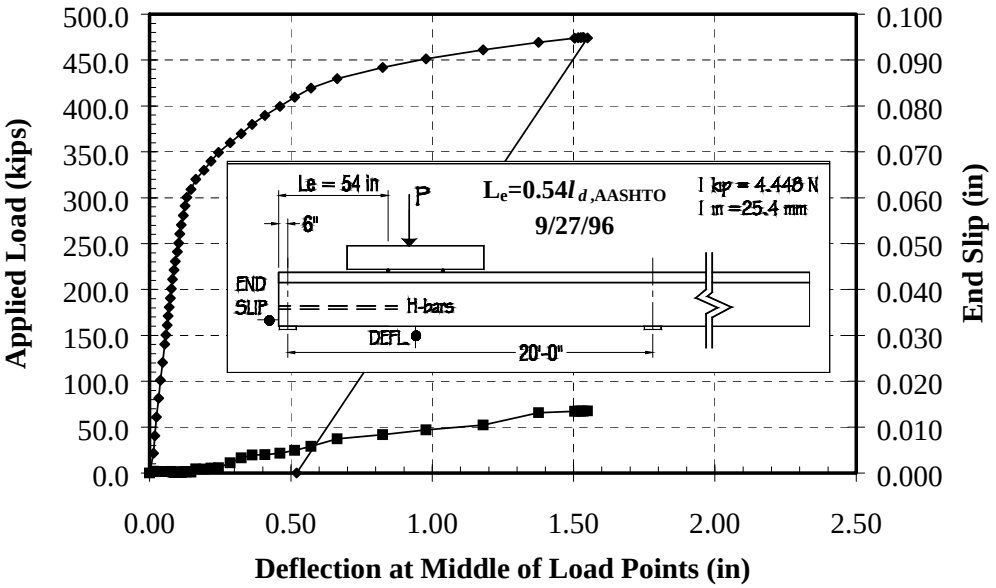

Figure F.8- Load and End Slip vs. Deflection Plot for M0B1B-4

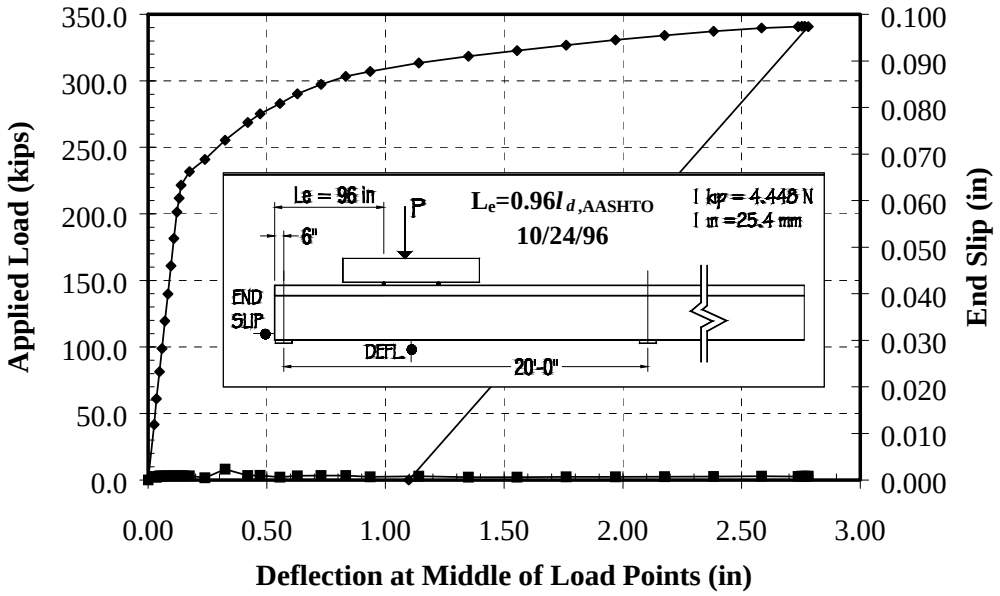

Figure F.9- Load and End Slip vs. Deflection Plot for H0B0A-1

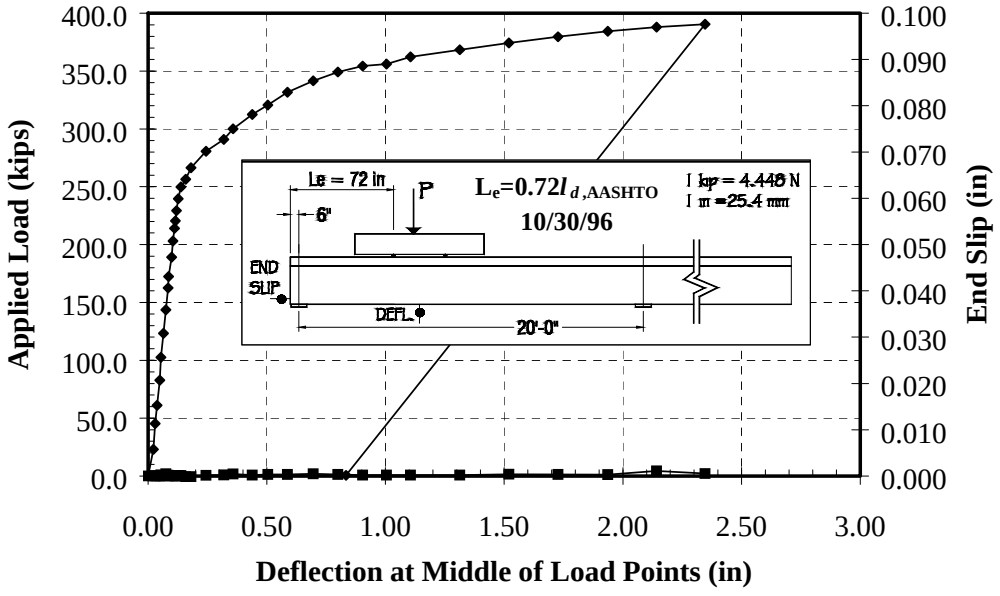

Figure F.10- Load and End Slip vs. Deflection Plot for H0B0B-2

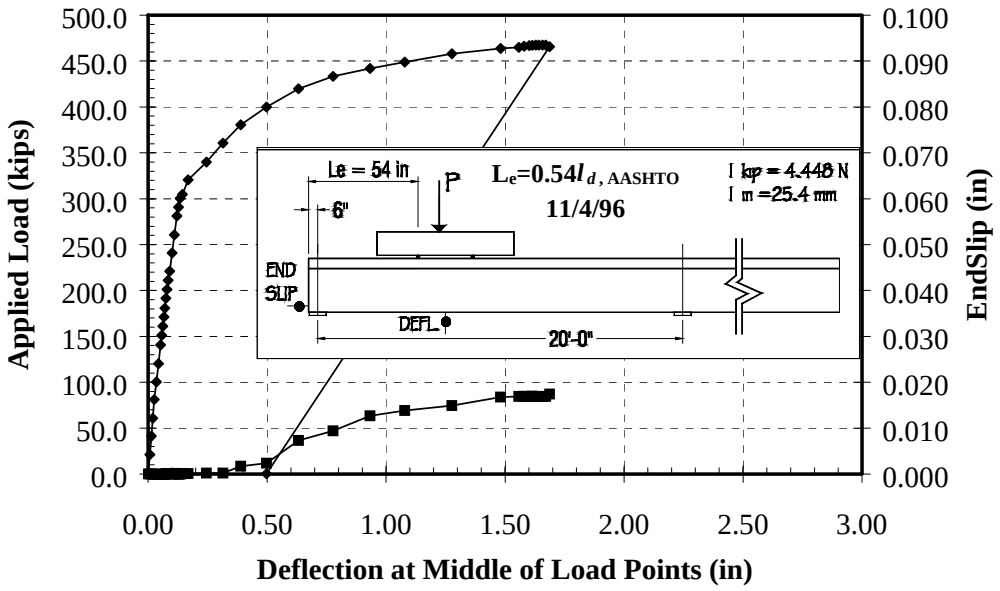

Figure F.11- Load and End Slip vs. Deflection Plot for H0B1A-3

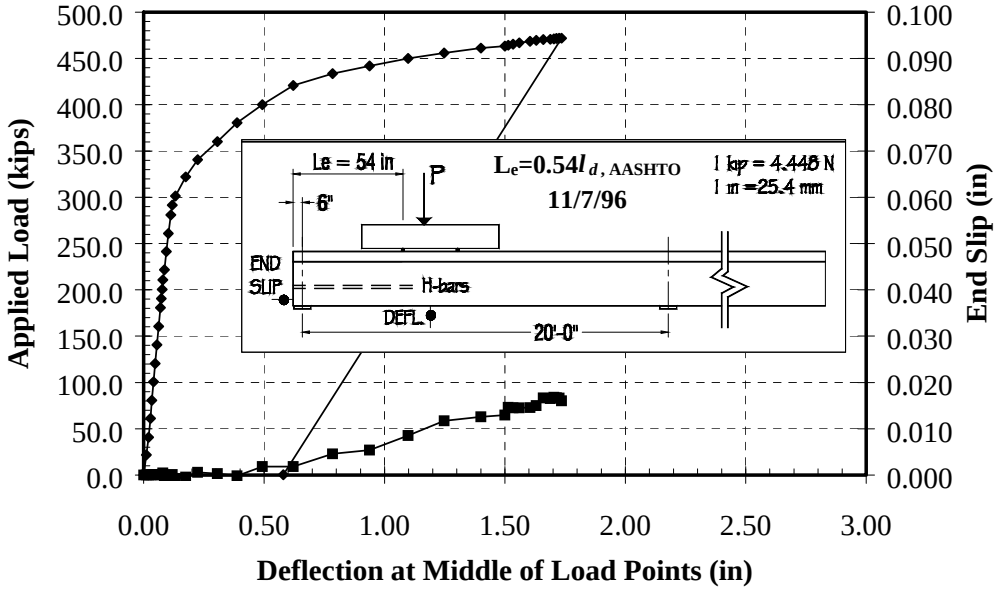

Figure F.12- Load and End Slip vs. Deflection Plot for H0B1B-4

APPENDIX G

CRACK PATTERNS

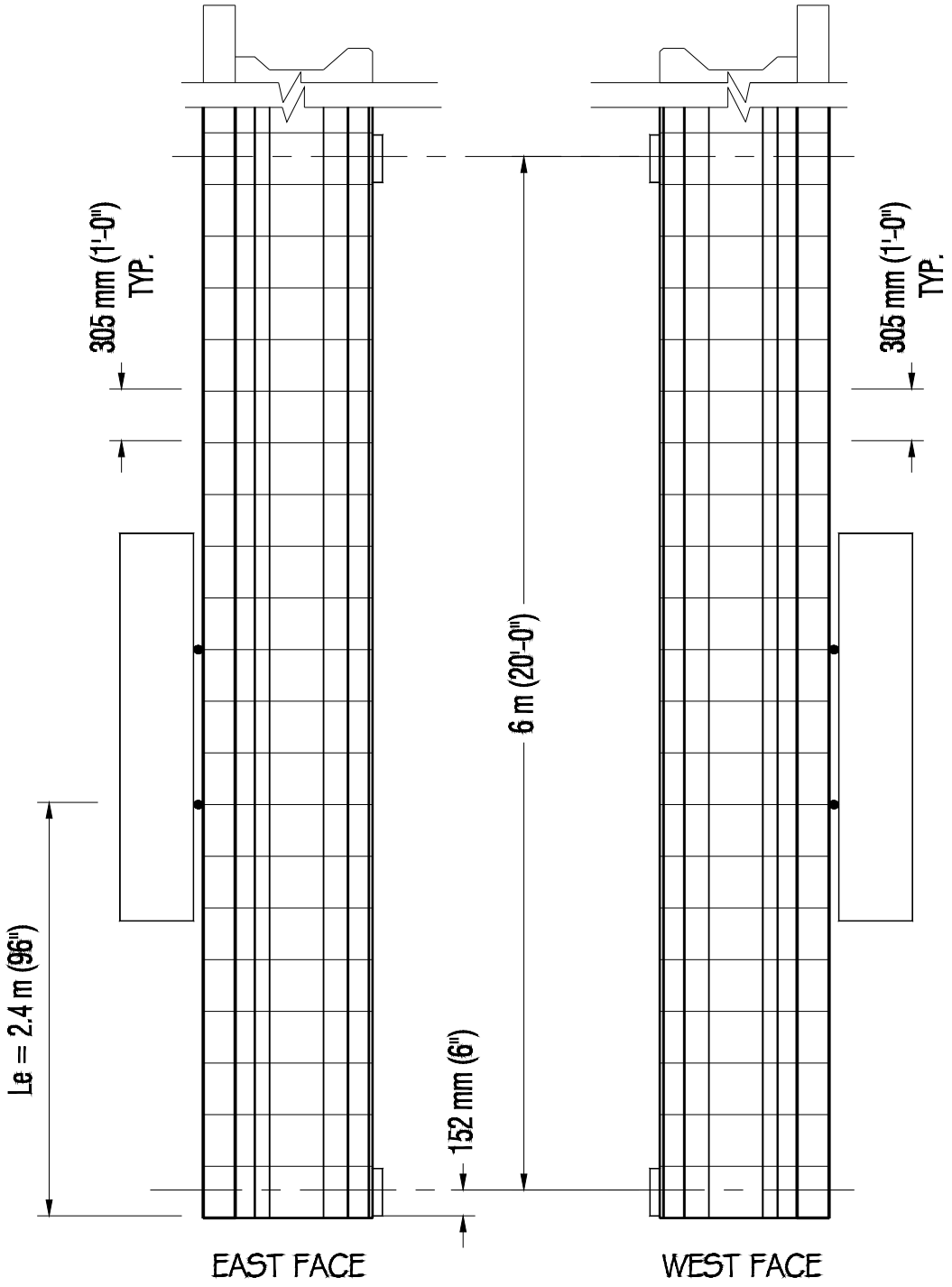

Figure G.1- Crack Patterns for L0B0A-1

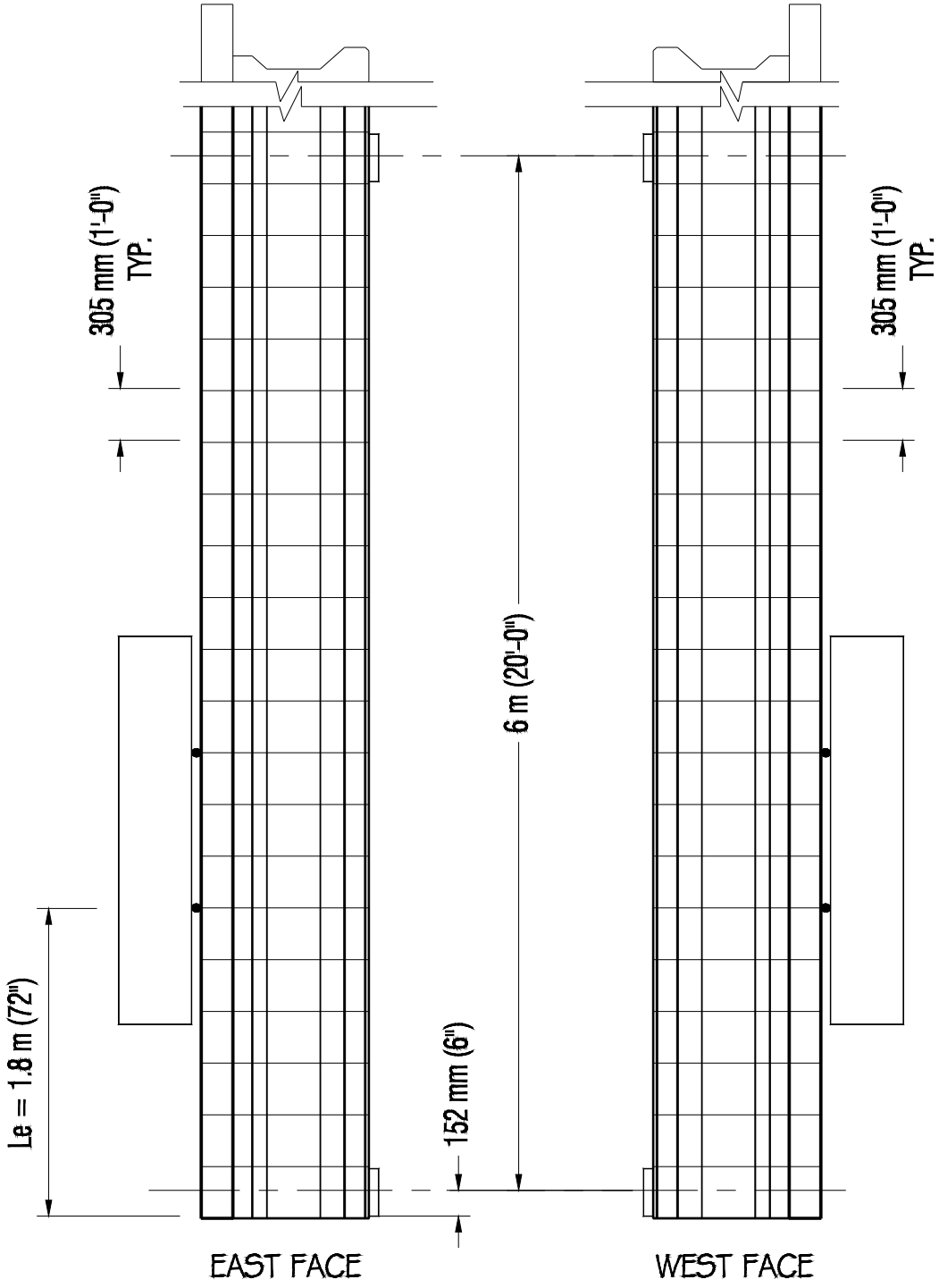

Figure G.2- Crack Patterns for L0B0B-2

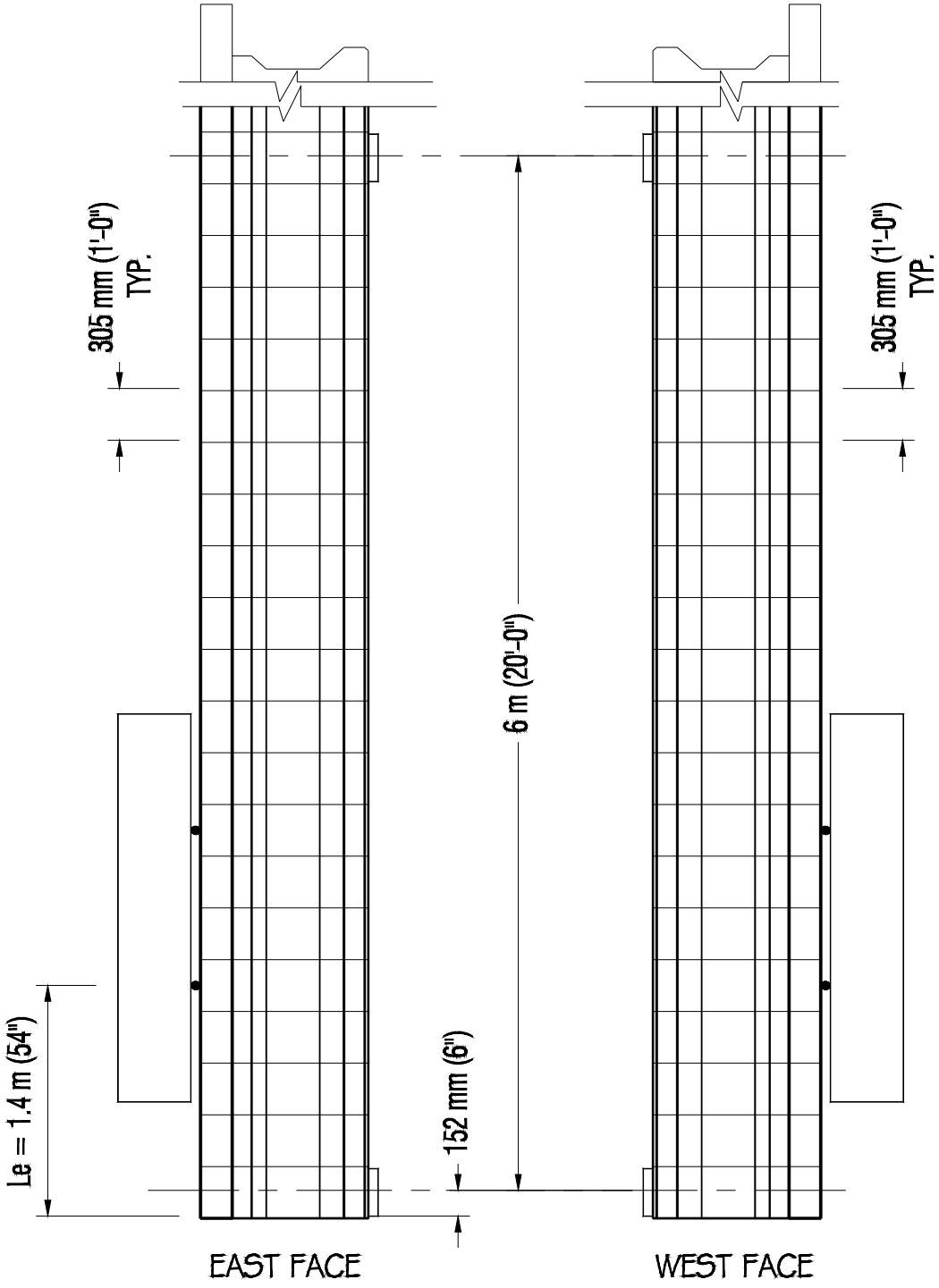

Figure G.3- Crack Patterns for L0B1A-3

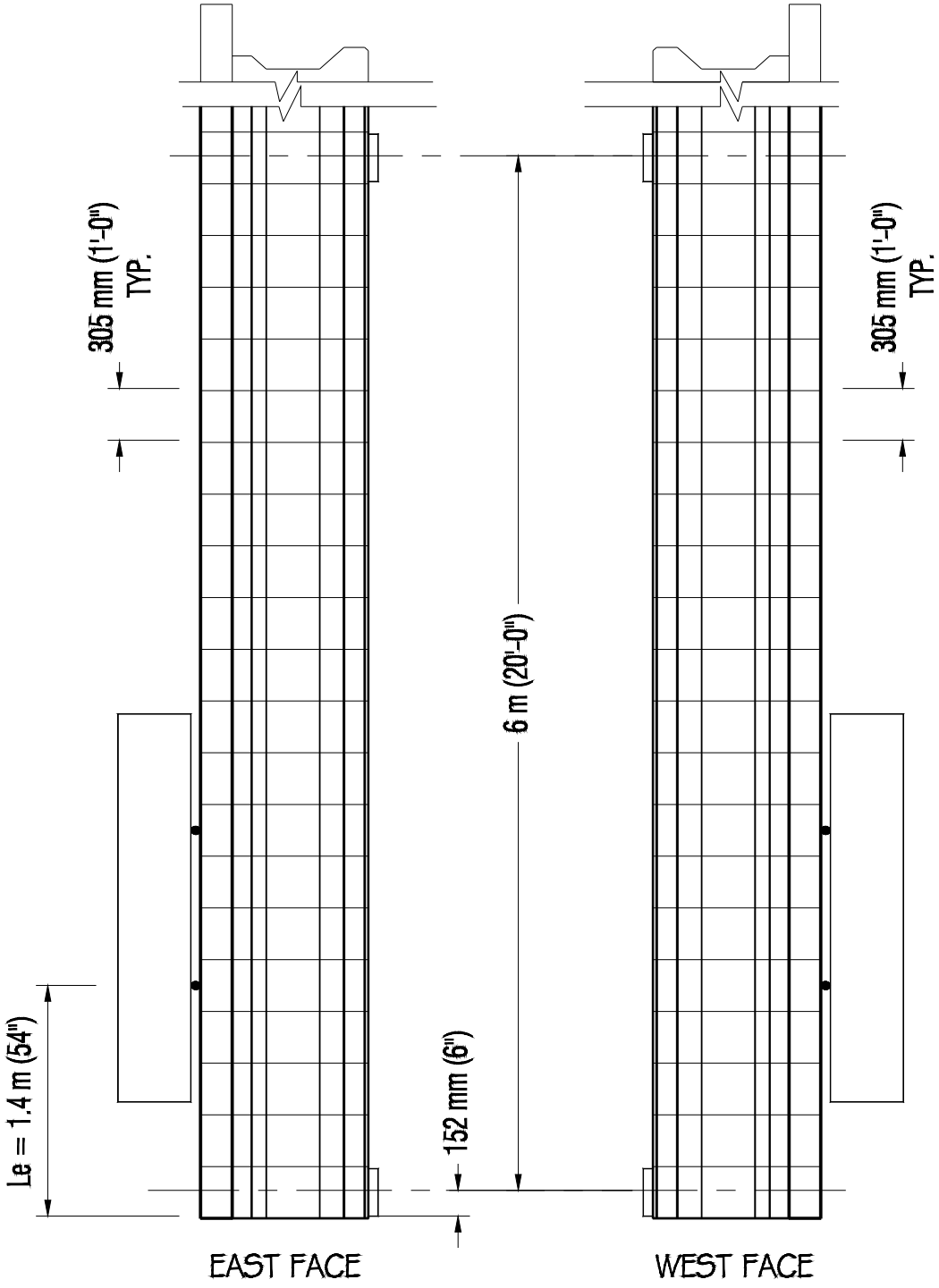

Figure G.4- Crack Patterns for L0B1B-4

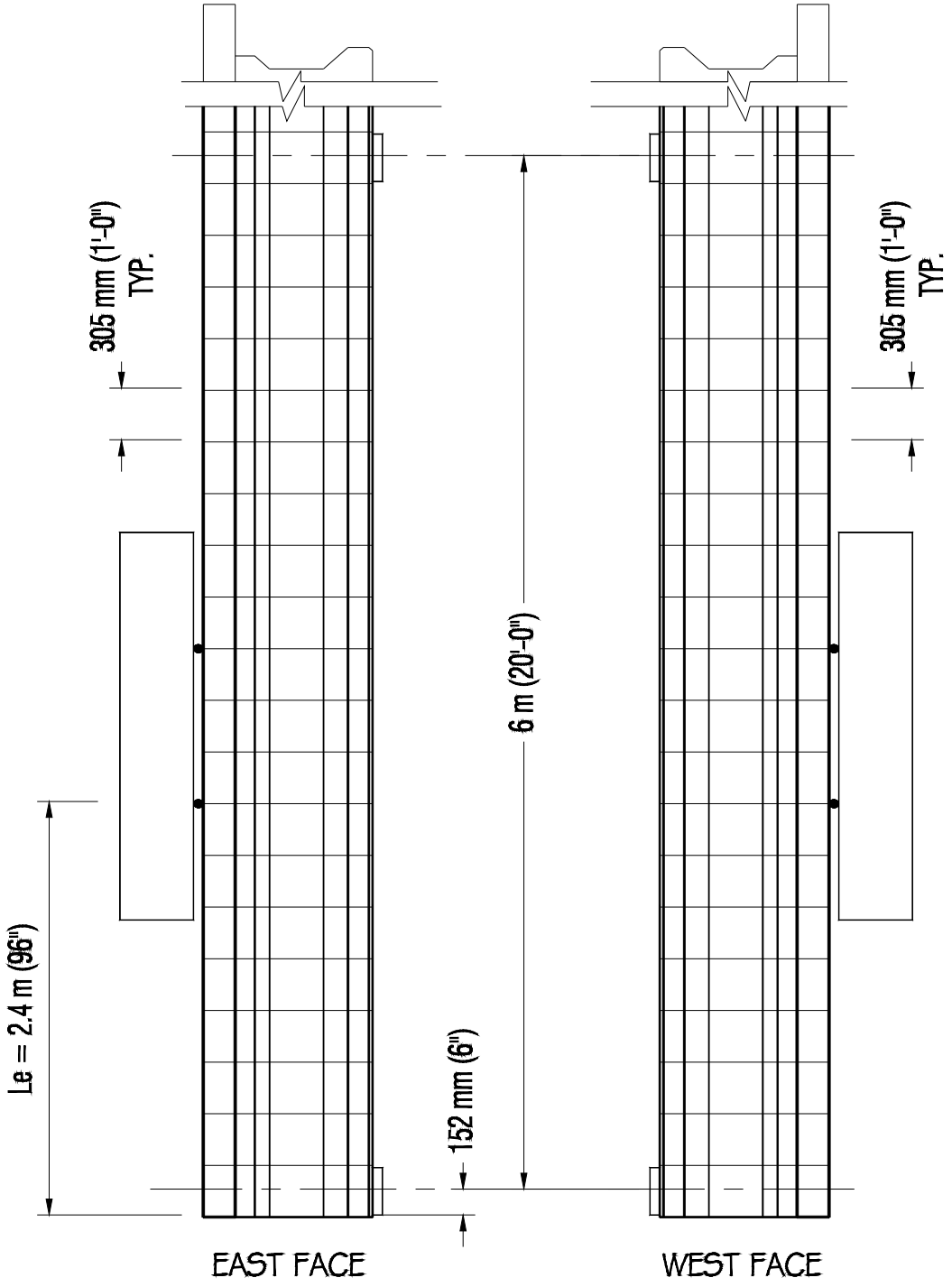

Figure G.5- Crack Patterns for M0B0A-1

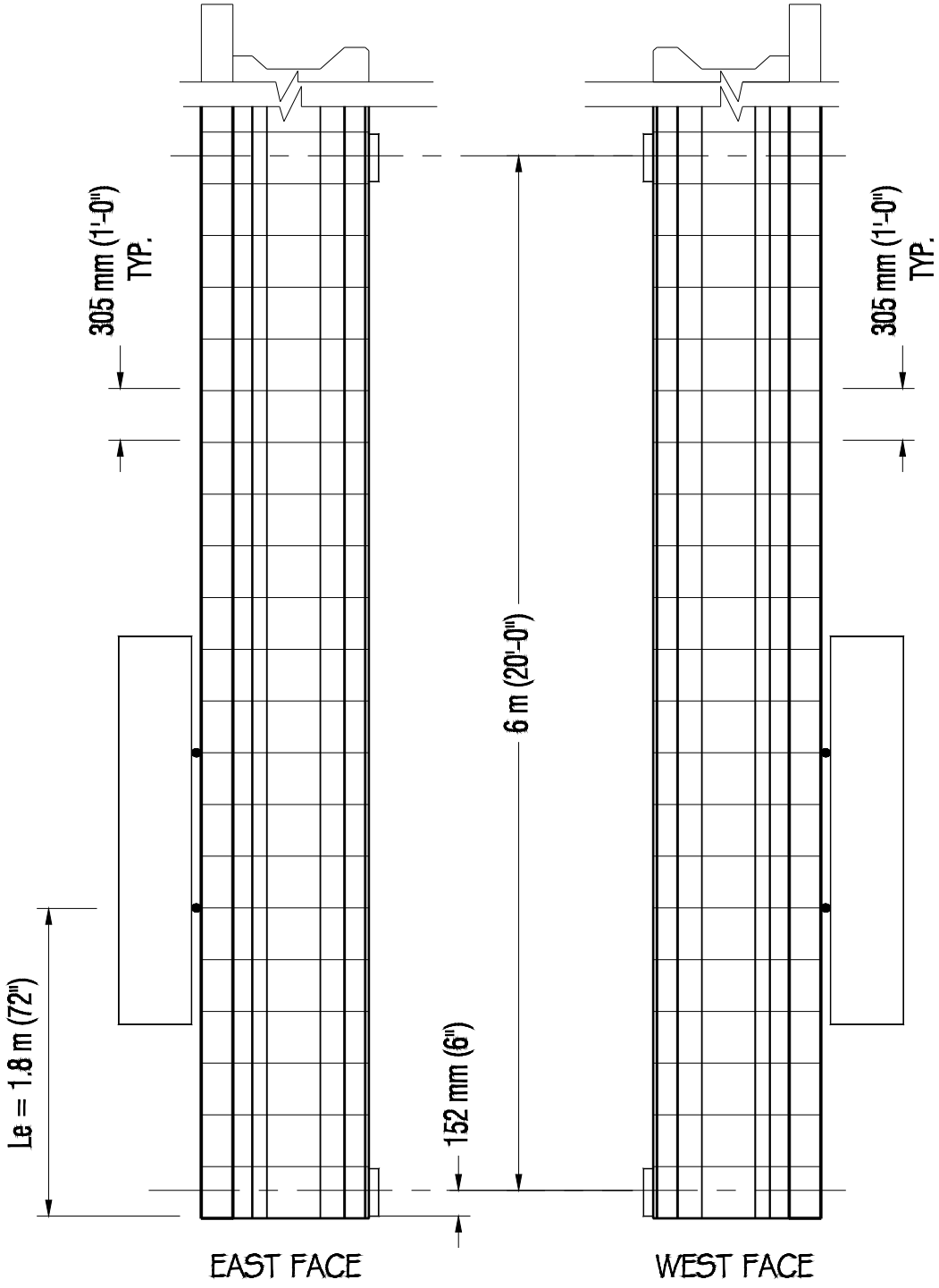

Figure G.6- Crack Patterns for M0B0B-2

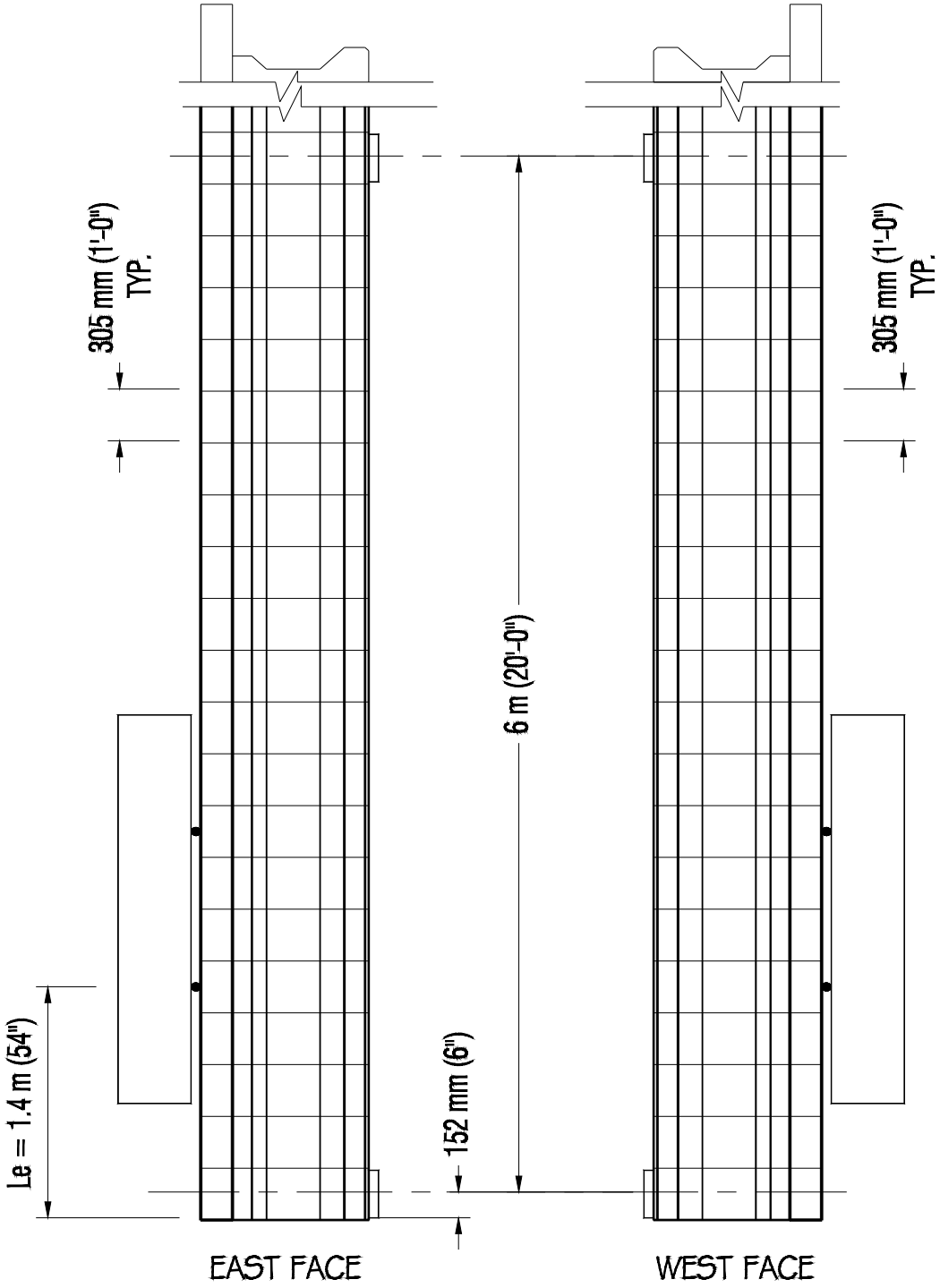

Figure G.7- Crack Patterns for M0B1A-3

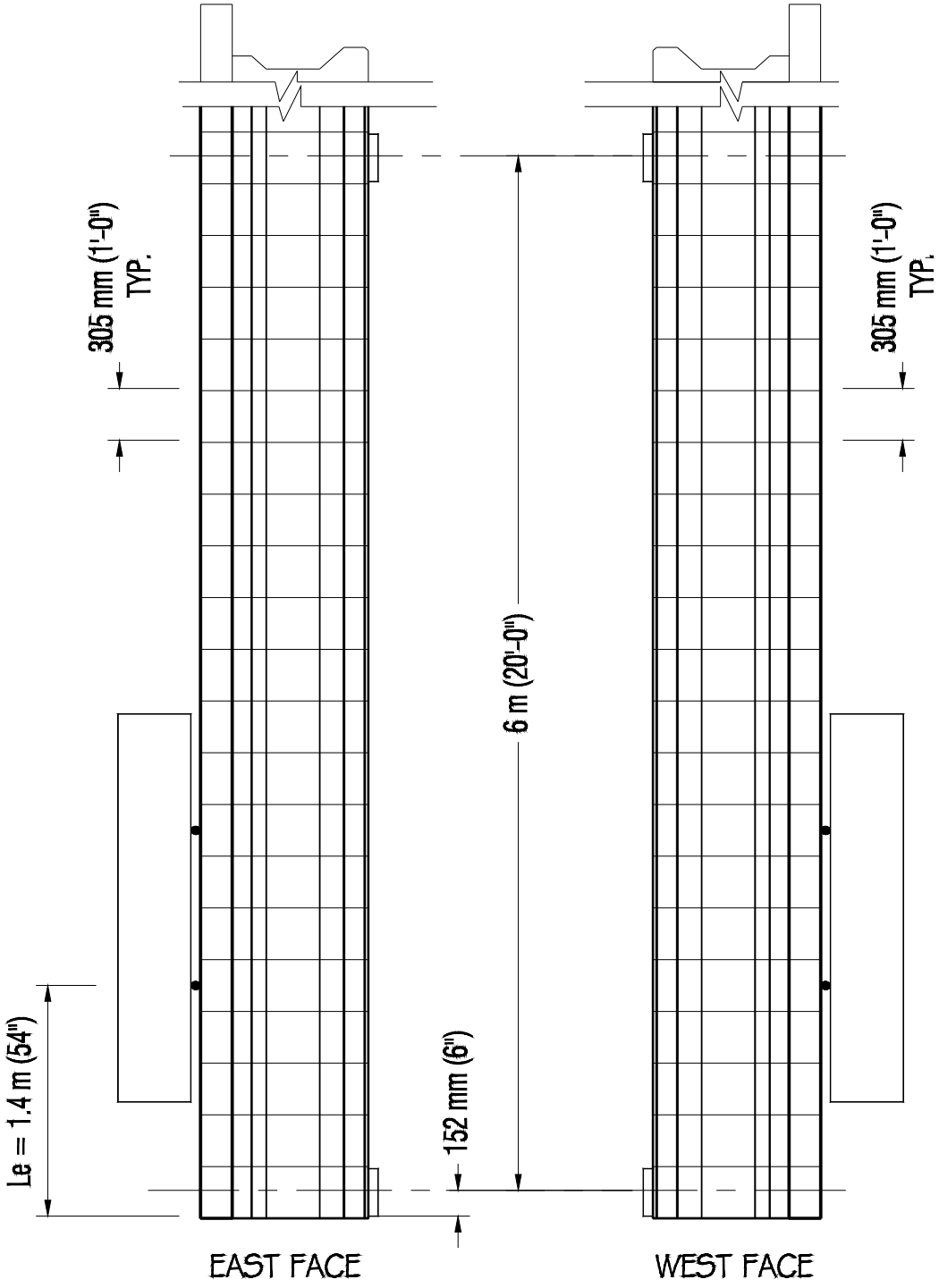

Figure G.8- Crack Patterns for M0B1B-4

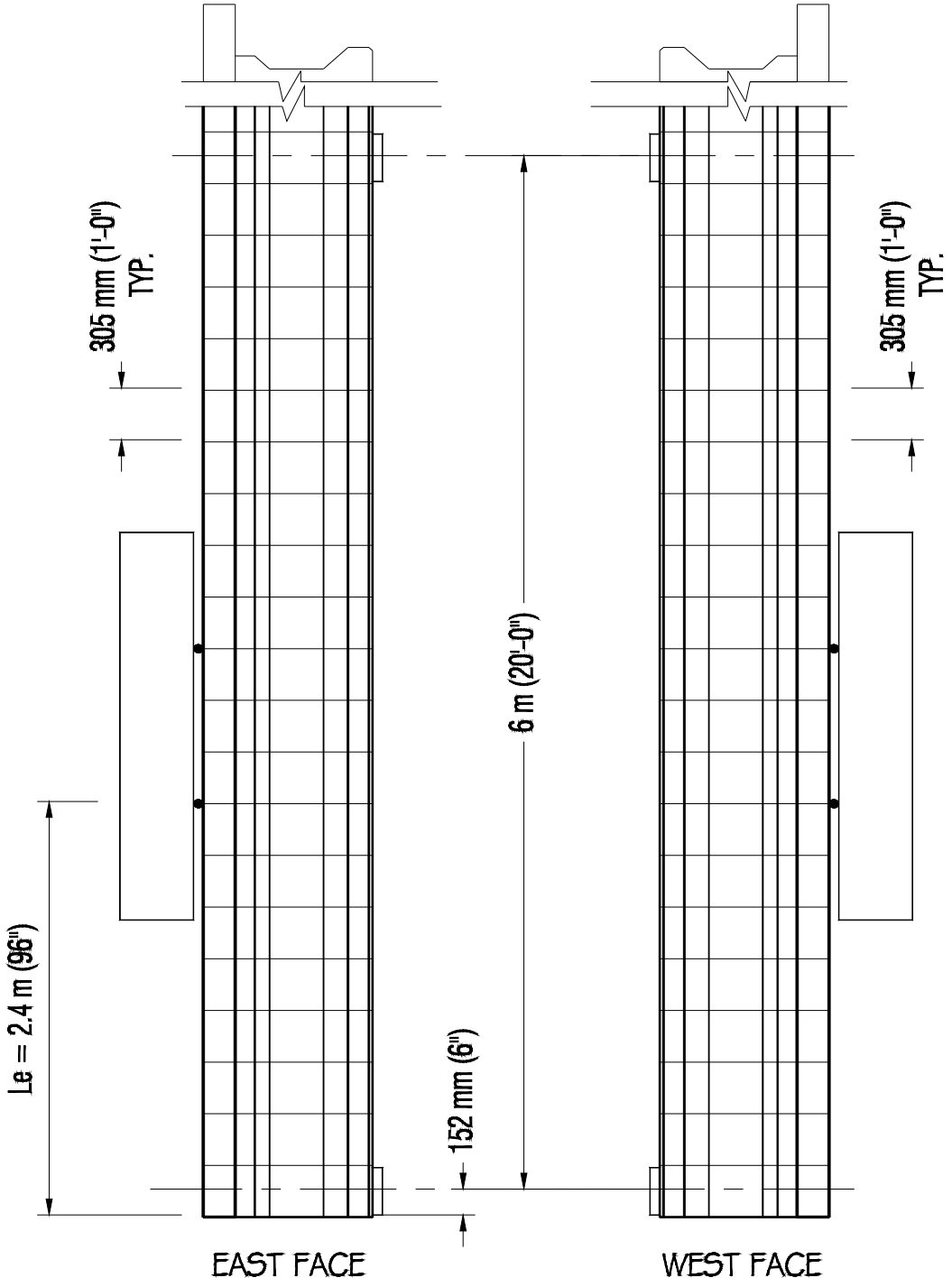

Figure G.9- Crack Patterns for H0B0A-1

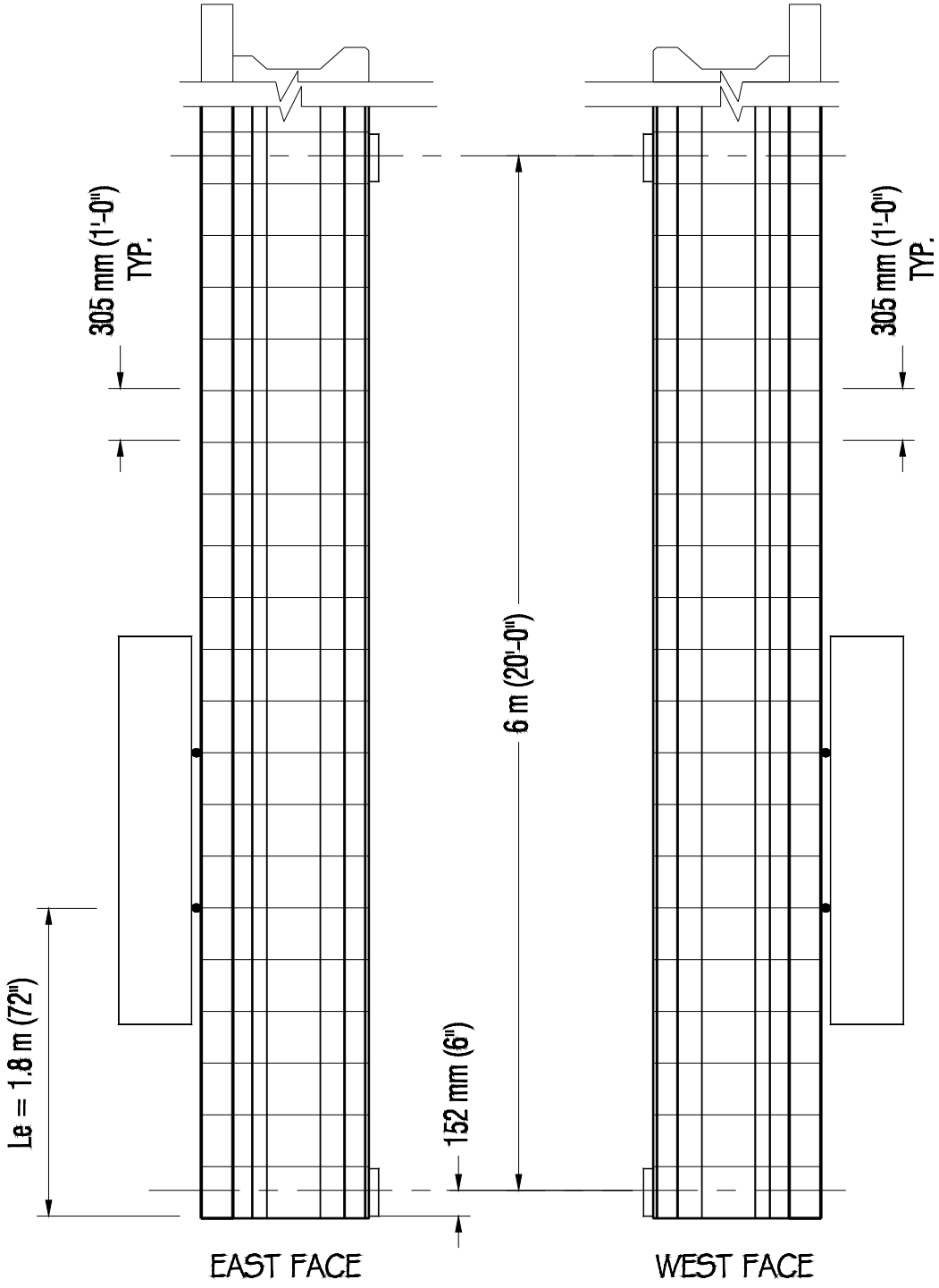

Figure G.10- Crack Patterns for H0B0B-2

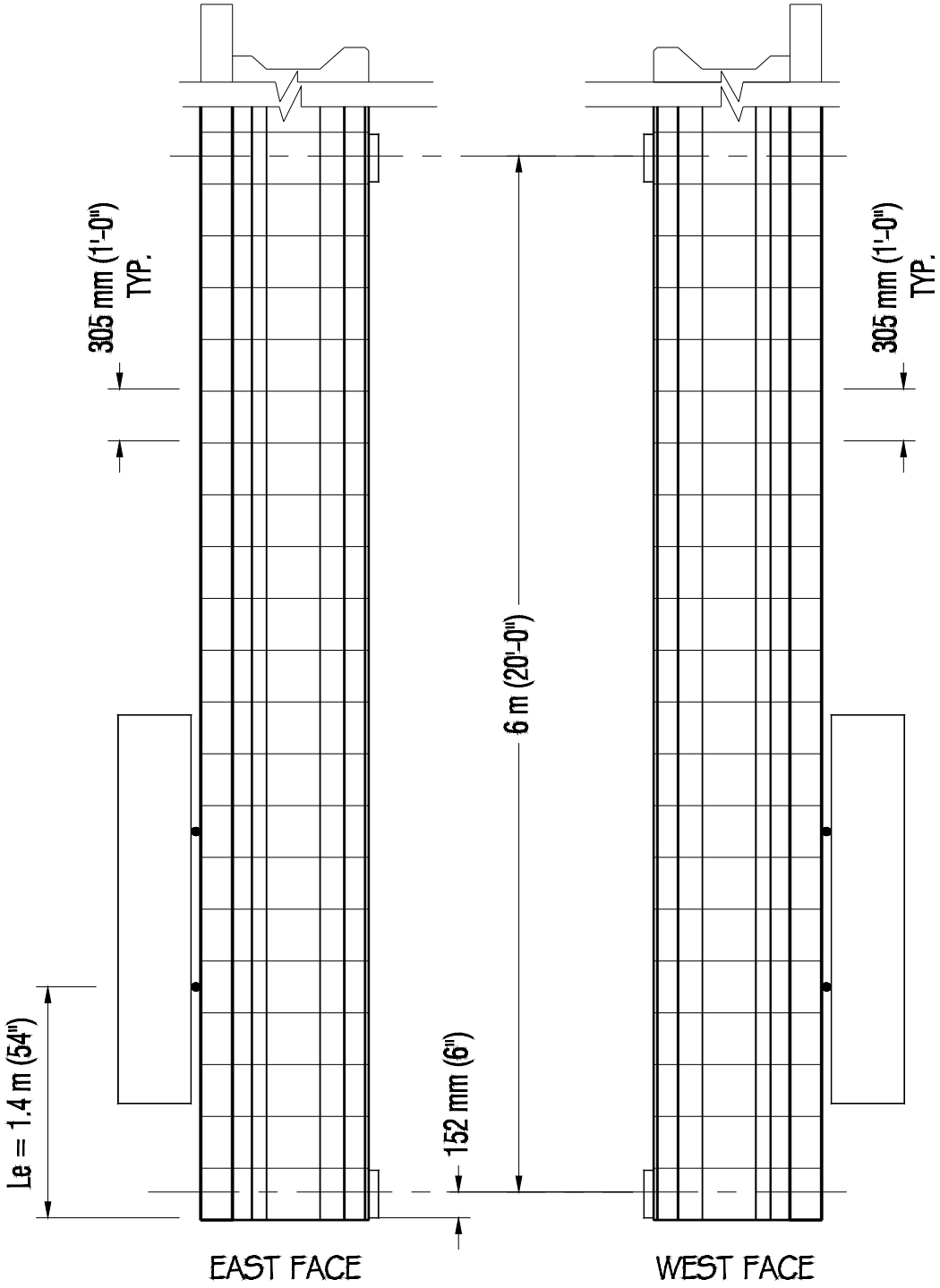

Figure G.11- Crack Patterns for H0B1A-3

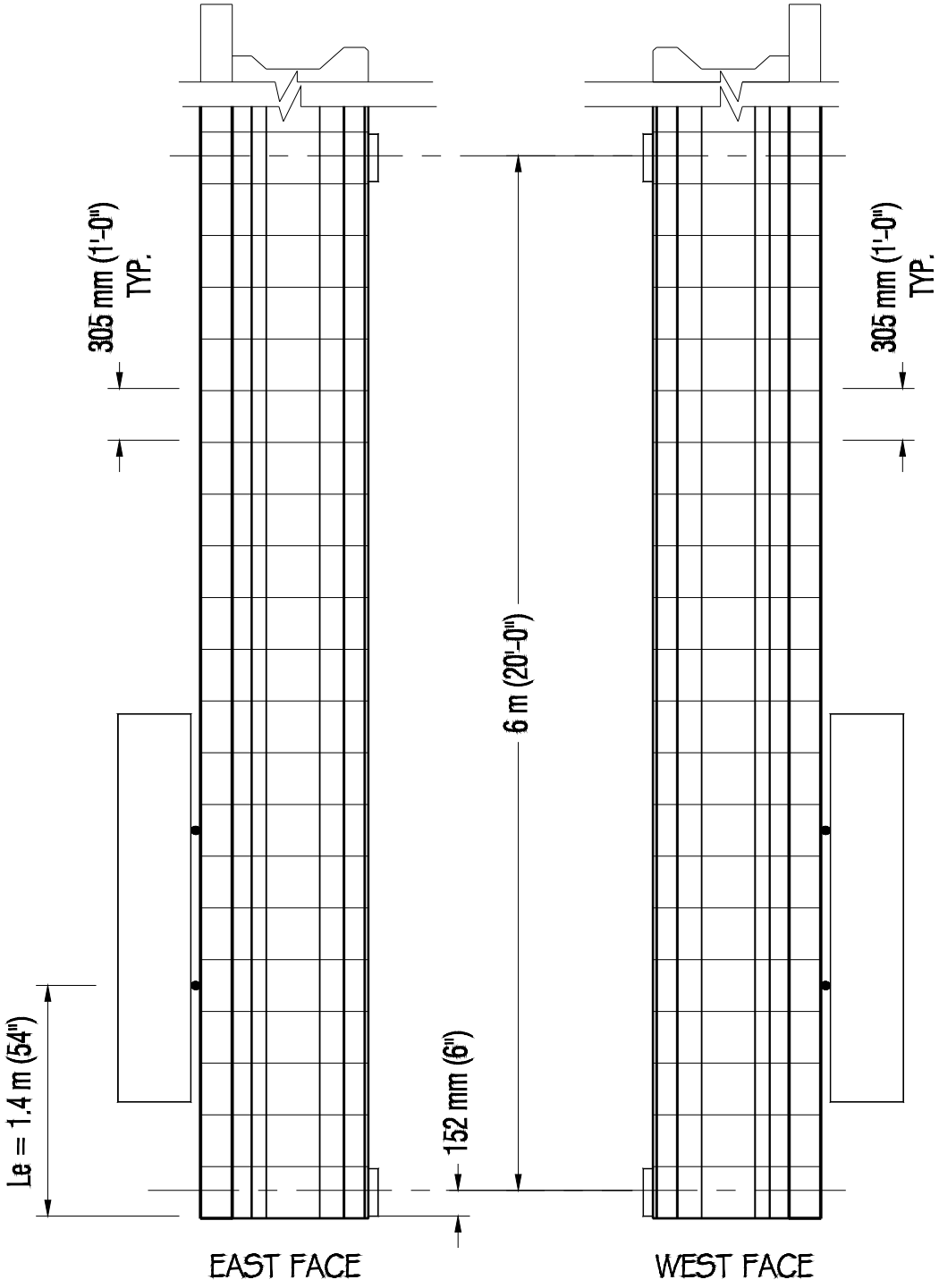

Figure G.12- Crack Patterns for H0B1B-4

APPENDIX H

STRAIN VS. LOAD PLOTS

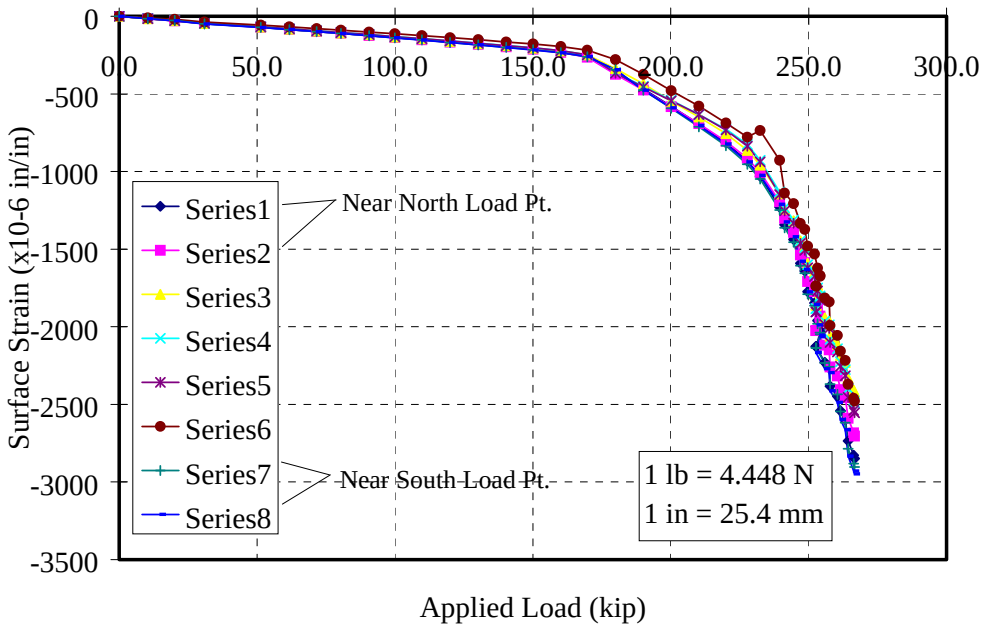

Figure H.1- Concrete Surface Strain vs. Applied Load for L0B0A-1

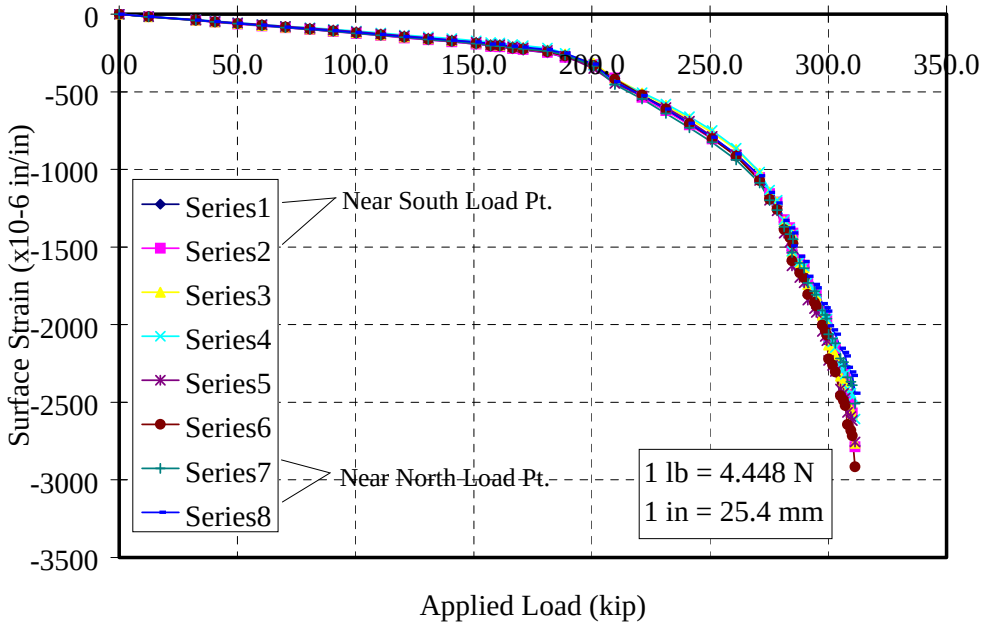

Figure H.2- Concrete Surface Strain vs. Applied Load for L0B0B-2

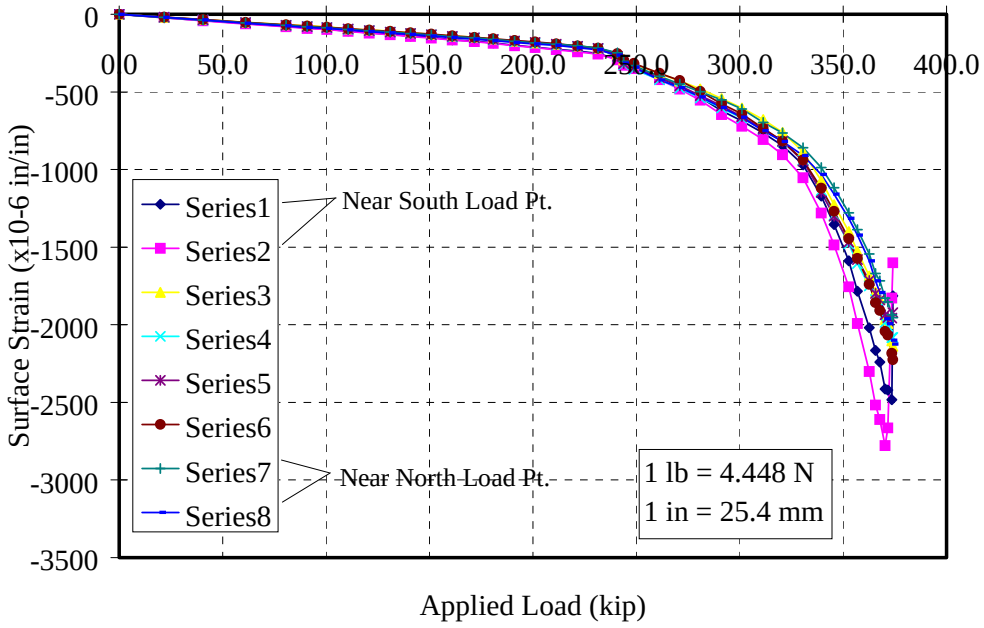

Figure H.3- Concrete Surface Strain vs. Applied Load for L0B1A-3

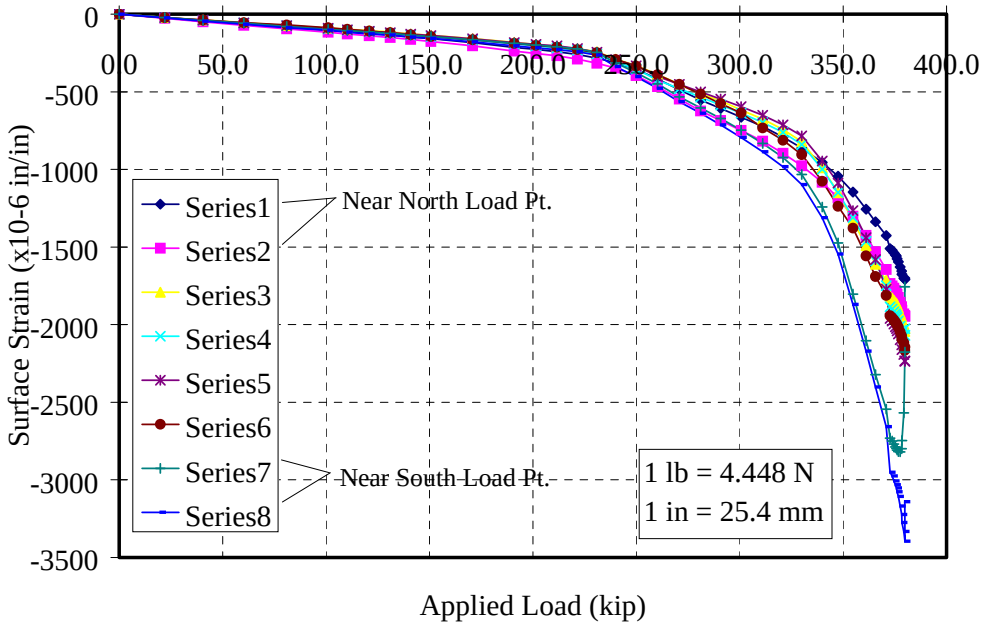

Figure H.4- Concrete Surface Strain vs. Applied Load for L0B0B-4

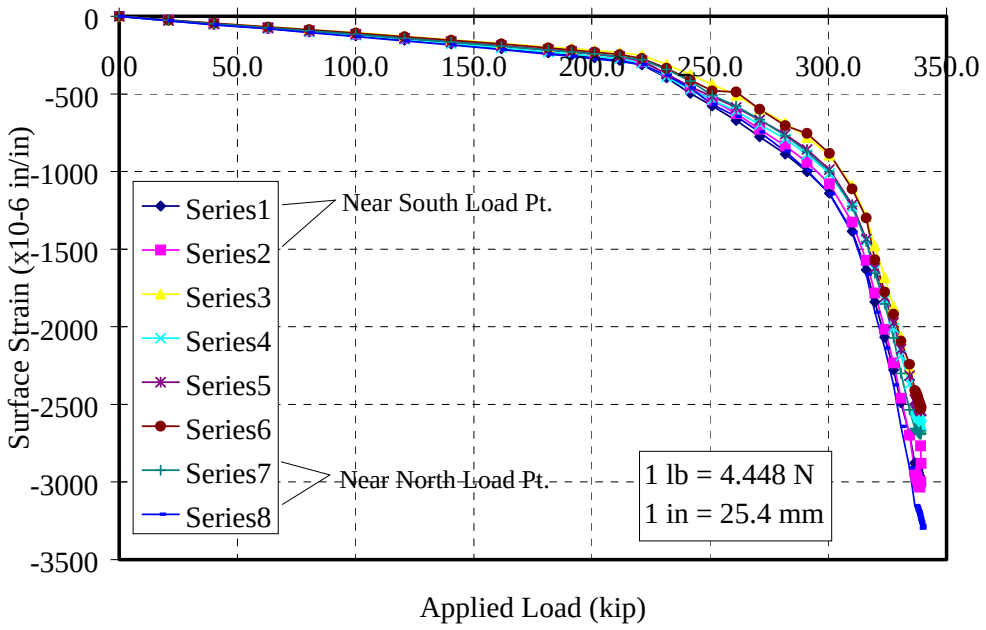

Figure H.5- Concrete Surface Strain vs. Applied Load for M0B0A-1

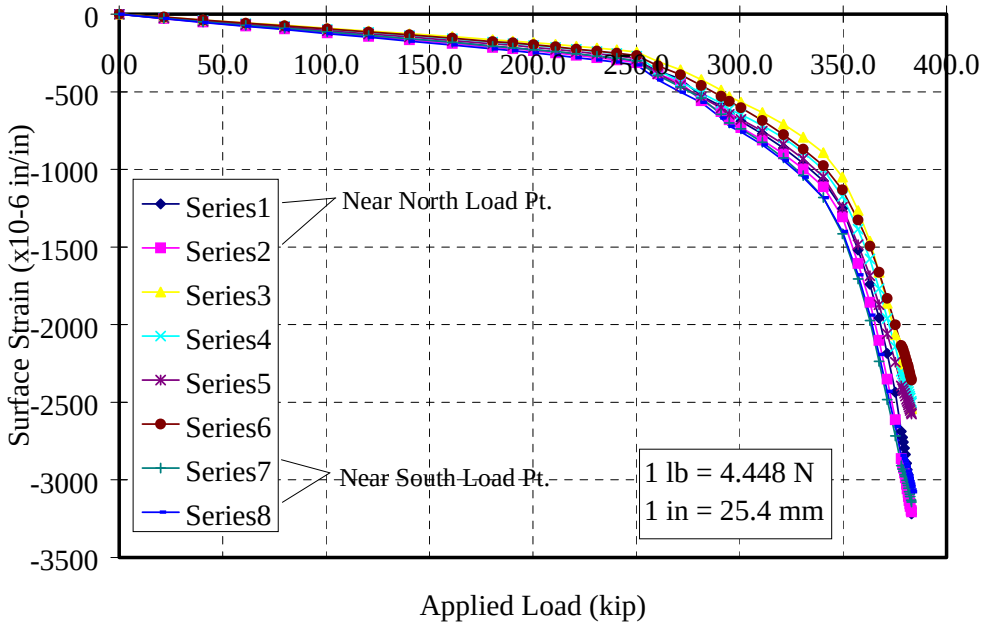

Figure H.6- Concrete Surface Strain vs. Applied Load for M0B0B-2

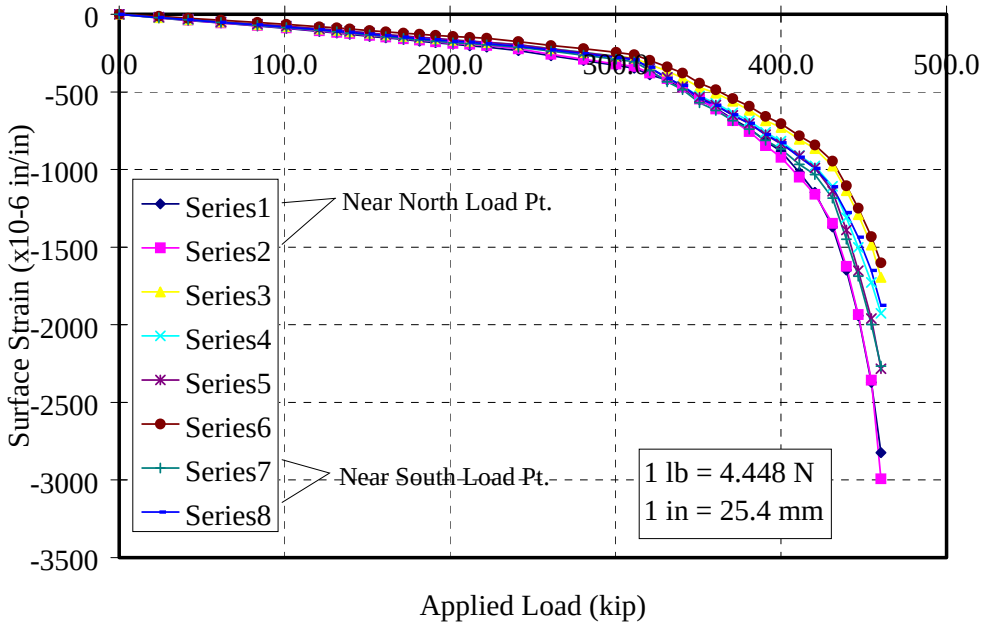

Figure H.7- Concrete Surface Strain vs. Applied Load for M0B1A-3

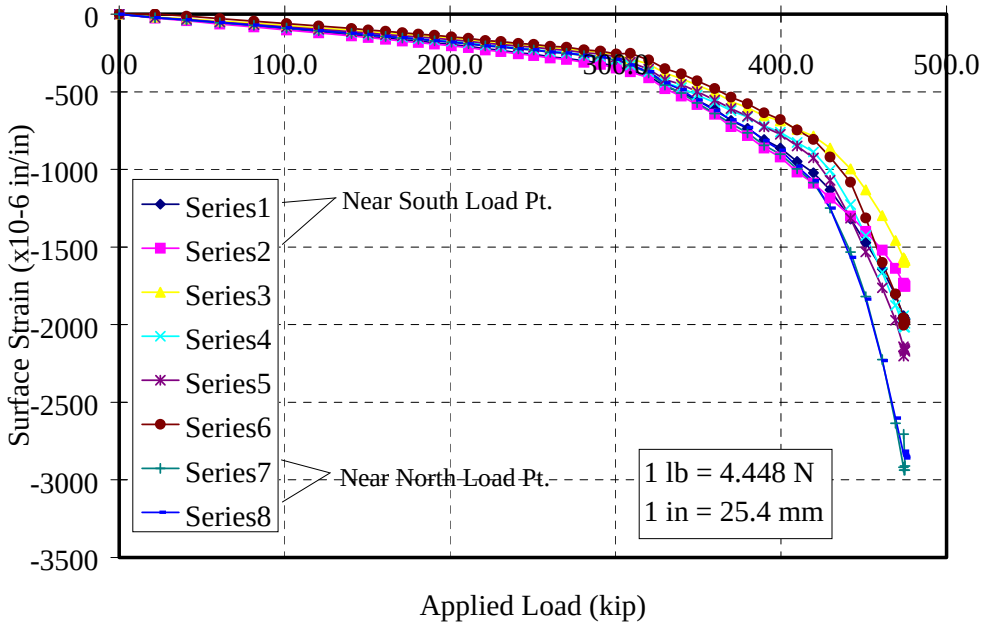

Figure H.8- Concrete Surface Strain vs. Applied Load for M0B0B-4

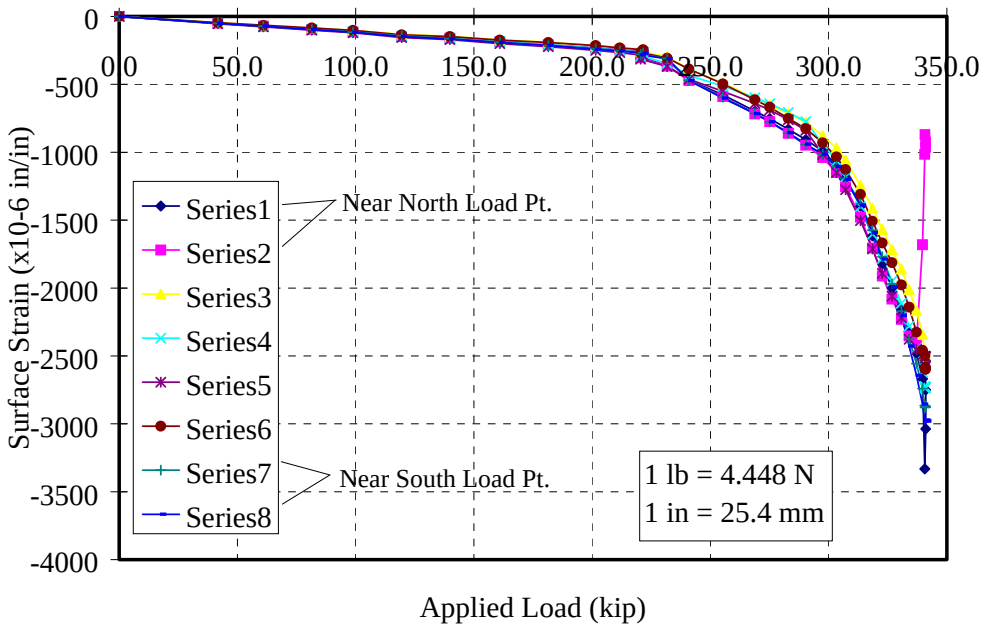

Figure H.9- Concrete Surface Strain vs. Applied Load for H0B0A-1

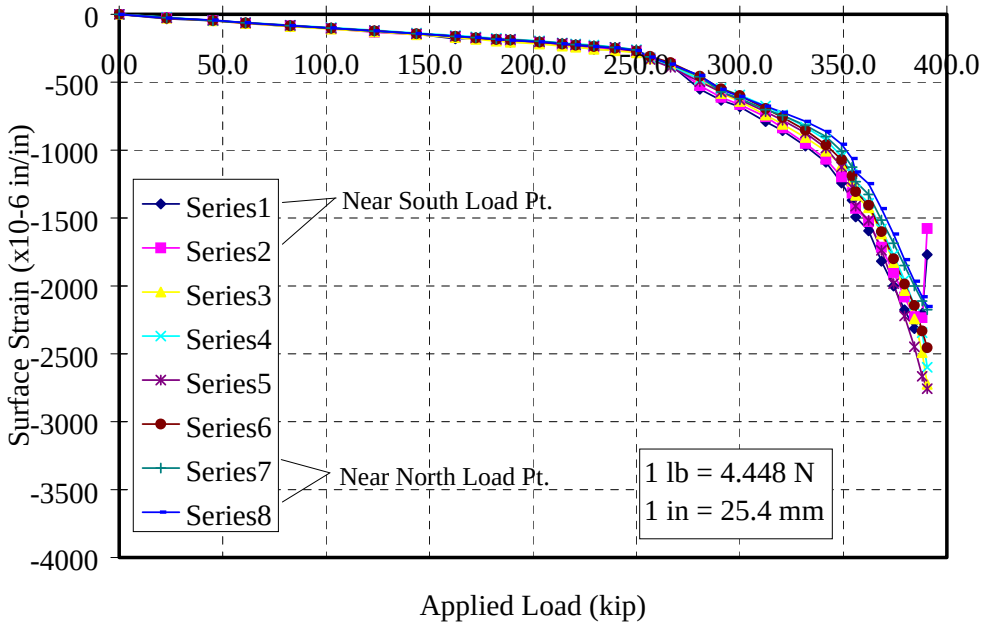

Figure H.10- Concrete Surface Strain vs. Applied Load for H0B0B-2

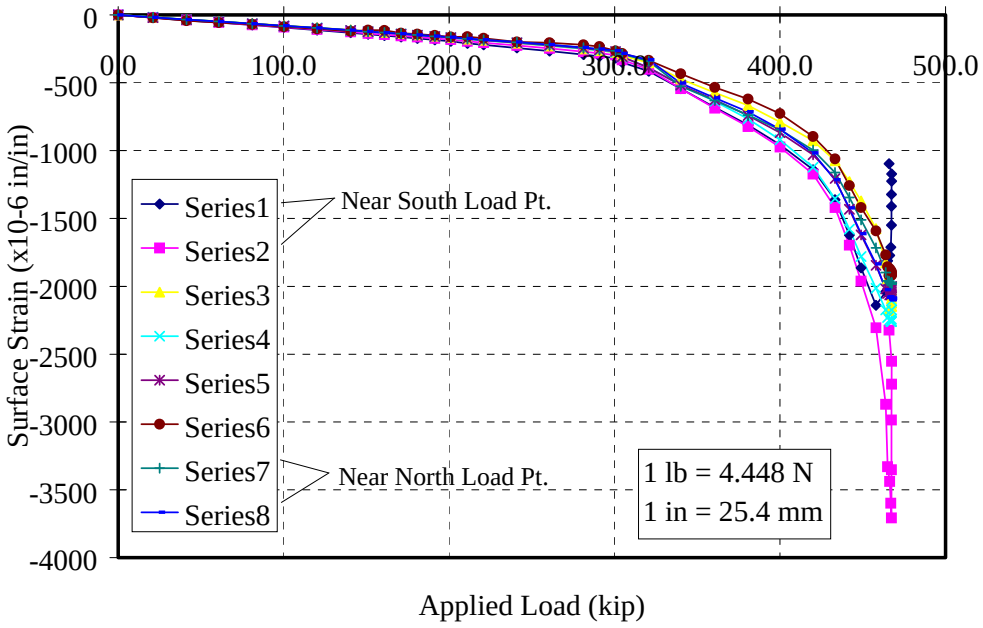

Figure H.11- Concrete Surface Strain vs. Applied Load for H0B1A-3

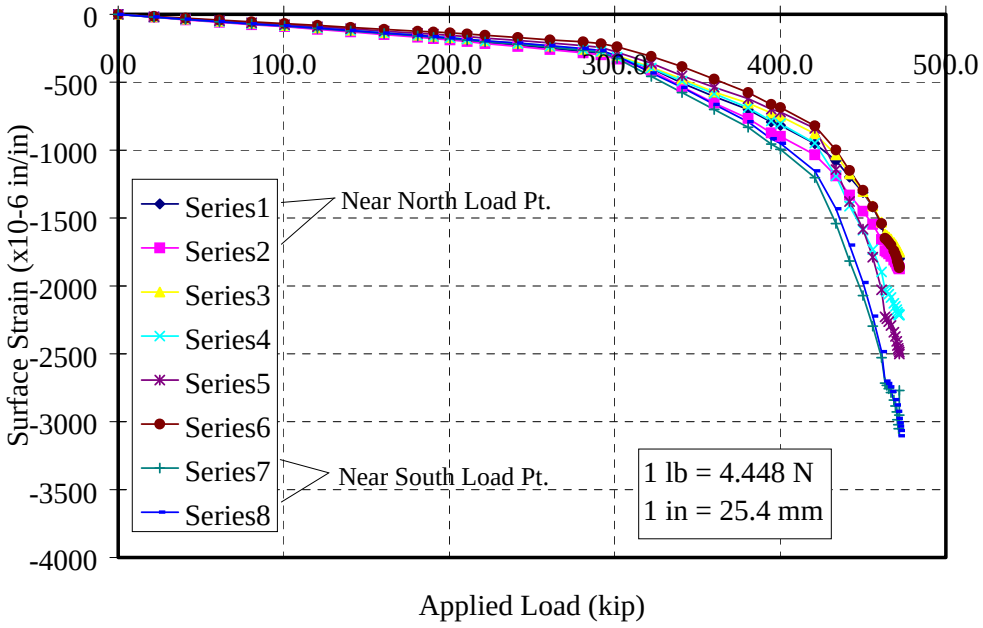

Figure H.12- Concrete Surface Strain vs. Applied Load for H0B0B-4

APPENDIX I

TXDOT BEAM REINFORCEMENT

AND BAR DETAILS

Figure I.1- TxDOT Mild Steel Reinforcement Details

Figure I.2- TxDOT Mild Steel Reinforcement Details (cont.)

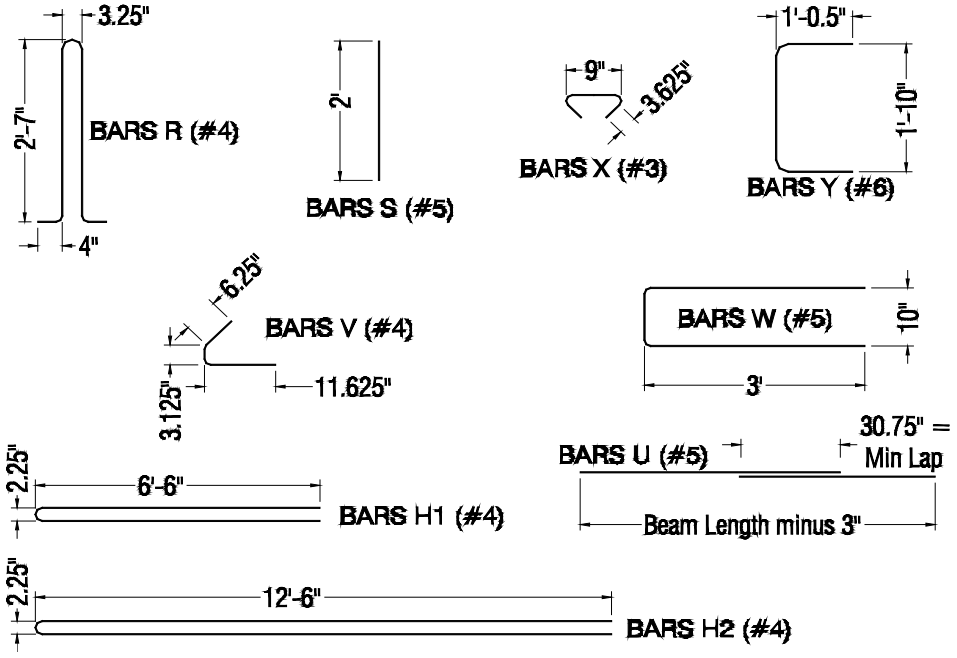

I.3- Reinforcing Steel Bar Details for the Prestressed Concrete Beams

REFERENCES

1. Cousins, Thomas E., Johnston, David W., and Zia, Paul, "Bond of Epoxy Coated Prestresing Strand," Research Report FHWA/NC/87-005, Center for Transportation Engineering Studies, Department of Civil Engineering, North Carolina State University, December, 1986.(a)

2. Cousins, Thomas E., Johnston, David W., and Zia, Paul, "Development Length of Epoxy-Coated Prestressing Strand," *ACI Materials Journal*, July-August, 1990, pp. 309-318.(b)

3. Cousins, Thomas E., Johnston, David W., and Zia, Paul, "Transfer Length of Epoxy-Coated Prestressing Strand," *ACI Materials Journal*, May-June, 1990, pp. 193-203.(c)

4. Cousins, T. E., Johnston, D. W., and Zia, P., "Transfer and Development Length of Epoxy Coated and Uncoated Prestressing Strand," PCI Journal, July-August, 1990, pp. 92-103.

5. Stocker, M. F., and Sozen, M. A., "Investigation of Prestressed Reinforced Concrete for Highway Bridges, Part V: Bond Characteristics of Prestressing Strand," Engineering Experiment Station 503, The University of Illinois, 1971. (d)

6. Russell, B. W., and Burns, N. H., "Design Guidelines for Transfer, Development and Debonding of Large Diameter Seven Wire Strands in Pretensioned Concrete Girders," Research Report 1210-5F. Center for Transportation Research, The University of Texas at Austin, January, 1993.(e)

7. Chief, Bridge Division, "Prestressing Strand for Pretension Applications-Development Length Revisited," *Memorandum*, Federal Highway Administration, October 26, 1988. (f)

8. Chief, Bridge Division, "Prestressing Strand for Pretension Applications Revisited," *Memorandum*, Federal Highway Administration, May 8, 1996.(g)

9. Janney, J. R., "Nature of Bond in Prestressed Concrete," *Journal of the American Concrete Institute*, May, 1954, pp. 717-736.(i)

10. Thorsen, Niels, "Use of Large Tendons in Pre-tensioned Concrete," *Journal of the American Concrete Institute*, February 1956, pp. 650-659.(j)

11. Hanson, Norman W., and Kaar, Paul H., "Flexural Bond Tests of Pretensioned Prestressed Beams," *Journal of the American Concrete Institute*, January 1959, pp. 783-802.(k)

12. Kaar, Paul H., LaFraugh, Robert W., and Mass, Mark A., "Influence of Concrete Strength on Strand Transfer Length," *Journal of the Prestressed Concrete Institute*, October, 1963, pp. 47-67.(l)

13. Zia, Paul and Mostafa, Talat, "Development Length of Prestressing Strands," *Journal of the Prestressed Concrete Institute*, Sept.-Oct., 1977, pp. 54-65.(m)

14. Loov, R. E., and Weerasekera, R., "Prestress Transfer Length," *Annual Conference of The Canadian Society for Civil Engineering*, Hamilton, Ontario, May 1990.(n)

15. Hoyer, E. And Fredrech, E., "Bietrag zür Frag der Nalftspannug in Eigen-beton-bauteinten," *Beton ünd Eisen*, V. 38, 1939.(o)

16. Unay, I.O., Russell, B. W., Burns, N. H., and Kreger, M., "Measurement of Transfer Length on Prestressing Strands in Prestressed Concrete Specimens," Research Report 1210-1, Center for Transportation Research, The University of Texas at Austin, March, 1991.(h)

17. ACI Committee 318, *Building Code Requirements for Reinforced Concrete Structures (ACI 318-95)*, American Concrete Institute, Detroit, Michigan, 1989.(cc)

18. Janney, J. R., "Report of Stress Transfer Length Studies on 270K Prestressing Strand," *PCI Journal*, February, 1963, pp. 41-45.(p)

19. Over, S. R. And Au, Tung, "Prestress Transfer Bond of Pretensioned Strands in Concrete," *Journal of the American Concrete Institute*, November, 1965, pp. 1451-1459.(q)

20. Deatherage, H. J. and Burdette, Edwin G., "Development Length and Lateral Spacing Requirements of Prestressing Strand for Prestressed Concrete Bridge Products," Final Report, The University of Tennessee, Knoxville, April, 1990.(v)

21. Malik, Raheel, "Measurement of Transfer Length of 0.5-inch and 0.6-inch Diameter Prestressing Strand in Single Strand specimens," Thesis, The University of Texas at Austin, May, 1990.(w)

22. Shahawy, M. A., Isa, M., and Batchelor, B. deV, "Strand Transfer Lengths in Full-Scale AASHTO Prestressed Concrete Girders," *PCI Journal*, V. 37, No. E, May-June, 1992, pp. 84-96.(z)

23. Lane, S. N., “Transfer Lengths in Regular Prestressed Concrete Concentric Beams,” Public Roads- A Journal of Highway Research and Development, Federal Highway Administration, V. 56, No. 2, September, 1992, pp. 67-71.(bb)

24. Kaar, P. H., Hanson, Norman W., “Bond Fatigue Tests of Beams Simulating Pretensioned Concrete Crossties,” *PCI Journal*, September-October, 1975, pp. 65-80.(s)

25. Dorsten, V., Hunt, F. F., Preston, H. K., “Epoxy-Coated Seven-Wire Prestressing Strand for Prestressed Concrete,” *PCI Journal*, July-August, 1984, pp. 120-129.(t)

26. Hanson, N. W., “Influence of Surface Roughness of Prestressing Strand on Bond Performance,” *PCI Journal*, V. 14, No. 1, February, 1969, pp. 32-45.(x)

27. Burdette, E.G., Deatherage, J. H., and Chew, C. K., “Development Length and Lateral Spacing Requirements of Prestressing Strand for Prestressed Concrete Bridge Girders,” *PCI Journal*, V. 39, No. 1, January-February, 1994, pp. 70-83.(aa)

28. Castrodale, Reid W., Burns, N. H., and Kreger, M. E., “A Study of Pretensioned High Strength Concrete Girders in Composite Highway Bridges-Laboratory Tests,” Research Report 381-3, Center for Transportation Research, The University of Texas at Austin, January 1988, pp. 9-24.(u)

29. Mitchell, D., Cook, W. D., Khan, A. A., and Tham, T., “Influence of High Strength Concrete on Transfer and Development Length of Pretensioning Strand,” *PCI Journal*, V. 38, No. 3, May-June, 1993, pp. 52-66.(y)

30. Kaar, P. H. and Magura, D. D., “Effect of Strand Blanketing on Performance of Pretensioned Girders,” *PCI Journal*, December, 1965, pp. 20-34.(r)

31. American Association of State Highway and Transportation Officials (AASHTO), Standard Specifications for Highway Bridges, Fifteenth Edition, AASHTO, Washington, D.C., 1992 (dd)

32. Tawfiq, K. S., “Cracking and Shear Capacity of High Strength Concrete Girders,” Final Report, FAMU/FSU College of Engineering, Tallahassee, Florida, January, 1995. (jj)

33. Gross, S.P., and Burns, N. H., “Transfer and Development Length of 15.2 mm (0.6 in) Diameter Prestressing Strand in High Performance Concrete: Results of the Hoblitzell-Buckner Beam Tests,” Research Report 580-2, Center for Transportation Research, The University of Texas at Austin, June, 1995. (mm)

34. Balazs, G. L., “Transfer Lengths of Prestressing Strand as a Function of Draw-in and Initial Prestress,” *PCI Journal*, V. 38, No. 2, March-April, 1993, pp. 86-93. (kk)

35. Loov, R., “A General Equation for the Steel Stress for Bonded Prestressed Concrete Members,” *PCI Journal*, V. 33, No. 6, November-December, 1988, pp. 108-148. (ll)

36. Buckner, C. D. “An Analysis of Transfer and Development Lengths for Pretensioned Concrete Structures,” Report No. FHWA-RD-94-049, Turner Fairbanks Highway Research Center, Federal Highway Administration, McLean, VA, December, 1994.(ff)

37. Martin, L. D. and Scott, N. L., “Development of Prestressing Strand in Pretensioned Members.” *ACI Journal*, Proceedings, V. 73, No. 8, August, 1976, pp. 453-456.(ee)

38. Logan, D. R., “Acceptance Criteria for Bond Quality of Strand for Pretensioned Prestressed Concrete Applications,” *PCI Journal*, V. 42, No. 2, March-April, 1997, pp. 52-90 (pp)

39. American Society for Testing and Materials (ASTM), *Standard Test Method for Static Modulus of Elasticity and Poisson’s Ratio of Concrete in Compression (C 469-94)*, ASTM, Philadelphia, Pennsylvania, July, 1994 (gg)

40. American Society for Testing and Materials (ASTM), *Test Method for Compressive Strength of Cylindrical Concrete Specimens (C39)*, Annual Book of ASTM Standards, V. 04.02, ASTM, Philadelphia, Pennsylvania. (hh)

41. American Society for Testing and Materials. *Method of Testing Multi-Wire Strand for Prestressed Concrete (A370)*, ASTM, Philadelphia, Pennsylvania, July, 1994. (ii)

42. Cordova, C. R., “Transfer and Development Length of 0.6-inch Diameter Prestressing Strand at Two Inch Spacing in Fully Bonded Normal Strength Concrete Composite Texas Type C Beams,” Master’s Thesis, The University of Texas at Austin, August, 1996. (oo)

43. Collins, M.P. and Mitchell, D., “Prestressed Concrete Structures,” Englewood Cliffs, NJ, Prentice-Hall, Inc., 1991. (tt)

44. Arrellaga, J. A., “Instrumentation Systems for Post-Tensioned Segmental Box Girder Bridges,” Master’s Thesis, The University of Texas at Austin, December, 1991. (qq)

45. FIP Report on Prestressing Steel 2, “Anchorage and Application of 7-Wire Strands,” FIP 5/4, London, June, 1978. (rr)

46. Uijil, J. A., “Tensile Stresses in the Transmission Zones of Hollow-Core Slabs Prestressed With Pretensioned Strands,” *Report 5-83-10*, Delft University of Technology, Delft, 1983. (ss)

47. Lin, T. Y., and Burns, N. H. *Design of Prestressed Concrete Structures*. Third Edition, John Wiley & Sons, New York, New York, 1981. (nn)